

CENTRAL HADRON PRODUCTION IN CROSSING OF DEDICATED
HADRONIC BEAMS: THE PHYSICS POTENTIAL OF AN IN-DEPTH
EXPERIMENTAL INVESTIGATION

PETER MINKOWSKI

Institute for Theoretical Physics, University of Bern, CH-3012 Bern, Switzerland

Dedicated to the memory of Professor Dubravko Tadić

Received 26 April 2004; Accepted 1 December 2005
Online 2 December 2005

The original aim of this work was to give a *brief* review of gluonic mesons, to be searched for in an experiment dedicated to central production of a relatively low mass hadronic system, whereby rapidity gaps are possible to impose, requiring initial hadron beams of sufficient energy and intensity. Sections 1 - 4 are devoted to this aim. The various theoretical ingredients, covering several decades of thinking by many, including the author, are contained in five appendices, dedicated to specifically gluonic binaries within QCD and their underlying Yang-Mills base structure

PACS numbers: 11.15.-q, 12.38.Aw, 13.85.-t

UDC 539.126

Keywords: QCD, central hadroproduction, gluonic binaries

Contents

1. Introduction	80
2. Theoretical expectations for primary gluonic binary (gb) Regge trajectories	81
3. Quantum numbers of binary gluonic mesons	83
4. Spectral patterns of gb - facts and fancy	90
5. Conclusion	98
Appendices	98
A.1 Spinor wave functions, spin states and transformation rules	98
A.2 Note on the complex Lorentz group and associated operations ...	103
A.3 Field strengths, potentials and adjoint string operators	104
A.4 Spin projection operations on adjoint string operators	118
A.5 Spin projection operations on adjoint string operators - extended ..	120
References	135

1. Introduction

I shall begin a historical survey, quoting a recent article [1] entitled "Central exclusive diffractive production as a spin-parity analyser: from hadrons to Higgs", written by four authors: A. B. Kaidalov, V. A. Khoze, A. D. Martin and

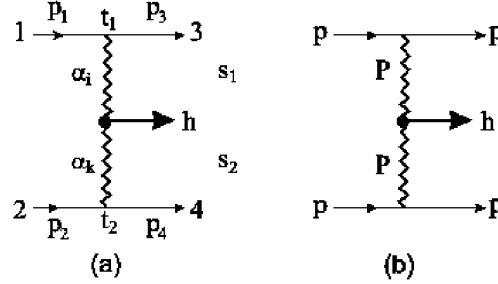


Fig. 1. (a) The central production of a state h by double Reggeon-exchange. (b) The double-Pomeron exchange contributions to $pp \rightarrow p + h + p$, which dominates at high energies, where the $+$ signs are used to indicate the presence of Pomeron-induced rapidity gaps.

M. G. Ryskin. 'Pour fixer les idées', let me reproduce the first figure of the above paper. In Fig. 1 the reaction of central type

$$\left\{ \begin{array}{l} H_1(p_1; q.\#1) \\ + H_2(p_2; q.\#2) \end{array} \right\} \rightarrow \left\{ \begin{array}{l} H_3(p_3; q.\#3) \\ + H_4(p_4; q.\#4) \\ + [h_c(p_c; q.\#c) + X_c] \end{array} \right\} \quad (1)$$

is represented with the following identifications:

- 1) Initial and tagged final hadron pairs inducing central production

$$\begin{array}{ll} H_{1,2} : & \text{initial hadron pair} & \text{with} & \left\{ \begin{array}{l} \text{momenta } p_{1,2} \\ \text{and } q.\# \quad q_{1,2} \end{array} \right\} \\ H_{3,4} : & \begin{array}{l} 3 (\leftarrow 1) \text{ and } 4 (\leftarrow 2) \\ \text{associated hadron pair} \end{array} & \text{with} & \left\{ \begin{array}{l} \text{momenta } p_{3,4} \\ \text{and } q.\# \quad q_{3,4} \end{array} \right\} \end{array} \quad (2)$$

- 2) Centrally produced (hadronic) system h_c conditioned by $h_c | X_c$

$$\begin{array}{ll} h_c : & \begin{array}{l} \text{centrally produced} \\ \text{system of interest} \end{array} & \text{with} & \left\{ \begin{array}{l} \text{momentum } p_c \\ \text{mass } M_c = \sqrt{p_c^2} \\ \text{and } q.\# \quad q_c \end{array} \right\} \\ X_c : & \text{specified conditions} & & \left\{ \begin{array}{l} \text{optimized to isolate } h_c \\ \text{from background.} \end{array} \right\} \end{array} \quad (3)$$

As is illustrated by the range of topics discussed in Ref. [1], the general issue of central production is not restricted to strong interactions, limited as far as quark and antiquark flavors are concerned to the three light ones u , d and s , denoted QCD_3 hereafter.

This is our main focus here.

Rather at sufficiently high c.m. energy, strong and electroweak synthesis of the central system ' h_c ' well includes the following processes, becoming dominantly reducible to fusion of virtual gauge boson pairs formed out of the sequence gluon (g), photon (γ), W and Z. We list only the combinations where $h_c = Q\bar{Q}$ $gg(g\gamma, \gamma\gamma) \rightarrow Q\bar{Q}$, $g\gamma \rightarrow Q\bar{Q}$ for heavy flavors $Q = c, b, t$ and the top quark induced hadronic production of Higgs boson(s), where $h_c = h^{JP} gg \rightarrow t\bar{t} \rightarrow h^{JP}$:

- i) Hadronic production of (single) heavy quark-antiquark pairs, both bound and open

$$h_c(QCD_6) = \left\{ \begin{array}{l} c\bar{c} : J/\Psi, \chi, \dots, D\bar{D}, \dots \\ b\bar{b} : Y, \chi_b, \dots, B\bar{B}, \dots \\ t\bar{t} \end{array} \right\} \quad (4)$$

$gg \rightarrow Q\bar{Q}$.

- ii) Hadronic production of (single) Higgs bosons h^{PC}

$$h_c(QCD_6, \mathcal{Y}_{h^{PC}t\bar{t}}) = \{ h^{++}, h^{-+} \} \quad (5)$$

$gg \rightarrow t\bar{t} \rightarrow h^{JP}$.

In Eq. (5), $\mathcal{Y}_{h^{PC}t\bar{t}}$ denotes the Yukawa coupling between the Higgs boson(s) and the top quark.

The association of central production with *perturbatively preconceived* gauge boson fusion is not fortuitous. It goes back to seminal work on multiparticle production mainly of electrons and positrons in QED, by Landau, Lifschitz, Pomeranchuk and others. I only wish to cite a selected subset for historical accuracy [2].

The perturbative approach to QED-governed high-energy elastic scattering amplitudes for initial particle pairs e^-e^\pm , e^-p , $e^-\gamma$, γp and $\gamma\gamma$ was pioneered by Cheng and Wu [3]. The proton can be replaced by a nucleus (A, Z), where the nuclear charge $Q = Ze$ serves to represent 'strong' coupling, for large Z .

2. Theoretical expectations for primary gluonic binary (gb) Regge trajectories

We follow the identification of the gluonic binary states lowest in mass discussed in Ref. [4]. It shall be clear, that here we follow a combination of *hypotheses and theoretical expectations*. We will comment on alternatives below.

We begin with the spectroscopic classification of gluonic binaries [5], which, apart from the confined nature of binary gluons, is identical to the classification of photon binaries [6, 7]. It will prove useful to obtain a ‘Richtwert’ for the inverse slope of the ϱ -Regge trajectory at 0 momentum transfer, since it is this quantity which sets the unit of mass square with respect to which hadronic resonances, gb and others, are to be placed in the simplified harmonic *and zero width*- approximation.

In this objective we define the quantity $m_\varrho^2(0 = t)$, which represents the ϱ mass square as seen in the limit of spacelike momentum transfer $t \rightarrow 0$ through the electromagnetic form factor of charged pions $F_\gamma^{\pi^+}(t)$

$$m_\varrho^{-2}(0) = \left. \frac{dF_\gamma^{\pi^+}(t)}{dt} \right|_{t=0} = \frac{1}{6} \langle r^2 \rangle_\gamma^{\pi^+}. \quad (6)$$

In Eq. (6) $\langle r^2 \rangle_\gamma^{\pi^+}$ denotes the e.m. mean square charge radius of charged pions. This quantity is presently being investigated by Caprini, Colangelo and Leutwyler [8], from where I quote the preliminary result

$$\langle r^2 \rangle_\gamma^{\pi^+} = \begin{cases} 0.4332 \pm 0.005 \text{ (stat.)} \pm 0.0004 \text{ (syst.)} \pm 0.0004 \text{ (P)} \\ \rightarrow 0.4332 \pm 1.3 \% \text{ fm}^2. \end{cases} \quad (7)$$

Converting to GeV units, we obtain

$$\begin{aligned} m_\varrho^2(0) &= 0.5393 \pm 1.3 \% \text{ GeV}^2 \\ m_\varrho^2(0) - m_{\pi_0}^2 &= 0.5211 \pm 1.3 \% \text{ GeV}^2 \\ &= (721.9 \pm 0.65 \% \text{ MeV})^2. \end{aligned} \quad (8)$$

The quantity $m_\varrho(0)$ in Eq. (8) deviates substantially from the resonance parameters of the ϱ , whether obtained from the pole position in the complex energy plane or other parametrizations of physical cross sections. For comparison I quote a recent determination by the KLOE collaboration [9]

$$\begin{aligned} m_\varrho &= 775.9 \pm 0.5 \pm 0.3 \text{ MeV} \\ \Gamma_\varrho &= 143.9 \pm 1.3 \pm 1.1 \text{ MeV}. \end{aligned} \quad (9)$$

The relation to the inverse Regge slope parameter $(\alpha')^{-1}$ is

$$\begin{aligned} (\alpha')^{-1} &= 2(m_\varrho^2(0) - m_{\pi_0}^2) \\ &= 1.0422 \pm 1.3 \% \text{ GeV}^2 \\ &= (1.0209 \pm 0.65 \% \text{ GeV})^2. \end{aligned} \quad (10)$$

We remark here, that the relation in Eq. (10) is *not* a rigorous one. We can compare with the direct $t > 0$ spectroscopic masses along the Λ baryon trajectory, assumed unperturbed

$$\begin{aligned} \frac{1}{2} (m^2(\Lambda^{5/2+}) - m^2(\Lambda^{1/2+})) &= (\alpha'_\Lambda)^{-1} = 1.034 \pm 0.010 \text{ GeV}^2 \\ \frac{1}{4} (m^2(\Lambda^{9/2+}) - m^2(\Lambda^{1/2+})) &= (\alpha'_\Lambda)^{-1} = 1.069 \pm 0.024 \text{ GeV}^2. \end{aligned} \quad (11)$$

3. Quantum numbers of binary gluonic mesons

The binary gluon system is only singled out in the present discussion, because it is expected to contain gluonic meson resonances, lower in mass than the ternary or more complex multi-gluonic mesons.

Let us first consider the finite dimensional (nonunitary) representations of $SL2C \times SL2C$ restricted and unrestricted to the covering group of the real Lorentz group. Details are presented in appendices A.1 and A.2. To this end, we associate with a bosonic resonance a free, massive state or collection of spin states. Let the total spin be J . The spinor wave functions are obtained by direct products of full and chiral spin 1/2 spinors, and the four-momenta p , neglecting here the width of the associated resonance.

$$\begin{aligned}
t_{\alpha_1 \alpha_2 \dots \alpha_N}(p; \{spin\}) e^{-ipx} &= \langle \Omega | \phi_{\alpha_1 \alpha_2 \dots \alpha_N}(x) | p; \{spin\} \rangle \\
N = 2J, \quad p^2 &= M^2, \quad p^0 = E \geq M \\
t_{\alpha_1 \alpha_2 \dots \alpha_N} &= t_{\underline{\alpha}} : \quad \text{totally symmetric under} & \alpha_1 \dots \alpha_N \\
& \quad \text{permutations of the indices} \\
\alpha_j &= 1, 2, \quad j = 1 \dots N
\end{aligned} \tag{12}$$

$$\begin{aligned}
\tilde{t}^{\hat{\gamma}_1 \hat{\gamma}_2 \dots \hat{\gamma}_N}(p; \{spin\}) e^{-ipx} &= \langle \Omega | \psi^{\hat{\gamma}_1 \hat{\gamma}_2 \dots \hat{\gamma}_N}(x) | p; \{spin\} \rangle \\
\tilde{t}^{\hat{\gamma}_1 \hat{\gamma}_2 \dots \hat{\gamma}_N} &= \tilde{t}^{\hat{\gamma}} : \quad \text{totally symmetric under} & \hat{\gamma}_1 \dots \hat{\gamma}_N \\
& \quad \text{permutations of the indices} \\
\hat{\gamma}_j &= 1, 2, \quad j = 1 \dots N.
\end{aligned}$$

In Eq. (12), $\{spin\}$ denotes the spin state, to be specified in a general frame of motion, and $(\phi_{\underline{\alpha}}, \psi^{\hat{\gamma}})$ a pair of free fields (right chiral, left chiral), associated with the particle in question.

The transformation rules of the spinor wave functions $(t_{\underline{\alpha}}, \tilde{t}^{\hat{\gamma}})$ are

$$\begin{aligned}
\{spin\} &\rightarrow s, \quad \#s = N + 1 \\
t_{\underline{\alpha}}(\Lambda p; s) &= S_{\underline{\alpha}}^{\underline{\beta}}(a) t_{\underline{\beta}}(p; s') D_{s s'} \\
\tilde{t}^{\hat{\gamma}}(\Lambda p; s) &= \tilde{S}^{\hat{\gamma}}_{\hat{\delta}}(b) \tilde{t}^{\hat{\delta}}(p; s') D_{s s'} \\
D_{s s'} &= D_{s s'}^J(\Lambda, p) ; \quad b = \bar{a}.
\end{aligned} \tag{13}$$

The sought representations of the Lorentz group are obtained as symmetric products of the spin 1/2 chiral spinors. They are presented in Appendix A.1.

There is a *small* step from binary photon to binary gluon compounds, even though their classification with respect to quantum numbers J^{PC} is identical. To see this, let me first discuss the $SU3_c$ gauge invariant binary gauge boson operator

$$\begin{aligned}
B_{[\mu_1 \nu_1], [\mu_2 \nu_2]}(x_1, x_2) &= \\
F_{[\mu_1 \nu_1]}(x_1; A) U(x_1, A; x_2, B) F_{[\mu_2 \nu_2]}(x_2; B) & \\
A, B, \dots &= 1, \dots, 8.
\end{aligned} \tag{14}$$

Adjoint representation indices referring to the color gauge group are denoted by A, B in Eq. (14). Summation over repeated such indices is implied. $F_{[\mu\nu]}(x; A)$ denote the color octet of field strengths. The quantity $U(x, A; y, B)$ in Eq. (14) denotes the octet string operator, i.e. the path ordered exponential over a straight line path \mathcal{C} from y to x .

$$U(x, A; y, B) = P \exp \left(\int_y^x \Big|_{\mathcal{C}} dz^\mu \frac{1}{i} V_\mu(z, D) \mathcal{F}_D \right)_{AB} \quad (15)$$

$$(\mathcal{F}_D)_{AB} = i f_{ADB}.$$

In Eq. (15), f_{ADB} denotes the structure constants of $SU3_c$ and \mathcal{F}_D the generators of its adjoint representation. $V_\mu(z, D)$ denote the octet of field potentials. Properties pertaining to the octet string operators, field strengths and their potentials are collected in Appendix A.3.

The extensive discussion of Stokes relations in Appendix A.3 serves here to present as clear an argument as possible, why the octet string operator $U(x, A; y, B)|_{\mathcal{C}}$, taken over a straight line path \mathcal{C} attached to two field strength operators $F_{[\mu_k \nu_k]}(x_k; A_k)$; $k = 1, 2$ at the ends of the string – as displayed in Eqs. (14) and (15) – form a configuration similar to an H_2 molecule, representing an energetically favored gluonic meson, i.e. a hadronic resonance susceptible of identification specifically in central production. The band structure of the H_2 molecule would then translate into the possible quantum numbers of the associated binary gluonic mesons, *so defined*, in appropriately adapted analogy. From a purely theoretical point of view, it has to be stressed, that this remains at the present stage a *hypothesis*, subject to further tests, extending the existing analyses in Refs. [4] and [5] as well as related and/or alternative points of view, to be substancified below.

To illustrate the molecular aspect, I reproduce in Fig. 2 the gauge boson action density in a lattice calculation of a nucleon [10].

The bilinear operator in Eq. (14) satisfies Bose symmetry

$$B_{[\mu_1 \nu_1], [\mu_2 \nu_2]}(x_1, x_2) = B_{[\mu_2 \nu_2], [\mu_1 \nu_1]}(x_2, x_1) \rightarrow$$

$$\widehat{C}^{-1} B_{[\mu_1 \nu_1], [\mu_2 \nu_2]}(x_1, x_2) \widehat{C} = B_{[\mu_1 \nu_1], [\mu_2 \nu_2]}(x_1, x_2). \quad (16)$$

In Eq. (16), \widehat{C} denotes the charge conjugation operator.

We shall consider matrix elements of the form

$$\langle \emptyset | B_{[\mu_1 \nu_1], [\mu_2 \nu_2]}(x_1, x_2) | gb(J^{PC}); p, \{spin\} \rangle \rightarrow$$

$$e^{-ipX} \tilde{t}_{\underline{z}}(z, p, J^{PC}; \cdot) \quad \text{with}$$

$$|\emptyset\rangle : \text{ground state} \quad , \quad X = \frac{1}{2}(x_1 + x_2) \quad , \quad z = (x_1 - x_2) \quad (17)$$

$$J^{PC} : \text{total spin, parity, C-parity} \quad ; \quad p : \text{c.m. four momentum}$$

$$\underline{z} : \text{spinor representation for } [\mu_1 \nu_1], [\mu_2 \nu_2]$$

$$\cdot : \text{spin state.}$$

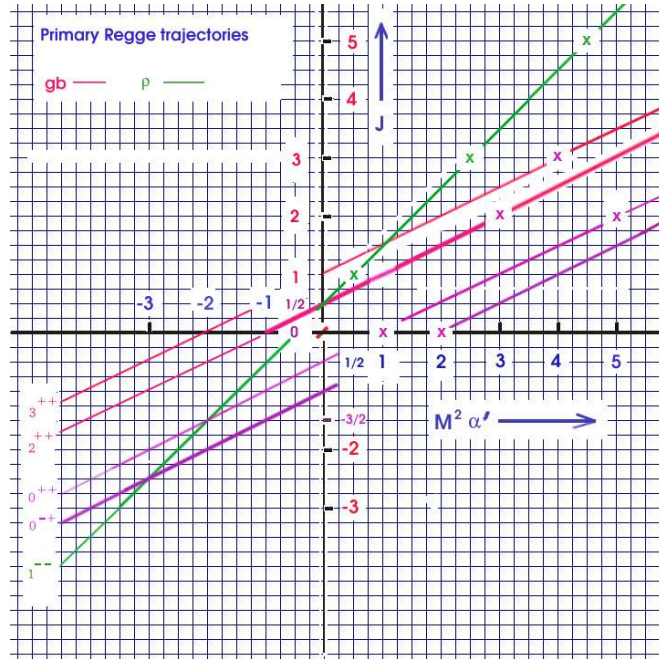


Fig. 2. Primary gluonic binary (gb) Regge trajectories in comparison with the $\rho - (q\bar{q})$ trajectory.

In Eq. (17) J^{PC} , p and $\cdot = \{spin\}$ refer to properties of the gluonic meson in question (gb), whereas $\cdot \leftrightarrow [\mu_1 \nu_1], [\mu_2 \nu_2]$ and z refer to variables intrinsic to the operator $B_{[\mu_1 \nu_1], [\mu_2 \nu_2]}(x_1, x_2)$.

The four-momentum p is introduced, as if $gb(J^{PC})$; $p, \{spin\}$ would correspond to a *stable* particle. This is at best approximately justified in the zero width approximation, which we shall *not* a priori assume to be valid.

Nevertheless gb -s will manifest themselves as poles in complex momentum planes, corresponding to analytic continuation of strong interaction scattering amplitudes. The latter refer to stable particles, like pions, kaons and baryons, in the limit where both electromagnetic and weak interactions are neglected.

Hence, ignoring the above complication for the time being, the mass of $gb(J^{PC})$ is defined through p

$$\begin{aligned} m^2 &= p_\mu p^\mu ; E_p = \sqrt{p^2 + m^2} \\ m &= m(gb(J^{PC})) . \end{aligned} \quad (18)$$

As a consequence of Eq. (16), we have for the *binary* gluonic mesons $C = +$ throughout

$$gb(J^{PC}) \rightarrow gb(J^{P+}) . \quad (19)$$

The relativistic spin \cdot , processed as outlined in Appendix A.1, combines the same way as in the nonrelativistic case to a total spin S_{12}

$$\begin{aligned} S_{12} &= S_{12}^+ + S_{12}^- \\ (S_{12}^+ = 0, 2 \leftrightarrow P = +) ; (S_{12}^- = 1 \leftrightarrow P = -) . \end{aligned} \quad (20)$$

The total spin states S_{12} in Eq. (20) are subject to transversity conditions, to which we will turn below. But independtly thereof the spectrum of $gb(J^{P+})$ at this stage splits into three

$$gb(J^{P+}) \begin{cases} \nearrow & gb(J^{++}) \quad , \quad S_{12}^+ = 2 \quad : \quad II^+ \\ \rightarrow & gb(J^{++}) \quad , \quad S_{12}^+ = 0 \quad : \quad I^+ \\ \searrow & gb(J^{-+}) \quad , \quad S_{12}^- = 1 \quad : \quad I^- . \end{cases} \quad (21)$$

The three spectral types shall be denoted as in Eq. (21) : II^+ , I^+ and I^- , where the superfix stands for parity.

To clarify the spin structure, we discuss the spectral classes I^\pm first. To this end we label the amplitudes $\tilde{t}_\pm(z, p, J^{PC}; \cdot)$ in Eq. (17)

$$\begin{aligned} \tilde{t}_\pm(z, p, J^{P+}; \cdot) &\rightarrow \tilde{t}_{\pm; S_{12}^\pm}(z, p, J^{\pm+}; \cdot) \\ \hline \tilde{t}_{\pm; S_{12}^\pm}(z, p, J^{\pm+}; \cdot) &\begin{cases} \nearrow & \tilde{t}_{\pm; II^+}(z, p, J^{++}; \cdot) \\ \rightarrow & \tilde{t}_{\pm; I^+}(z, p, J^{++}; \cdot) \\ \searrow & \tilde{t}_{\pm; I^-}(z, p, J^{-+}; \cdot) \end{cases} \\ \pm; S_{12}^\pm &\rightarrow \pm \rightarrow [\mu_1 \nu_1] , [\mu_2 \nu_2] . \end{aligned} \quad (22)$$

The two spectral classes I^\pm exhibit the relativistic factorization patterns

$$\begin{aligned} \tilde{t}_{\pm; I^\pm}(z, p, J^{\pm+}; \cdot) &= \left(\begin{array}{c} (K^\pm)_{[\mu_1 \nu_1][\mu_2 \nu_2]} \\ \times \tilde{t}_{I^\pm}(z, p, J^{\pm+}; \cdot) \end{array} \right) \\ (K^+)_{[\mu_1 \nu_1][\mu_2 \nu_2]} &= g_{\mu_1 \mu_2} g_{\nu_1 \nu_2} - g_{\mu_1 \nu_2} g_{\mu_2 \nu_1} \\ (K^-)_{[\mu_1 \nu_1][\mu_2 \nu_2]} &= \varepsilon_{\mu_1 \mu_2 \nu_1 \nu_2} . \end{aligned} \quad (23)$$

In Eq. (23), K^\pm denote the two Lorentz invariant tensors with parity \pm , respectively, and $g_{\mu\nu}$ the Lorentz metric tensor.

The tensors K^\pm form projection operations on the octet string operators

$$B_{[\mu_1 \nu_1], [\mu_2 \nu_2]}(x_1, x_2) ,$$

introduced in Eq. (14) and described in Appendix A.4. The projections yield

$$B_{[\mu_1 \nu_1], [\mu_2 \nu_2]}(x_1, x_2) = \left(\begin{array}{c} (K^+)_{[\mu_1 \nu_1], [\mu_2 \nu_2]} B^{(+)} \\ + (K^-)_{[\mu_1 \nu_1], [\mu_2 \nu_2]} B^{(-)} \\ + B'_{[\mu_1 \nu_1], [\mu_2 \nu_2]} \end{array} \right) , \quad (24)$$

where the quantities $B^{(\pm)}$ are derived in Appendix A.4. They are of the form given

in Eq. (160) reproduced below

$$\begin{aligned}
B^{(+)}(x_1, x_2) &= \\
&= \frac{1}{12} F_{[\alpha\beta]}(x_1; A) U(x_1, A; x_2, B) F^{[\alpha\beta]}(x_2; B) \\
\hline
B^{(-)}(x_1, x_2) &= \\
&= -\frac{1}{12} F_{[\alpha\beta]}(x_1; A) U(x_1, A; x_2, B) \tilde{F}^{[\alpha\beta]}(x_2; B) \\
&= -\frac{1}{12} \tilde{F}_{[\alpha\beta]}(x_1; A) U(x_1, A; x_2, B) F^{[\alpha\beta]}(x_2; B) \\
\hline
\tilde{F}_{[\alpha\beta]}(x_2; B) &= \frac{1}{2} \varepsilon_{\alpha\beta\gamma\delta} F^{[\gamma\delta]}(x_2; B) \\
\text{and } (x_2; B) &\leftrightarrow (x_1; A).
\end{aligned} \tag{25}$$

Returning to the (spin-) reduced amplitudes $\tilde{t}_{I^\pm}(z, p, J^{\pm+}; \cdot)$ introduced in Eq. (23) we obtain using the notation of Eq. (17)

$$\begin{aligned}
\langle \emptyset | B^{(\pm)}(x_1, x_2) | gb_{I^\pm}(J^{\pm+}); p, \{spin\} \rangle \\
= e^{-ipX} \tilde{t}_{I^\pm}(z, p, J^{\pm+}; \cdot),
\end{aligned} \tag{26}$$

with $B^{(\pm)}$ given in Eq. (25). In Eq. (26), the suffix I^\pm of the states gb_{I^\pm} indicates, that these are restricted to the spectral types denoted I^\pm in eq. (21). In the local limit of $z \rightarrow 0$, i.e. shrinking the extension of the adjoint string to zero length, we recognize in $B^{(\pm)}$ two local operators shaping the dynamics of QCD. We ignore here for clarity all short-distance singularities, in this limit.

$$\begin{aligned}
z \rightarrow 0 \quad : \quad \begin{array}{l} B^{(+)} \rightarrow \frac{1}{12} F_{[\mu\nu]}(X; A) F^{[\mu\nu]}(X; A) \\ B^{(-)} \rightarrow -\frac{1}{12} F_{[\mu\nu]}(X; A) \tilde{F}^{[\mu\nu]}(X; A) \end{array} \rightarrow \\
\hline
\begin{array}{l} 3 B^{(+)} \Big|_0 = \mathcal{L}^{(+)}(X) \quad \Big| \quad \mathcal{L}^{(+)}(X) = g^2 s(X) \\ -3 B^{(-)} \Big|_0 = \mathcal{L}^{(-)}(X) \quad \Big| \quad \mathcal{L}^{(-)}(X) = 8\pi^2 ch_2(X) \end{array} \\
\hline
\mathcal{L}^{(+)}(X) = \frac{1}{4} F_{[\mu\nu]}(X; A) F^{[\mu\nu]}(X; A) \\
\mathcal{L}^{(-)}(X) = \frac{1}{4} F_{[\mu\nu]}(X; A) \tilde{F}^{[\mu\nu]}(X; A).
\end{aligned} \tag{27}$$

In Eq. (27), s denotes the action density pertaining to gauge bosons and g the (strong) coupling constant, while ch_2 represents the density of the second Chern character.

We return to the wave functions $\tilde{t}_{I^\pm}(z, p, J^{\pm+}; \cdot)$ defined in Eqs. (23) and (26) pertaining to the gb spectral types I^\pm in eq. (26). As a consequence of Eq. (16), they satisfy the Bose symmetry relation

$$\tilde{t}_{I^\pm}(z, p, J^{\pm+}; \cdot) = \tilde{t}_{I^\pm}(-z, p, J^{\pm+}; \cdot). \tag{28}$$

We meet a problem of interpretation of the bilinear wave functions \tilde{t}_{I^\pm} and the symmetry in eq. (28), known (also) from the study of $q\bar{q}$ and 3 q composite systems

[11]. This is recognized, decomposing the Lorentz four vector z into parallel and transverse components relative to the c.m. momentum p

$$z = z_p + \eta p / m^2; \quad \eta = z_p \rightarrow z_p p = 0. \quad (29)$$

In the c.m. system, the scalar product η in Eq. (29) becomes relative time, which is not a genuine degree of freedom of the dynamical system in question.

$$\begin{aligned} \text{c.m. : } p &\rightarrow p_{c.m.} (m, \vec{0}) \\ \eta &\rightarrow m z_0 = m t_{rel}. \end{aligned} \quad (30)$$

Let me illustrate what is addressed here, considering the decay $\varrho^0 \rightarrow 2\pi$. First, we shall assume pions to be absolutely stable. Then the decay

$$\varrho^0 \rightarrow 2\pi^0$$

is forbidden by Bose symmetry. Next, we take into account, that π^0 's decay (mainly) into two photons, over the width of π^0 . The latter is according to the PDG [12]

$$\tau_{\pi^0} = (8.4 \pm 0.6) 10^{-17} \text{ s} \leftrightarrow \Gamma_{\pi^0} = (7.84 \pm 0.53) \text{ eV}. \quad (31)$$

To be specific, we consider the reaction

$$e^+ e^- \rightarrow \varrho^0 \rightarrow 4\gamma \quad (32)$$

and ask the question, whether it can proceed, when the two pairs of photons, $\gamma_1 \gamma_2$ and $\gamma_3 \gamma_4$ say, form each a π^0 , with invariant masses m_{12} and m_{34} differing by a well defined fraction of Γ_{π^0}

$$\begin{aligned} f_+ \Gamma_{\pi^0} &\geq |m_{12} - m_{34}| \geq f_- \Gamma_{\pi^0} \\ \text{with } f_+ &= 1, \quad f_- = 0.1 \text{ say.} \end{aligned} \quad (33)$$

The answer relevant here is, that there is a *multitude* of equivalent irreducible wave functions out of the *family* defined in Eqs. (23) and (26),

$$\tilde{t}_{I\pm}(z, p, J^{\pm+}; \cdot) = \tilde{t}_{I\pm}(z_p, p, \eta, J^{\pm+}; \cdot), \quad (34)$$

distinguished by the *parameter* η as defined in Eqs. (29) and (30). Thus we choose the representative with $\eta = 0$

$$t_{I\pm}(z_p, p, J^{\pm+}; \cdot) = \tilde{t}_{I\pm}(z_p, p, \eta = 0, J^{\pm+}; \cdot). \quad (35)$$

The above procedure illustrates the *difference* between decay amplitudes of resonances into two photons and their selection rules, derived in Refs. [6] and [7], and the wave functions of binary gluonic mesons.

The irreducible wave functions $t_{I\pm}$ can readily be discussed in the rest system of the momentum p , where

$$\begin{aligned} \text{c.m. : } (\eta = 0, z_p) &\rightarrow z_p = (0, \vec{z}) \rightarrow \vec{z} \\ t_{I\pm}(z_p, p, J^{\pm+}; \cdot) &\rightarrow t_{I\pm}(\vec{z}, J^{\pm+}; \cdot). \end{aligned} \quad (36)$$

The procedure outlined above implies that the octet string bilinear operators

$$B_{[\mu_1 \nu_1], [\mu_2 \nu_2]}(x_1, x_2), \quad (37)$$

defined in Eq. (14), are to be evaluated for spacelike relative positions $z = x_1 - x_2$ only.

Now Eq. (28) takes the form

$$t_{I^\pm}(\vec{z}, J^{\pm+}; \cdot) = t_{I^\pm}(-\vec{z}, J^{\pm+}; \cdot). \quad (38)$$

The consequence for the angular momentum composition of the spectral types I^\pm is indeed identical to the situation of decay into two photons [6, 7]

$$\begin{aligned} t_{I^\pm}(\vec{z}, J^{\pm+}; \cdot) &\rightarrow t_{I^\pm}(\vec{z}, J^{\pm+}; M) \\ t_{I^\pm}(\vec{z}, J^{\pm+}; M) &= R_{I^\pm}^J(r) Y_M^J(\vec{e}) \quad ; \quad J = \text{even} \\ r = |\vec{z}| \quad , \quad \vec{e} &= \vec{z}/r \end{aligned} \quad (39)$$

$$I^+ \quad : \quad J^{PC} = 0^{++}, 2^{++}, 4^{++} \dots$$

$$I^- \quad : \quad J^{PC} = 0^{-+}, 2^{-+}, 4^{-+} \dots$$

In Eq. (39), Y_M^J denote the orbital spherical harmonics with angular momentum J , while $\{R_{I^\pm}^J\}$ stand for a *family* of radial wave functions. Neither nature nor extension of this family, nor its ordering in mass can be deduced from the spectral type. For the sake of absolute clarity let me emphasize that the family of wave functions (of all types pertinent to binary gluonic mesons) can be empty, since no first principle proof to the contrary exists.

Quantum numbers of binary gluonic mesons continued

The II^+ spectral type

We turn to the remaining spectral type denoted II^+ in Eq. (21). The properties of this spectral series, represented by the quantities $B'_{[\mu_1 \nu_1], [\mu_2 \nu_2]}$ defined in Eq. (24) are derived in Appendix A.5. As shown there the wave functions of the gb spectral type II^+ are uniquely associated with the classical energy momentum bilinear pertaining to gauge bosons. We retain here the characteristic composition of the wave function associated bilinears B' in Eqs. (218) and (219) in the summary remarks of Appendix A.5:

$$B_{[\mu_1 \nu_1], [\mu_2 \nu_2]} = \left\{ \begin{array}{l} \frac{1}{2} \left(\begin{array}{l} g_{\mu_1 \mu_2} \varrho_{\nu_1 \nu_2} - g_{\nu_1 \mu_2} \varrho_{\mu_1 \nu_2} \\ -g_{\mu_1 \nu_2} \varrho_{\nu_1 \mu_2} + g_{\nu_1 \nu_2} \varrho_{\mu_1 \mu_2} \end{array} \right) \\ + K_{[\mu_1 \nu_1], [\mu_2 \nu_2]}^+ B^{(+)} \\ + K_{[\mu_1 \nu_1], [\mu_2 \nu_2]}^- B^{(-)} \end{array} \right\} \quad (40)$$

$$\text{with : } g^{\mu_1 \mu_2} B_{[\mu_1 \nu_1], [\mu_2 \nu_2]} = R_{\nu_1 \nu_2}$$

$$-\varrho^{\mu\nu} = -R^{\mu\nu} + \frac{1}{4} g^{\mu\nu} R = \vartheta_{cl}^{\mu\nu}$$

$$R = g^{\nu_1 \nu_2} R_{\nu_1 \nu_2} = 12 B^{(+)}.$$

The bilinears B' are thus given by

$$B'_{[\mu_1\nu_1],[\mu_2\nu_2]} = \frac{1}{2} \begin{pmatrix} g_{\mu_1\mu_2} \varrho_{\nu_1\nu_2} - g_{\nu_1\nu_2} \varrho_{\mu_1\mu_2} \\ -g_{\mu_1\nu_2} \varrho_{\nu_1\mu_2} + g_{\nu_1\nu_2} \varrho_{\mu_1\mu_2} \end{pmatrix} \quad (41)$$

$$B' \leftrightarrow \{II^+\} \longleftrightarrow \vartheta_{cl}^{\mu\nu}.$$

The three spectral types are given in Eq. (42) below, completing the types I^\pm in Eq. (39)

$$\begin{aligned} t_{I^\pm}(\vec{z}, J^{\pm+}; \cdot) &\rightarrow t_{I^\pm}(\vec{z}, J^{\pm+}; M) \\ t_{I^\pm}(\vec{z}, J^{\pm+}; M) &= R_{I^\pm}^J(r) Y_M^J(\vec{e}) \quad ; \quad J = \text{even} \\ r = |\vec{z}| \quad , \quad \vec{e} &= \vec{z}/r \end{aligned}$$

$$\begin{aligned} I^+ &: J^{PC} = 0^{++}, 2^{++}, 4^{++} \dots \\ I^- &: J^{PC} = 0^{-+}, 2^{-+}, 4^{-+} \dots \end{aligned}$$

$$\begin{aligned} t_{II^+}(\vec{z}, J^{\pm+}; \cdot) &\rightarrow t_{II^+}(\vec{z}, J^{II^+}; M, \vec{E}_\pm) \\ t_{II^+}(\vec{z}, J^{II^+}; M, \vec{E}_\pm) &= \\ &= R_{II^+}^J(r, \vec{E}_\pm) D_{M\pm 2}^J(\vec{e}, \vec{E}_\pm) \\ II^+ &: J^{PC} = 2^{++}, 3^{++}, 4^{++}, 5^{++} \dots \end{aligned} \quad (42)$$

In Eq. (42), the chromoelectric field strengths \vec{E}_\pm are retained in the arguments of the wave functions.

The functions $D_{M\sigma}^J(\vec{e}, \vec{E}_\pm)$, with $\sigma = \pm 2$, denote the eigenfunctions of a (symmetric) top, with the full orientation involving three Euler angles provided by the correlation between the two chromoelectric field strengths \vec{E}_\pm of the adjoint string, discussed in Appendix A.5.

Let us end here the theoretical discussion of binary gluonic modes associated with the octet gauge boson string. Theoretical expectations of spectral characteristics of states representing the spectral types I^\pm and II^+ shall be addressed in the next section.

4. Spectral patterns of gb - facts and fancy

a) Lattice QCD calculations

The most promising and widely accepted framework to derive spectral patterns of hadrons, including gluonic mesons, is the lattice gauge theory and therein the restriction to gauge boson degrees of freedom only. I shall quote several papers instead of a review [13–14]. I shall discuss the above papers one by one. In Ref. [13], a careful and dedicated study is devoted to the determination of the mass of $gb(0^{++})$, the lowest lying gluonic meson in pure Yang-Mills theory based on $SU3_c$, and also $gb(2^{++})$, with the results

$$\begin{aligned} m(gb(0^{++})) &= 1627 \pm 83 \text{ MeV} \rightarrow m^2 = 2.65 \pm 0.27 \text{ GeV}^2 \\ m(gb(2^{++})) &= 2354 \pm 95 \text{ MeV} \rightarrow m^2 = 5.54 \pm 0.6 \text{ GeV}^2. \end{aligned} \quad (43)$$

The main result refers to $gb(0^{++})$ and is in very good agreement with all lattice gauge theory calculations, concerning the same state.

I compare the above results with the assignment made here in Fig. 3

$$\begin{aligned} m^2 (gb(0^{++})) &= 1.04 \text{ GeV}^2 \\ m^2 (gb(2^{++})) &= 3.13 \text{ GeV}^2. \end{aligned} \quad (44)$$

Direct Measurement of Y-type Flux-Tube Formation in Lattice QCD

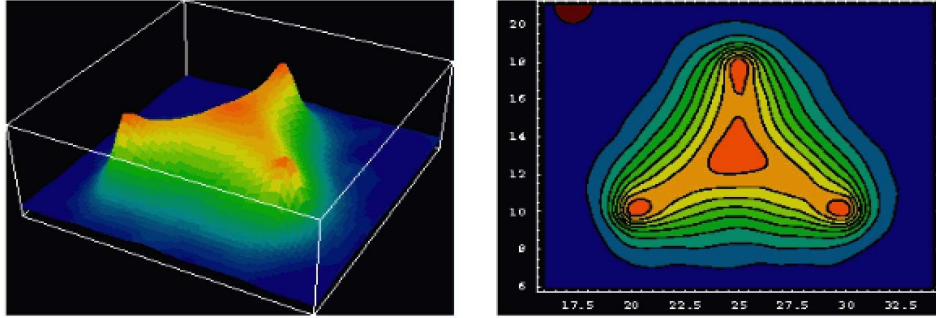


Fig. 3. Gauge boson action density for a nucleon in lattice simulation of QCD.

While it is difficult to associate an error with the tentative pattern represented in Fig. 3 and Eq. (44), to which I will return below, the essentially smaller mass square scale, by factors of ~ 2.5 and ~ 1.8 for $gb(0^{++})$ and $gb(2^{++})$, respectively, is indeed a *basic* controversy, seemingly disproving the mass square range considered in eq. (44).

In Ref. [14], an attempt is made to align gb resonances on the Pomeron trajectory, as done here in Fig. 3, but with very different assignments: the slope of the Pomeron trajectory is assumed to be

$$\begin{aligned} [14] : \alpha'_P &= \alpha'_{gb} \sim 0.22 \pm 0.4 \text{ GeV}^{-2} \\ \text{here : } \alpha'_{gb} &= \frac{1}{2} \alpha' = 0.5211 \pm 1.3\% \text{ GeV}^{-2}. \end{aligned} \quad (45)$$

Again a factor of two opens up, with respect to the value of α'_{gb} , between Ref. [14] and our present discussion, where indeed the relation $\alpha'_{gb} = \frac{1}{2} \alpha'$, also discussed below, can be in doubt.

As a consequence of the calculations in Ref. [14], the deduced mass square value for $gb(2^{++})$, which is supposed to lie on the Pomeron trajectory, becomes

$$\begin{aligned} [14] : m^2 (gb(2^{++})) &= 4.4 \pm 1.2 \text{ GeV}^2 \\ \text{here : } m^2 (gb(2^{++})) &= 3.13 \text{ GeV}^2 \\ (m^2 (gb(3^{++}))) &= 4.17 \text{ GeV}^2. \end{aligned} \quad (46)$$

Comparing the mass square values of Ref. [14] in Eq. (46) with the one of Ref. [13] in Eq. (43), we see (marginal) agreement.

In Ref. [15], lattice calculations are presented to determine the masses of hybrid mesons, composed of at least one gluon bound with a (nonstrange) $q\bar{q}$ pair, and exhibiting $q\bar{q}$ exotic quantum numbers, such as

$$J^{PC} = 0^{--}, 0^{+-}, 1^{-+}, 2^{+-} \dots$$

The lightest hybrid states with nonstrange quarks is found with characteristics

$$\begin{aligned} [15] : J^{PC} = 1^{-+} \quad ; \quad m_{hyb} = 1.9 \pm 0.2 \text{ GeV} \\ \rightarrow m_{hyb}^2 = 3.6 \pm 0.6 \text{ GeV}^2. \end{aligned} \quad (47)$$

Also in lattice calculations of hybrid meson masses, agreement between different groups is very satisfactory. The above is not directly related to the discussion of binary gluonic mesons, but the result in Eq. (47) is apparently contradicted by the experimental finding of (at least) two exotic mesons with $J^{PC} = 1^{-+}$ quantum numbers in p wave decay to $\eta\pi$ and $\eta'\pi$ [17]. These resonances carry the name $\pi_1(1400)$ and $\pi_1(1600)$, where the mass in MeV is the argument.

The two resonances in question were attributed the following characteristics [17] (beyond $J^{PC} = 1^{-+}$)

$$\begin{aligned} \pi_1(1400) \quad : \quad m = 1370 \pm 16 \begin{matrix} +50 \\ -30 \end{matrix} \text{ MeV} \\ \Gamma = \quad 385 \pm 40 \begin{matrix} +65 \\ -105 \end{matrix} \text{ MeV} \\ \pi_1(1600) \quad : \quad m = 1597 \pm 10 \begin{matrix} +45 \\ -10 \end{matrix} \text{ MeV} \\ \Gamma = \quad 340 \pm 40 \begin{matrix} +50 \\ -50 \end{matrix} \text{ MeV}. \end{aligned} \quad (48)$$

In the first paper in Ref. [17], the authors remark that the exotic quantum numbers violate $SU(3)_f$ symmetry, in the decay $\pi_1(1400) \rightarrow \pi\eta_8$, assigning pure flavor octet quantum numbers to η , unless it is not a hybrid meson but rather composed of two quarks and two antiquarks. There is a $\sim 20^\circ$ singlet octet mixing between η and η' , which, given the mass of $\pi_1(1400)$, i.e. below decay threshold for $\pi\eta'$ (modulo the width) becomes essential, even though we would then expect a reduction of the width by a factor of ~ 5 .

Alternatively, it can not be excluded that $\pi(1400)$ is in a quark flavor configuration corresponding to $q\bar{q}q\bar{q}$, and thus is not a hybrid meson in the first place. This discussion, even if at the side of the issue of gluonic mesons, gives a taste of the *interpretation* difficulties, facing the recognition of gb-s.

But even if we assume that precisely $\pi(1600)$ is a genuine hybrid meson, and further that the result given in Ref. [15] can be made to agree with a mass value of 1600 MeV, it is difficult to conceive that $gb(0^{++})$ would have a mass in excess of 1600 MeV as indicated in the value given in Ref. [13]. To be fair to all lattice calculations, let me stress that the mass values of gluonic mesons refer to the (unrealistic) case of no quark flavors (or all quark flavors very heavy), and that a considerable shift in mass of, e.g., $gb(0^{++})$ can be the result of the light quark flavors, unaccounted for in Ref. [13] and all comparable calculations.

In Ref. [16], the calculations focus on the question of low-mass scalar mesons, not gb-s. This issue is a prerequisite for the successful identification of $gb(0^{++})$,

lowest in mass and thus was examined as to the structure of the scalar $q\bar{q}$ nonet, lowest in mass, in Ref. [4], where this nonet was *assumed* to be identifiable.

In Ref. [16] the local, composite field called σ was investigated on the lattice

$$\sigma(x) = \frac{1}{\sqrt{2}} (\bar{u}_c(x) u_c(x) + \bar{d}_c(x) d_c(x)) . \quad (49)$$

where the suffix c denotes triplet color.

Irrespective of the pattern of the full nonet it is valid to consider the two point function of two σ fields, on the lattice, and to deduce the mass of the lowest scalar resonance, coupling to the σ field.

The authors of Ref. [16] declare their calculation preliminary, so it is not yet possible to evaluate the error of their mass determination. Nevertheless, they indicate the following result

$$\begin{aligned} [16] : m_\pi < m_\sigma < m_\rho \sim 776 \text{ MeV} \\ [4] : \sigma(q\bar{q}) \rightarrow f_0(980); m_{f_0} \sim 980 \text{ MeV}. \end{aligned} \quad (50)$$

We continue the discussion of the scalar $q\bar{q}$ nonet, beyond lattice calculations only, in the next subsection.

b) $\pi\pi$ – and related ps-ps scattering and scalars

In this context, let me start with quoting a recent paper devoted to $\pi\pi$ elastic scattering in the framework of chiral perturbation theory, and the Roy equation for full control of analyticity, unitarity and crossing relations [18].

In Ref. [18], in a dedicated chapter "Poles on the second sheet", *op. cit.*, the following pole parameters are quoted for the s wave $I = 0$, $\pi\pi$ partial wave amplitude

$$\begin{aligned} [18] : \sqrt{s} &= (430 \pm 30 - i(295 \pm 20)) \text{ MeV} \rightarrow \\ s &= (0.098 \pm 0.037 - i(0.254 \pm 0.032)) \text{ GeV}^2 \\ s_{\text{thr}} &= 4 m_\pi^2 = 0.078 \text{ GeV}^2. \end{aligned} \quad (51)$$

The result in Eq. (51) is indeed of highest interest.

Within the quoted errors, the resonance parameters are compatible with a *threshold* resonance, when considered in the complex s plane. For the properties of Jost functions in this and in general cases, I refer to Res Jost's original work [19].

The deeper question related to the existence (or nonexistence) of the threshold resonance, as derived in Ref. [18] is, whether there exists a symmetry, which would enforce the stability of the resonance position, in particular in the chiral limit, i.e. of

$$s_R = \Re s \sim s_{\text{thr}} \rightarrow 0. \quad (52)$$

The role of the threshold resonance is then apparently that of a dilaton zero mode, arising from spontaneous breaking of dilatation invariance. It is the trace anomaly, which prevents the dilatation symmetry to be broken *exclusively* spontaneously.

The relations with respect to the (Lorentz) invariant amplitude are

$$\begin{aligned}
T_0(s) &= \frac{1}{2} \int_{-1}^{+1} dz T(s, z) ; f_0(s) = \frac{1}{8\pi\sqrt{s}} T_0(s) \\
f_0(s) &= \frac{1}{q} t(q) ; t(q) = (S(q) - 1) / (2i) \\
t(q) &= \frac{1}{16\pi} \sqrt{1 - s_{\text{thr}}/s} T_0(s) \\
\sigma_{el}(s) &= 4\pi |f_0(s)|^2 \text{ for } s \text{ real } \geq s_{\text{thr}}.
\end{aligned} \tag{53}$$

In Eq. (53) q denotes the c.m. momentum.

Assuming indeed a threshold resonance with $s_R = \Re s|_R = s_{\text{thr}}$ and $\Im s_R = -\gamma_R$, the function $S(q)$ is of the form

$$S(q) = \frac{s_R + i\gamma_R - s}{s_R - i\gamma_R - s} S_1(q). \tag{54}$$

The most interesting situation arises if *first* we assume that S_1 tends to 1 at threshold

$$\begin{aligned}
S_1(q \rightarrow 0) &\rightarrow 1 \\
&\rightarrow f_0 \sim a \rightarrow i/q
\end{aligned} \tag{55}$$

The behaviour displayed in Eq. (55) is obviously at variance with the restrictions imposed by (approximate) chiral symmetry, but this is not the interesting part, due to a threshold resonance. Rather it is the intrinsic interdependence of the *remaining* contribution $S_1(q \sim 0)$ near threshold with the threshold phase of 90° of the threshold resonance, which is most striking. The latter must be moved either backward or forward by another 90° at threshold in order to achieve a finite scattering length. It is this interdependence, which is unlikely not to move the threshold resonance even very far from its initial threshold position.

A measure for the width of the deduced threshold resonance is the ratio

$$\gamma_R / s_R \sim 2.5 \leftrightarrow \Gamma = 590 \pm 40 \text{ MeV}, \tag{56}$$

as obtained in Ref. [18]. While we do not pursue the above discussion further here, it is necessary to retain that the value of the mass derived in Ref. [18], $m_R = 430 \pm 30 \text{ MeV}$, especially when the width is just ignored, leads to an increased uncertainty concerning the very possibility of recognizing the mass and mixing pattern of scalar mesons, in the sense of spectroscopy.

Alternative discussions of scalar resonances

Besides the new derivation of the $I = 0$ s-wave $\pi\pi$ scattering amplitude in Ref. [18], the phase shifts in this channel are by now fairly well established from threshold to a c.m. energy of $\sim 1400 \text{ MeV}$ [20], but only as far as resolution of phase ambiguities is concerned.

The $I = 0$ s-wave amplitude from the second reference in [20] is reproduced below. It becomes clear from the errors both in the phase shift (Fig. 4a) as well

as in the inelasticity (Fig. 4b) that the details are, despite a remarkable effort in analysis, rather uncertain in the range of c.m. energies $600 \text{ MeV} \leq \sqrt{s} \leq 1600 \text{ MeV}$.

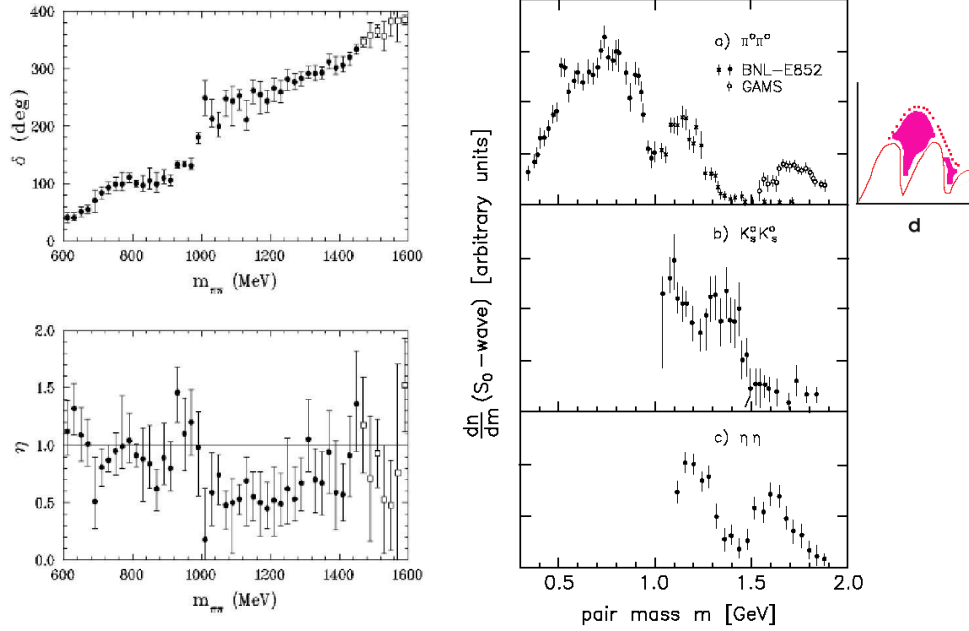


Fig. 4 (left). a) phase shifts δ and b) inelasticities η for “down-flat” solution (circles). Squares denote data from Ref. [21].

Fig. 5. a) $\pi^0 \pi^0$, b) $K_s K_s$, c) $\eta \eta$, d) red dragon in full.

The red dragon and “ σ ” in $\pi\pi$; $I = 0$ s wave

The discussion of the partial wave amplitude, corresponding to the projection on $I = 0$ and on the s wave, denoted $t(q)$ in Eq. (53)

$$t(q) = (S(q) - 1) / (2i), \quad (57)$$

has been the subject of many recent papers, to which we turn now. But we first show the result of combining elastic and quasi elastic pseudoscalar meson scattering, corresponding to the same quantum numbers, performed in Ref. [4]. For a detailed discussion I refer back to Ref. [4].

The absolute values $|t(q)|^2$ (with only relative normalization) for $\pi\pi \rightarrow \pi\pi$, $K\bar{K}$, $\eta\eta$ are shown in Fig. 5 together with the full shape of the red dragon, amputating the negative interference due to $f_0(980)$ and $f_0(1500)$.

Several comments are necessary here:

- i) “data”.

The compilation of Figs. 5a - c makes it appear as if actual data are displayed. This is by no means the case, rather between the real data from the reactions

$$\pi \mathcal{N} \rightarrow \begin{cases} \pi^0 \pi^0 \mathcal{N}(\Delta) \\ K_s K_s \mathcal{N}(\Delta) \\ \eta \eta \mathcal{N}(\Delta) \end{cases}$$

and the displayed absolute values there is a *series* of analysis steps. The latter make it difficult to assess the overall errors.

ii) the second interference minimum due to $f_0(1500)$.

The pattern showing two interfering narrow states: $f_0(980)$ and $f_0(1500)$ by today's notation, has been inferred from the peripheral $\pi \mathcal{N}$ reactions listed above. The latter resonance has clearly been observed in $p\bar{p}$ annihilation at rest by the Crystal Barrel collaboration at the Lear facility of CERN [22], adding a new element with high statistics and precision of analysis.

iii) the red dragon proper.

The unfolding of the interference due to $f_0(980)$ and $f_0(1500)$ reveals a broad structure, the red dragon proper, as sketched in Fig. 5d. The c.m. energy over which this structure is extended comprises the range $400 \text{ MeV} \leq \sqrt{s} \leq 1600 \text{ MeV}$. Within all Breit-Wigner like strong interaction resonances, there does not exist a comparably wide one. This establishes the singular feature of the $\pi\pi$ s wave scattering amplitude in this range, and also considerably below 400 MeV, i.e. down to the two pion threshold, as well as above 1600 MeV.

The combined experimental and theoretical evaluation of data, which led to the clear picture represented by the red dragon in Fig. 5 is *not* subject to the remaining large inherent errors of details of the respective scattering amplitudes. This contrasts with all attempts, [4], [18] and those discussed below, where further *interpretation* of details of the red dragon are undertaken.

$\sigma(\sim 500)$ and/or $\kappa(\sim 750)$ scalar mesons

The claims of the existence of an isospin singlet, nonstrange scalar state σ in a mass region clearly below $f_0(980)$ are numerous besides Ref. [18]. Another light scalar state, κ with isospin 1/2, well below $K_0^*(1430)$ has also received much attention. These claims have been recently repeated on various grounds. We cite two reviews compiled within the PDG [12]: on scalar mesons [23] and on non $q\bar{q}$ candidates [24].

A new window has opened up in the study of the decay of charmed [25, 26] and b -flavored mesons [27, 28].

What is emerging from c - and b -flavored meson decays is the clear fact, that in three pseudoscalar meson (π and K) decays, two out of the three pseudoscalars are produced amply in their relative s wave. This is quite in line with analogous decays from $p\bar{p}$ and hence the analysis in terms of two body amplitudes, the third

pseudoscalar being treated as ‘kinematical spectator, modulo constraints from Bose statistics’, was performed in all reactions in a similar way.

A few decays are listed below for definiteness

$$\begin{aligned}
 D^+ & \rightarrow \pi^- \pi^+ \pi^+ & ; & [25], [26] \\
 D_s^+ & \rightarrow \pi^- K^+ \pi^+ & ; & [27], [28] \\
 B^+ & \rightarrow K^- K^+ K^+ & ; & [27], [28] \\
 p\bar{p} & \rightarrow \pi^- \pi^+ \eta & ; & [29]
 \end{aligned}
 \tag{58}$$

The present results from the study of the above decays do favour the derived existence of a ‘ σ ’ isoscalar state, called $f_0(600)$ by the PDG [12] as well as indications of an isospin 1/2 state called ‘ κ ’, with masses ~ 500 MeV for σ and ~ 750 MeV for κ respectively. The determination of the widths is rather uncertain, but follows the widths of peaks in the projected Dalitz plot distributions of the order of 200–400 MeV.

It is fair to say that, as welcome as these new channels are, the present stage of analysis has not led to a clear picture of scalar meson states.

c) Central production experiments

The first experiment searching for gluonic mesons in central production was performed at the ISR at CERN [30], at $\sqrt{s} = 63$ GeV. I reproduce here the invariant mass distribution of $\pi^+ \pi^-$ pairs as observed in Ref. [30]. Even though Fig. 6 represents the (absolute) square of an amplitude and Fig. 5 the square of *another* amplitude, the similarity and shape of the red dragon is clearly visible. This similarity does not need any further analysis.

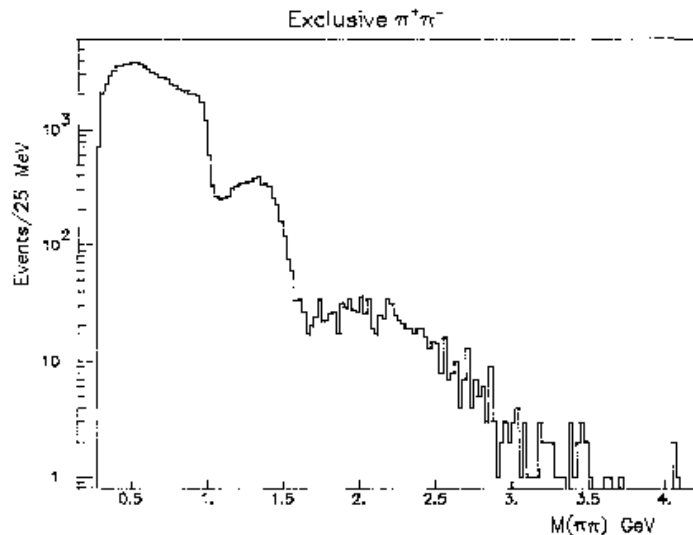


Fig. 6. Invariant mass distribution of π^\pm pairs in central $pp \rightarrow pp X_c$ production at $\sqrt{s} = 63$ GeV [30].

The more recent experiment WA102 and its predecessor WA76 are using a fixed target configuration and thus the c.m. energies studied are lower, $\sqrt{s} \leq 29$ GeV [31].

Despite dedicated studies [32], no clear understanding of central production *and* spectroscopic information encoded in ps-ps scattering amplitudes (section b) of this chapter) nor any convincing evidence for the mass region from lattice QCD calculations (section a) of this chapter) for the gluonic binary $gb(0^{++})$ is emerging. Rather a choice of apparent possibilities is offered, where in order not to offend any individuals, I follow the PDG [12]

$$f_0 : 600, 980, 1370, 1500, 1710 \dots \text{ MeV}. \quad (59)$$

The present *controversial* situation does - in my opinion - reflect human shortcomings more than intrinsic difficulty to understand the strong interaction dynamics underlying gluonic binaries as well as $q\bar{q}$ scalar mesons.

5. Conclusion

In view of the previous sentence and in summary of the present outline, I think that a dedicated experiment of central production, at the highest achievable c.m. energies as well as with an optimally adapted detector is scientifically worth while.

Appendix A.1 Spinor wave functions, spin states and transformation rules

We present the spin 1/2 chiral building blocks below, as they determine the general spin transformation rules defined in Eq. (13).

$$S_{\underline{\alpha}}^{\underline{\beta}}(a) = \{ S_{\alpha_1}^{\beta_1}(a) \times \dots \times S_{\alpha_N}^{\beta_N}(a) \}_{\text{symm}}. \quad (60)$$

The irreducible blocks $S_{\alpha_j}^{\beta_j}(a)$ in Eq. (60) correspond to spin 1/2

$$a = (a_0, a_1, a_2, a_3) = a_\mu : \begin{array}{l} \text{complex four-vector} \\ \text{not a Lorentz vector} \end{array}$$

$$S_{\alpha}^{\beta}(a) = S_1^1(a) = \left(a_0 \Sigma_0 + \frac{1}{i} \vec{a} \vec{\Sigma} \right)_{\alpha}^{\beta} \quad (61)$$

$$S_1^1(a) = \begin{pmatrix} a_0 - i a_3 & -a_2 - i a_1 \\ a_2 - i a_1 & a_0 + i a_3 \end{pmatrix}$$

$$a^2 = a_0^2 + \vec{a}^2 = \text{Det } S_1^1 = 1.$$

The quadratic constraint restricts S_1^1 as defined in Eq. 61 to be unimodular (i.e. to have $\text{Det} = 1$). Rotations (by half angles in bosonic terms) correspond to a_μ real. This is parametrizing the sphere (over the real numbers): $S_3 \equiv SU2$. Lorentz boosts (by hyperbolic half angles in bosonic terms) correspond to a_0 real, \vec{a} pure

imaginary. This is parametrizing the double hyperboloid (over the real numbers) :
 $(\Re a_0)^2 - (\Im \vec{a})^2 = 1$.

The matrices Σ_0, Σ_k ; $k = 1, 2, 3$ are the Pauli matrices, as arising in the right chiral representation of the full γ - matrix algebra.

$$\begin{aligned} (\sigma_{\mu\nu})_{\alpha}^{\beta} &\leftrightarrow P_R \frac{i}{2} [\gamma_{\mu}, \gamma_{\nu}] P_R \quad ; \quad P_R = \frac{1}{2} (1 + \gamma_5 R) \\ \gamma_5 R &= \frac{1}{i} \gamma_0 \gamma_1 \gamma_2 \gamma_3 \\ (\sigma_{\mu\nu})_{\alpha}^{\beta} &= \begin{pmatrix} -i \Sigma_k \\ \varepsilon_{mnr} \Sigma_r \end{pmatrix}_{\alpha}^{\beta} \quad \begin{array}{l} \text{for } \mu = 0, \nu = k = 1, 2, 3 \\ \text{for } \mu = m, \nu = n; \\ m, n, r = 1, 2, 3. \end{array} \end{aligned} \quad (62)$$

The right-chiral quantities $(\sigma_{\mu\nu})_{\alpha}^{\beta}$ in Eq. (62) satisfy the duality relation

$$(\sigma_{\mu\nu})_{\alpha}^{\beta} \rightarrow \sigma_{\mu\nu}^R \quad ; \quad \sigma_{\mu\nu}^R = -i \frac{1}{2} \varepsilon_{\mu\nu\varrho\tau} \sigma^{\varrho\tau R}. \quad (63)$$

Half angles (6), rotational and hyperbolic - a) to the right

An infinitesimal Lorentz transformation is covered by the spin 1/2 half angles $\omega^{\mu\nu}$, defined below, multiplying the (right chiral) base transformations $\sigma_{\mu\nu}^R$

$$\begin{aligned} \omega^{\mu\nu} &= \frac{1}{2} \Omega^{\mu\nu} \\ \omega^{\mu\nu} &= \begin{pmatrix} 0 & \varepsilon_1 & \varepsilon_2 & \varepsilon_3 \\ -\varepsilon_1 & 0 & \Theta_3 & -\Theta_2 \\ -\varepsilon_2 & -\Theta_3 & 0 & \Theta_1 \\ -\varepsilon_3 & \Theta_2 & -\Theta_1 & 0 \end{pmatrix} = \omega^{\mu\nu} (\vec{\Theta}, \vec{\varepsilon}). \end{aligned} \quad (64)$$

Projecting ω onto σ^R , we obtain

$$\begin{aligned} (\omega^R)_{\alpha}^{\beta} &\rightarrow \omega_{\alpha}^{\beta} \\ \omega_{\alpha}^{\beta} &= \frac{1}{2} \omega^{\mu\nu} (\sigma_{\mu\nu})_{\alpha}^{\beta} = i \left(\left\{ \vec{\Theta} - i \vec{\varepsilon} \right\} \frac{1}{i} \vec{\Sigma} \right)_{\alpha}^{\beta} \\ &\rightarrow \vec{\omega} \equiv \vec{\omega}^R = \vec{\Theta} - i \vec{\varepsilon}. \end{aligned} \quad (65)$$

S_1^1 in Eq. (61) then represents the exponential of $(\omega)_{\alpha}^{\beta}$ (multiplied with $\frac{1}{i}$)

$$S_{\alpha}^{\beta}(a) = \exp \left(\frac{1}{i} \omega \right)_{\alpha}^{\beta} = \exp \left(\frac{1}{i} \vec{\omega} \vec{\Sigma} \right)_{\alpha}^{\beta}. \quad (66)$$

Leaving out the (right chiral) spinor indices eq. (66) becomes

$$S(a) = \cos(\vec{\omega} \vec{\Sigma}) - i \sin(\vec{\omega} \vec{\Sigma}). \quad (67)$$

Thus we introduce the orthogonal complex invariant of $\vec{\omega}$

$$\begin{aligned} Z(\omega) &= z^2(\omega) = \vec{\omega}^2 = \left\{ \vec{\Theta}^2 - \vec{\varepsilon}^2 \right\} - i \left\{ 2 \vec{\Theta} \vec{\varepsilon} \right\} \\ &\rightarrow S(a) = \cos(z) \Sigma_0 - i [\sin(z)/z] \vec{\omega} \vec{\Sigma} \\ a &= a(\omega) \quad ; \quad a_0 = \cos(z) \quad ; \quad \vec{a} = [\sin(z)/z] \vec{\omega}. \end{aligned} \quad (68)$$

The square-root ambiguity of $z(\omega) = \pm \sqrt{Z(\omega)}$ does not affect the functional relation $a = a(\omega)$, as becomes clear from Eq. (68).

From right chiral to left chiral spinors

The right-chiral base representations of $SL2C_R$ are by construction not parity invariant, nor are the matrices $S(a) \equiv \mathcal{A}$ over the real numbers. So we shall transform the defining equations (60–62) to the left-chiral side

$$\begin{aligned} S_{\underline{\alpha}}^{\underline{\beta}}(a) &= \{ S_{\alpha_1}^{\beta_1}(a) \times \cdots \times S_{\alpha_N}^{\beta_N}(a) \}_{\text{symm}} \rightarrow \\ \rightarrow \tilde{S}_{\underline{\delta}}^{\underline{\gamma}}(b) &= \left\{ \tilde{S}_{\delta_1}^{\gamma_1}(b) \times \cdots \times \tilde{S}_{\delta_N}^{\gamma_N}(b) \right\}_{\text{symm}}, \end{aligned} \quad (69)$$

$$b = (b_0, b_1, b_2, b_3) = b_{\mu} : \quad \begin{array}{l} \text{complex four-vector} \\ \text{not a Lorentz vector} \end{array}$$

$$\begin{aligned} \tilde{S}_{\underline{\delta}}^{\underline{\gamma}}(b) &= \tilde{S}_2^2(b) = \left(b_0 \tilde{\Sigma}_0 + \frac{1}{i} \vec{b} \vec{\Sigma} \right)_{\underline{\delta}}^{\underline{\gamma}} \\ \tilde{S}_2^2(b) &= \begin{pmatrix} b_0 - i b_3 & -b_2 - i b_1 \\ b_2 - i b_1 & b_0 + i b_3 \end{pmatrix} \\ b^2 &= b_0^2 + \vec{b}^2 = \text{Det} \tilde{S}_2^2 = 1. \end{aligned} \quad (70)$$

The transformation from \mathcal{A} to \mathcal{B} corresponds to the substitution

$$\mathcal{A} \rightarrow (\mathcal{A}^\dagger)^{-1} = \mathcal{B}. \quad (71)$$

The substitution in Eq. (71) makes use of the four base representations of $SL2C$, best represented in the associated quadrangle

$$\begin{array}{ccc} \mathcal{A} & \longleftrightarrow & (\mathcal{A}^T)^{-1} \\ \uparrow \equiv c.c. & & \uparrow \equiv c.c. \\ \bar{\mathcal{A}} & \longleftrightarrow & (\mathcal{A}^\dagger)^{-1}. \end{array} \quad (72)$$

In the quadrangle in Eq. (72) the up-down operation means complex conjugation of each matrix element, forming the involutory chains

$$\begin{aligned} \mathcal{A} &\rightarrow \bar{\mathcal{A}} \rightarrow \mathcal{A} \\ &\text{and} \\ (\mathcal{A}^T)^{-1} &\rightarrow (\mathcal{A}^\dagger)^{-1} \rightarrow (\mathcal{A}^T)^{-1} \end{aligned}$$

whereas the left-right operation associates the symplectic dual, forming the equally involutory chains

$$\begin{aligned} \mathcal{A} &\rightarrow (\mathcal{A}^T)^{-1} \rightarrow \mathcal{A} \\ &\text{and} \\ \bar{\mathcal{A}} &\rightarrow (\mathcal{A}^\dagger)^{-1} \rightarrow \bar{\mathcal{A}}. \end{aligned}$$

Thus both up-down and left-right transformations along the quadrangle in Eq. (72) are commutative as well as involutory.

Yet the left-right transformation associates equivalent representations, contrary to the up-down one, which associates inequivalent representations, of which we have chosen the two residing in the upper-left and lower-right corners of the triangle in Eq. (72).

The symplectic equivalence is realized in the right-chiral basis by

$$(\mathcal{A}^T)^{-1} = s \mathcal{A} s^{-1} \quad ; \quad s = (\pm) i \sigma_2 = (\pm) \begin{pmatrix} 0 & 1 \\ -1 & 0 \end{pmatrix}, \quad (73)$$

The base Pauli matrices go into each other under the substitution in Eq. (71)

$$\begin{aligned} \Sigma_\mu &= \Sigma_\mu^\dagger = (\Sigma_\mu)^{-1} = (\Sigma_\mu^\dagger)^{-1} \\ &\rightarrow \left(\tilde{\Sigma}_0, \vec{\tilde{\Sigma}} \right) = \left(\Sigma_0, \vec{\Sigma} \right). \end{aligned} \quad (74)$$

Hence we have

$$\begin{aligned} \mathcal{A} &\rightarrow (\mathcal{A}^\dagger)^{-1} = \mathcal{B}(\mathcal{A}) \\ b &= \bar{a} \quad ; \quad \forall \text{ components.} \end{aligned} \quad (75)$$

Thus the quadrangle in Eq. (72) leads to the right- and left-chiral reality restricted form of $SL2C_R \times SL2C_L$

$$\begin{aligned} \{spin\} &\rightarrow s, \quad \#s = N + 1; \quad D_{s s'} = D_{s s'}^J(\Lambda, p) \\ R &: t_\alpha(\Lambda p; s) = S_\alpha^\beta(a) \quad t_\beta(p; s') \quad D_{s s'} \\ L &: \tilde{t}_\delta^\dagger(\Lambda p; s) = \tilde{S}_{\delta}^{\dot{\gamma}}(b) \quad \tilde{t}^{\dot{\delta}}(p; s') \quad D_{s s'}. \end{aligned} \quad (76)$$

While we proceed in steps, let me quote Res Jost [33], illustrating the L-R chiral aspects. The decomposition in Eq. (60) expands (doubles) into

$$\begin{aligned} R &: S_\alpha^\beta(a) = \left\{ S_{\alpha_1}^{\beta_1}(a) \times \cdots \times S_{\alpha_N}^{\beta_N}(a) \right\}_{\text{symm}} \\ L &: \tilde{S}_{\delta}^{\dot{\gamma}}(b) = \left\{ \tilde{S}_{\delta_1}^{\dot{\gamma}_1}(b) \times \cdots \times \tilde{S}_{\delta_N}^{\dot{\gamma}_N}(b) \right\}_{\text{symm}}, \end{aligned} \quad (77)$$

and then reduces to the R-L spin 1/2 building blocks

$$\begin{aligned} R &: S_\alpha^\beta(a) = S_1^1(a) \equiv \mathcal{A}(a) = \left(a_0 \Sigma_0 + \frac{1}{i} \vec{a} \vec{\Sigma} \right)_\alpha^\beta \\ L &: \tilde{S}_{\delta}^{\dot{\gamma}}(b) = \tilde{S}_2^2(b) \equiv \mathcal{B}(b) = \left(b_0 \tilde{\Sigma}_0 + \frac{1}{i} \vec{b} \vec{\tilde{\Sigma}} \right)_\delta^{\dot{\gamma}} \\ &\tilde{\Sigma}_\mu = \Sigma_\mu. \end{aligned} \quad (78)$$

The reality condition corresponds to a diagonal in the quadrangle in Eq. (72)

$$\begin{array}{ccc} \mathcal{A}(a) & \longleftrightarrow & \mathcal{B}(b) \\ \swarrow & & \searrow \\ \mathcal{A} & = & (\mathcal{B}^\dagger)^{-1} \\ \downarrow & & \downarrow \\ a & = & \bar{b} \end{array} \quad (79)$$

The so constrained pair

$$(\mathcal{A}(a), \mathcal{B}(\bar{a})) \equiv \text{spin}(1, 3; \mathfrak{R}) \simeq SL2C \quad (80)$$

defines the (self covered) group $\text{spin}(1, 3; \mathfrak{R})$: \mathfrak{R} indicates that the spin group is over the *real* numbers, whereas 1, 3 denote the signature of the derived metric, i.e. 1 time and 3 space (real) dimensions.

Half angles (6), rotational and hyperbolic - b) to the left

The left-chiral representation of $\text{spin}(1, 3; \mathfrak{R})$ complements the right-chiral one defined in Eq. (62)

$$\begin{aligned} (\sigma_{\mu\nu})_{\dot{\delta}}^{\dot{\gamma}} &\leftrightarrow P_L \frac{i}{2} [\gamma_{\mu}, \gamma_{\nu}] P_L; \quad P_L = \frac{1}{2}(1 - \gamma_5 R) \\ \gamma_5 R &= \frac{1}{i} \gamma_0 \gamma_1 \gamma_2 \gamma_3 \\ (\sigma_{\mu\nu})_{\dot{\delta}}^{\dot{\gamma}} &= \begin{pmatrix} i \Sigma_k & \\ & \varepsilon_{mnr} \Sigma_r \end{pmatrix}_{\dot{\delta}}^{\dot{\gamma}} \quad \begin{array}{l} \text{for } \mu = 0, \nu = k = 1, 2, 3 \\ \text{for } \mu = m, \nu = n; \\ m, n, r = 1, 2, 3. \end{array} \end{aligned} \quad (81)$$

In principle we should have distinguished the left-chiral matrices $\tilde{\Sigma}_{\mu}$ characterizing the left chiral SL2C basis in Eq. (81), but we have chosen (without loss of generality) to identify $\tilde{\Sigma}_{\mu} = \Sigma_{\mu}$ as specified in Eq. (78).

The left chiral variant of Eq. (63) becomes

$$\begin{aligned} (\sigma_{\mu\nu})_{\alpha}^{\beta} &\rightarrow \sigma_{\mu\nu}^R; \quad \sigma_{\mu\nu}^R = -i \frac{1}{2} \varepsilon_{\mu\nu\varrho\tau} \sigma^{\varrho\tau R} \\ &\rightarrow (\sigma_{\mu\nu})_{\dot{\delta}}^{\dot{\gamma}} \rightarrow \sigma_{\mu\nu}^L; \quad \sigma_{\mu\nu}^L = +i \frac{1}{2} \varepsilon_{\mu\nu\varrho\tau} \sigma^{\varrho\tau L}. \end{aligned} \quad (82)$$

Eq. (65) when reflected to the left takes on the form

$$\begin{aligned} (\omega^L)_{\dot{\delta}}^{\dot{\gamma}} &\rightarrow \tilde{\omega}_{\dot{\delta}}^{\dot{\gamma}} \\ \tilde{\omega}_{\dot{\delta}}^{\dot{\gamma}} &= \frac{1}{2} \omega^{\mu\nu} (\sigma_{\mu\nu})_{\dot{\delta}}^{\dot{\gamma}} = i \left(\left\{ \vec{\Theta} + i \vec{\varepsilon} \right\} \frac{1}{i} \vec{\Sigma} \right)_{\dot{\delta}}^{\dot{\gamma}} \\ &\rightarrow \vec{\tilde{\omega}} \equiv \vec{\omega}^L = \vec{\Theta} + i \vec{\varepsilon}; \quad \vec{\omega} \equiv \vec{\omega}^R = \vec{\Theta} - i \vec{\varepsilon}. \end{aligned} \quad (83)$$

\tilde{S}_2^2 in Eq. (78) is along with the right counterpart in Eq. (66)

$$\begin{aligned} S_{\alpha}^{\beta}(a) &= \exp \left(\frac{1}{i} \omega \right)_{\alpha}^{\beta} = \exp \left(\frac{1}{i} \vec{\omega} \vec{\Sigma} \right)_{\alpha}^{\beta} \\ &\rightarrow \tilde{S}_{\dot{\delta}}^{\dot{\gamma}}(b) = \exp \left(\frac{1}{i} \tilde{\omega} \right)_{\dot{\delta}}^{\dot{\gamma}} = \exp \left(\frac{1}{i} \vec{\tilde{\omega}} \vec{\Sigma} \right)_{\dot{\delta}}^{\dot{\gamma}}. \end{aligned} \quad (84)$$

Equation (67) extends to

$$\begin{aligned} S(a) &= \cos(\vec{\omega} \vec{\Sigma}) - i \sin(\vec{\omega} \vec{\Sigma}) \\ \rightarrow \tilde{S}(b) = S(b) &= \exp \left(\frac{1}{i} \tilde{\omega} \right) = \cos(\vec{\tilde{\omega}} \vec{\Sigma}) - i \sin(\vec{\tilde{\omega}} \vec{\Sigma}) \\ \vec{\tilde{\omega}} = \vec{\omega} &; \quad b = \bar{a} \\ S(a) &= a_0 \Sigma_0 + \frac{1}{i} \vec{a} \vec{\Sigma}; \quad S(b) = b_0 \Sigma_0 + \frac{1}{i} \vec{b} \vec{\Sigma}. \end{aligned} \quad (85)$$

Equation (68) completes to

$$\begin{aligned}
 Z(\omega) &= z^2(\omega) = \vec{\omega}^2 = \left\{ \vec{\Theta}^2 - \vec{\varepsilon}^2 \right\} - i \left\{ 2 \vec{\Theta} \vec{\varepsilon} \right\} \\
 \rightarrow S(a) &= \cos(z) \Sigma_0 - i [\sin(z)/z] \vec{\omega} \vec{\Sigma} \\
 a &= a(\omega) \ ; \ a_0 = \cos(z) \ ; \ \vec{a} = [\sin(z)/z] \vec{\omega} \\
 \rightarrow Z(\tilde{\omega}) &= z^2(\tilde{\omega}) = \vec{\tilde{\omega}}^2 = \left\{ \vec{\Theta}^2 - \vec{\varepsilon}^2 \right\} + i \left\{ 2 \vec{\Theta} \vec{\varepsilon} \right\} \\
 Z(\tilde{\omega}) &= z^2(\tilde{\omega}) = \overline{Z}(\omega) = \overline{z^2}(\omega) \\
 S(b) &= \cos(\bar{z}) \Sigma_0 - i [\sin(\bar{z})/\bar{z}] \vec{\omega} \vec{\Sigma} \\
 b &= a(\tilde{\omega}) = \overline{a(\omega)}.
 \end{aligned} \tag{86}$$

Realization of (half) angles through an antisymmetric pair of vectors

The complex three vectors defining the half angles $\omega^{\mu\nu}$ in Eq. (64)

$$\vec{\omega}^R = \vec{\Theta} - i \vec{\varepsilon} \ ; \ \vec{\omega}^L = \vec{\Theta} + i \vec{\varepsilon}. \tag{87}$$

can be realized as antisymmetric combinations of two real Lorentz vectors x^μ, y^ν .

This is however a restricted realization.

Here Lorentz vector does not distinguish between vector and axial vector. In fact we shall think of x as a genuine Lorentz four vector and of y as an axial vector.

$$\begin{aligned}
 \omega_{\mu\nu}([x, y]) &= \varepsilon_{\mu\nu\sigma\tau} x^\sigma y^\tau \\
 \omega_{0k} &= (\vec{x} \wedge \vec{y})^k \ ; \ \omega_{mn} = \varepsilon_{mnr} (x^0 y^r - x^r y^0) \\
 \vec{\varepsilon} &= -\vec{x} \wedge \vec{y} \ ; \ \vec{\Theta} = x^0 \vec{y} - y^0 \vec{x} \ : \ \vec{\Theta} \vec{\varepsilon} = 0 \\
 \rightarrow \vec{\omega}^R &= x^0 \vec{y} - y^0 \vec{x} + i (\vec{x} \wedge \vec{y}) \\
 \vec{\omega}^L &= x^0 \vec{y} - y^0 \vec{x} - i (\vec{x} \wedge \vec{y}).
 \end{aligned} \tag{88}$$

The invariants $Z(\omega), Z(\tilde{\omega})$ in Eqs. (68) and (86) are purely real

$$Z(\omega) = (\vec{\omega}^R)^2 = (xy)^2 - x^2 y^2 = (\vec{\omega}^L)^2 = Z(\tilde{\omega}). \tag{89}$$

In Eq. (89), we used the timelike Lorentz scalar product $x^2 = (x^0)^2 - \vec{x}^2$.

The realization given in Eqs. (88) and (89) is useful when x^μ is proportional to a four-velocity, i.e. $x^0 \geq \lambda > 0$, $x^2 = \lambda^2$ and y describes a spin direction, chosen in such a way that $xy = 0$, and $y^2 = -1$.

Appendix A.2

Note on the complex Lorentz group and associated operations

We recall the reality constrained covering of the Lorentz group $spin(1, 3; \mathfrak{R})$ defined in Eq. (80)

$$(\mathcal{A}(a), \mathcal{B}(\bar{a})) \equiv spin(1, 3; \mathfrak{R}) \simeq SL2C. \tag{90}$$

I list the operations on amplitudes or fields, which demand an extension of spin representations to *covering* of the complex Lorentz group. This latter extension is denoted by \xrightarrow{C} , defined in Eq. (91) below

$$\begin{aligned} spin(1, 3; \mathfrak{R}) &\xrightarrow{C} spin(1, 3; C) \simeq SL2C \times SL2C \\ (\mathcal{A}(a), \mathcal{B}(\bar{a})) &\xrightarrow{C} (\mathcal{A}(a), \mathcal{B}(b)) \quad ; \quad a, b \text{ unrestricted.} \end{aligned} \tag{91}$$

In the list below, we number and specify the operation in the first and second columns, the operand in the third, inducing the parallel operation \xrightarrow{C}

	operation	operand	\xrightarrow{C}
1	crossing	scattering amplitudes	\checkmark
2	extension to complex momenta	scattering amplitudes	\checkmark
3	extension to Euclidean space	local fields	\checkmark

(92)

Operations 1 - 3 in Eq. (92) are *not* independent of each other. A profound consequence is the symmetry under the antiunitary CPT transformation [33] for local field theories.

Appendix A.3 Field strengths, potentials and adjoint string operators

Potentials and field strengths have been introduced in Eqs. (14) and (15). We shall specify their local gauge transformation properties below. For simplicity, we shall only discuss the octet or adjoint representation of $SU3_c$.

The Lie algebra generators of the octet representation $(\mathcal{F}_D)_{AB} = if_{ADB}$ in Eq. (15) lead to the finite (local) transformations

$$\begin{aligned} \Omega_{AB}(x) &= \exp\left(\frac{1}{i}\omega_D(x)\mathcal{F}_D\right)_{AB} \\ [\mathcal{F}_A, \mathcal{F}_B] &= if_{ABC}\mathcal{F}_C. \end{aligned} \tag{93}$$

The $SU3_c$ angles $\omega_D(x)$ shall not be confused with the Euler half angles $\omega^{\mu\nu}$ in Eq. (67), while the group analogy is obvious. $\omega_D(x)$ shall be chosen varying over space time x , restricted by differentiability requirements.

Let $X(x, A)$ be a classical field transforming under the local octet transformations Ω

$$\begin{aligned} X^\Omega(x, A) &= \Omega_{AB}(x)X(x, B) \\ \text{in short : } X^\Omega(x) &= \Omega(x)X(x) \rightarrow X^\Omega = \Omega X. \end{aligned} \tag{94}$$

The extension of the local *adjoint* transformations in Eq. (94) to other representations of $SU3_c$ is straightforward. Ω are real, orthogonal 8×8 matrices with determinant 1.

Here we treat gauge potentials and field strengths as classical fields (test fields in the sence of distributions). The potentials $V_\mu(x, D)$ are defined through the

**Please,
check Eq. (93).**

(octet) covariant derivatives acting on X

$$\begin{aligned}
(D_\mu)_{AB} &= \partial_\mu \delta_{AB} + (\mathcal{W}_\mu)_{AB}; \quad \partial_\mu = \partial / \partial x^\mu \\
(\mathcal{W}_\mu)_{AB} &= iV_\mu(x, D) (\mathcal{F}_D)_{AB} = V_\mu(x, D) f_{DAB} \\
\text{in short : } \mathcal{W}_\mu &= iV_{\mu D} \mathcal{F}_D; \quad D_\mu = \partial_\mu + \mathcal{W}_\mu.
\end{aligned} \tag{95}$$

In Eq. (95), the quantities $V_\mu(x, D)$ and $(\mathcal{W}_\mu)_{AB}(x)$ are real.

Parallel transport

We turn to the parallel transport operators, defined in Eq. (15) repeated below

$$\begin{aligned}
U(x, A; y, B) &= P \exp \left(\int_y^x \Big|_{\mathcal{C}} dz^\mu \frac{1}{i} V_\mu(z, D) \mathcal{F}_D \right)_{AB} \\
&= P \exp \left(- \int_y^x \Big|_{\mathcal{C}} dz^\mu \mathcal{W}_\mu(z, D) \mathcal{F}_D \right)_{AB} \\
(\mathcal{F}_D)_{AB} &= i f_{ADB}; \quad \mathcal{W}_\mu(z, D) = iV_\mu(z, D) \\
\mathcal{W}_{\mu; AB}(z) &= \mathcal{W}_\mu(z, D) (\mathcal{F}_D)_{AB} \\
\text{in short : } U(x; y) &= P \exp \left(- \int_y^x \Big|_{\mathcal{C}} dz^\mu \mathcal{W}_\mu \right).
\end{aligned} \tag{96}$$

For classical field configurations, $U(x; y)|_{\mathcal{C}}$ is the operation of parallel transport of a tangent (octet) vector, e.g. $X(y) \{ \rightarrow X(y, B) \}$, at the point y along the curve \mathcal{C} to x .

$$\begin{aligned}
X(y, B) &\xrightarrow{\mathcal{C}} X_{\parallel}(x, A) = U(x, A; y, B) X(y, B) \\
X(y) &\xrightarrow{\mathcal{C}} X_{\parallel}(x) = U(x; y) X(y) \\
y &\xrightarrow{\mathcal{C}} x \\
U(x; y) &= U(x; y)|_{\mathcal{C}}.
\end{aligned} \tag{97}$$

If $X(x)$ is itself an octet field defined at all x , then $X_{\parallel}(x)|_{x \xrightarrow{\mathcal{C}} y}$ has to be distinguished from the given value $X(x)$.

$U(x; y)|_{\mathcal{C}}$ defined in Eqs. (96) and (97) follows from the parallel transport differential equation, using a parameter representation of the curve \mathcal{C}

$$\begin{aligned}
\mathcal{C} : \left\{ 1 \geq \tau \geq 0 \left| \begin{array}{l} z = z(\tau) \\ z(0) = y \\ z(1) = x \end{array} \right. \right\} \\
v(\tau) = \dot{z}(\tau) = (d/d\tau) z(\tau).
\end{aligned} \tag{98}$$

Let us follow the τ development of the family of parallel transports from y along \mathcal{C} to the point $z(\tau)$, as the latter moves from y to x

$$\begin{aligned}
U(\tau) &= U(z(\tau); y)|_{\mathcal{C}} \\
\mathcal{W}_\mu(\tau) &= \mathcal{W}_\mu(z(\tau)) \rightarrow \\
(d/d\tau)U(\tau) &= -v^\mu(\tau)\mathcal{W}_\mu(\tau)U(\tau) \\
U(0) &= \mathbb{1} \leftrightarrow U(y, A; y, B) = \delta_{AB}.
\end{aligned} \tag{99}$$

The parallel transport equation (99) is subjected to the initial conditions defined in its last line. It can be integrated by successive iterations

$$\begin{aligned}
U(\tau) &= \sum_{n=0}^{\infty} \int_0^\tau d\tau_1 \int_0^{\tau_1} d\tau_2 \cdots \int_0^{\tau_{n-1}} d\tau_n \\
&\quad \times w(\tau_1)w(\tau_2)\cdots w(\tau_n) \\
w(\tau) &= w_{AB}(\tau) = -v^\mu(\tau)\mathcal{W}_{\mu;AB}(z(\tau)) \\
\tau \geq \tau_1 \geq \tau_2 \cdots ; \quad U(1) &= U(x; y)|_{\mathcal{C}} \\
&\rightarrow U(xA; yB)|_{\mathcal{C}} = \\
&= P \exp \left(- \int_y^x \Big|_{\mathcal{C}} dz^\mu \mathcal{W}_\mu(z, D) \mathcal{F}_D \right)_{AB},
\end{aligned} \tag{100}$$

The path ordering in Eq. (96) reflects the path ordered sequence $\tau \geq \tau_1 \geq \tau_2 \cdots$ in the multiple integrals in Eq. (100), thus established.

Parallel transport and gauge transformations

We go back to Eqs. (94) and (95), implying the action of a local gauge transformation on the connection $\mathcal{W}_\mu(x, D)\mathcal{F}_D$

$$\begin{aligned}
D_\mu &= \partial_\mu + \mathcal{W}_\mu ; \quad D_\mu^\Omega = \partial_\mu + \mathcal{W}_\mu^\Omega \\
X^\Omega(x) &= \Omega(x)X(x) \rightarrow D_\mu^\Omega X^\Omega = \Omega D_\mu X.
\end{aligned} \tag{101}$$

The local gauge transformation Ω thus induces the transformation law for the connection

$$\mathcal{W}_\mu^\Omega = \Omega \partial_\mu \Omega^{-1} + \Omega \mathcal{W}_\mu \Omega^{-1}. \tag{102}$$

The parallel transport of tangent vectors $X^\Omega(y)$ along the curve \mathcal{C} with connection \mathcal{W}_μ^Ω should be equivalent to the same operation on tangent vectors $X(y)$ with \mathcal{W} modulo the transformation induced on the tangent vectors. Using the relations in Eq. (97), this implies

$$\begin{aligned}
X^\Omega(x) &= \Omega(x)X(x) \leftrightarrow X^\Omega(y) = \Omega(y)X(y) \rightarrow \\
X^\Omega(y) &\xrightarrow{\mathcal{C}} X_{\parallel}^\Omega(x) = U^\Omega(x; y)X^\Omega(y) \\
X(y) &\xrightarrow{\mathcal{C}} X_{\parallel}(x) = U(x; y)X(y) \\
y &\xrightarrow{\mathcal{C}} x.
\end{aligned} \tag{103}$$

Thus we expect the relations

$$\begin{aligned} X_{\parallel}^{\Omega}(x) &= \Omega(x) X_{\parallel}(x) \leftrightarrow X^{\Omega}(y) = \Omega(y) X(y) \rightarrow \\ \Omega(x) U(x; y) X(y) &= U^{\Omega}(x; y) \Omega(y) X(y) \forall X(y) \rightarrow \\ U^{\Omega}(x; y) &= \Omega(x) U(x; y) \Omega^{-1}(y). \end{aligned} \quad (104)$$

We want to verify the relation inferred in Eq. (104). To this end we form the two, a priori different, matrix valued functions of τ along \mathcal{C}

$$\begin{aligned} U_1(\tau) &= U^{\Omega}(\tau) \leftrightarrow U_2(\tau) = \Omega(z_{\tau}) U(\tau) \Omega^{-1}(y) \\ z_{\tau} &= z(\tau). \end{aligned} \quad (105)$$

From Eq. (99) we infer

$$\begin{aligned} \partial_{\tau} U_1(\tau) &= -v^{\mu}(\tau) \mathcal{W}_{\mu}^{\Omega}(\tau) U_1(\tau) \\ \partial_{\tau} U_2(\tau) &= \left[\begin{array}{l} (\partial_{\tau} \Omega(z_{\tau})) \Omega^{-1}(z_{\tau}) - \\ -v^{\mu}(\tau) \Omega(z_{\tau}) \mathcal{W}_{\mu}(\tau) \Omega^{-1}(z_{\tau}) \end{array} \right] U_2(\tau). \end{aligned} \quad (106)$$

The expression in the first line of the bracket in Eq. (106) transforms into

$$(\partial_{\tau} \Omega(z_{\tau})) \Omega^{-1}(z_{\tau}) = -v^{\mu}(\tau) \Omega(z_{\tau}) \partial_{z^{\mu}} \Omega^{-1}(z_{\tau}). \quad (107)$$

Thus the differential equation for $U_2(\tau)$ in Eq. (106) takes the form

$$\begin{aligned} \partial_{\tau} U_2(\tau) &= -v^{\mu}(\tau) \left[\begin{array}{l} \Omega(z_{\tau}) \partial_{z^{\mu}} \Omega^{-1}(z_{\tau}) \\ + \Omega(z_{\tau}) \mathcal{W}_{\mu}(\tau) \Omega^{-1}(z_{\tau}) \end{array} \right] U_2(\tau) \\ &= -v^{\mu}(\tau) \left[\begin{array}{l} \mathcal{W}_{\mu}^{\Omega}(\tau) \end{array} \right] U_2(\tau) \end{aligned} \quad (108)$$

$$\mathcal{W}_{\mu}^{\Omega}(z) = \Omega(z) \partial_{z^{\mu}} \Omega^{-1}(z) + \Omega(z) \mathcal{W}_{\mu}(z) \Omega^{-1}(z).$$

Comparing Eqs. (106) and (108), we see that U_1 and U_2 fulfill the same differential equation, as a consequence of the gauge transformation law of the connection \mathcal{W} . They also have the same initial value

$$\begin{aligned} U_1(0) &= U_2(0) = \mathbb{1} \rightarrow U_1(\tau) = U_2(\tau) \\ \rightarrow U^{\Omega}(x; y) &= \Omega(x) U(x; y) \Omega^{-1}(y) \quad \text{qed.} \end{aligned} \quad (109)$$

On the nonabelian Stokes relation

For our purpose here, to describe the degrees of freedom of *binary* gluonic mesons, the set of parallel transport matrices (matrix valued bilocal field operators) as displayed in Eq. (100)

$$\begin{aligned} U(xA; yB)|_{\mathcal{C}} &= (U(x; y)|_{\mathcal{C}})_{AB} \\ &= P \exp \left(- \int_y^x \Big|_{\mathcal{C}} dz^{\mu} \mathcal{W}_{\mu}(z, D) \mathcal{F}_D \right)_{AB} \\ U^{\Omega}(x; y) &= \Omega(x) U(x; y) \Omega^{-1}(y), \end{aligned} \quad (110)$$

along *straight line* paths \mathcal{C} restricting general ones, as defined in Eq. (98), are sufficient.

$$\begin{aligned} \overleftarrow{\mathcal{C}} : \left\{ 1 \geq \tau \geq 0 \left| \begin{array}{l} z = z(\tau) = y + \tau(x - y) \\ z(1) = x \longleftarrow z(0) = y \end{array} \right. \right\} \\ v(\tau) = \dot{z}(\tau) = z = x - y. \end{aligned} \quad (111)$$

Parallel transport being generated by the connection 1-form

$$\begin{aligned} \left(\mathcal{W}^{(1)} \equiv dz^\mu \mathcal{W}_\mu(z, D) \mathcal{F}_D \right)_{AB} \rightarrow \\ U(x; y) = P \exp \left(- \int_y^x \Big|_{\mathcal{C}} \mathcal{W}^{(1)} \right); \quad P \equiv P^{(1)}. \end{aligned} \quad (112)$$

the matrix valued 1-forms naturally acquire the line ordering, appropriate for one dimensional integrals.

Yet connection 1-forms and their path $P^{(1)}$ ordered integrals do not exhaust the range of r -forms and their r -dimensional $P^{(r)}$ ordered integrals, associated with nonabelian degrees of freedom.

Next in line are the curvature 2-form and its *surface* $P^{(2)}$ ordered integral. We follow the covariant derivative path with the octet field $X(x)$ introduced in Eqs. (93)–(95)

$$\begin{aligned} D_\mu X(x) &= (\partial_\mu + \mathcal{W}_\mu) X(x) \\ (D_\mu D_\nu - D_\nu D_\mu) X(x) &= \mathcal{W}_{[\mu\nu]} X(x). \end{aligned} \quad (113)$$

In Eq. (113), $\mathcal{W}_{[\mu\nu]}$ denotes the (antisymmetric Yang-Mills) curvature tensor, i.e. the field strengths

$$\begin{aligned} \mathcal{W}_{[\mu\nu]} &= \partial_\mu \mathcal{W}_\nu - \partial_\nu \mathcal{W}_\mu + [\mathcal{W}_\mu, \mathcal{W}_\nu] \\ \mathcal{W}_{[\mu\nu]}(x) &= \mathcal{W}_{[\mu\nu]}(x, D) \mathcal{F}_D = \\ &= \left[\begin{array}{l} (\partial_\mu \mathcal{W}_\nu(x, D) - \partial_\nu \mathcal{W}_\mu(x, D)) \mathcal{F}_D \\ + \mathcal{W}_\mu(x, A) \mathcal{W}_\nu(x, B) [\mathcal{F}_A, \mathcal{F}_B] \end{array} \right] \\ \mathcal{W}_\mu(z, D) &= iV_\mu(z, D) \quad ; \quad [\mathcal{F}_A, \mathcal{F}_B] = if_{ABC} \mathcal{F}_C. \end{aligned} \quad (114)$$

In Eq. (114), we have included the relations in Eqs. (93) and (96).

The form of the curvature tensor $\mathcal{W}_{[\mu\nu]}$ in Eq. (114) becomes

$$\begin{aligned} \mathcal{W}_{[\mu\nu]}(x, D) &= \frac{1}{i} F_{[\mu\nu]}(x, D) = \\ &= \left[\begin{array}{l} \partial_\mu \mathcal{W}_\nu(x, D) - \partial_\nu \mathcal{W}_\mu(x, D) \\ + i \mathcal{W}_\mu(x, A) \mathcal{W}_\nu(x, B) f_{ABD} \end{array} \right] \\ F_{[\mu\nu]}(x, D) &= \\ &= \left[\begin{array}{l} \partial_\nu V_\mu(x, D) - \partial_\mu V_\nu(x, D) \\ - V_\nu(x, A) V_\mu(x, B) f_{ABD} \end{array} \right]. \end{aligned} \quad (115)$$

We recast the quantities $\mathcal{W}_{[\mu\nu]}$ in Eqs. (114) and (115) into their Lie algebra valued form

$$\begin{aligned}\mathcal{W}_{[\mu\nu][AB]}(x) &= (\mathcal{W}_{[\mu\nu]}(x, D)\mathcal{F}_D)_{AB} \\ &= (F_{[\mu\nu]}(x, D)L_D)_{AB} \\ (L_D)_{AB} &= \frac{1}{i}(\mathcal{F}_D)_{AB} = f_{ADB} \quad ; \quad [L_R, L_S] = f_{RST}L_T.\end{aligned}\tag{116}$$

We also cast Eq. (112) into the L_D form

$$\begin{aligned}(\mathcal{W}^{(1)} \equiv dz^\mu \mathcal{W}_\mu(z, D)\mathcal{F}_D)_{AB} &\rightarrow \\ \mathcal{W}_\mu(z, D)\mathcal{F}_D = i\mathcal{W}_\mu(z, D)L_D = -V_\mu(z, D)L_D &\rightarrow \\ \mathcal{W}_{\mu[AB]}(x) = -V_\mu(x, D)(L_D)_{AB}.\end{aligned}\tag{117}$$

Comparing the connection and curvature representations in Eqs. (116) and (117), we learn that the local quantities $\mathcal{W}_{\mu[AB]}(x)$ and $\mathcal{W}_{[\mu\nu][AB]}(x)$, as well as the components $-V_\mu(x, D)$ and $F_{[\mu\nu]}(x, D)$ are real. This is usual in the mathematical literature.

Local gauge transformations as defined for the connection in Eqs. (102) and (108) are naturally extended to the curvature

$$\begin{aligned}\left\{ \begin{array}{l} \mathcal{W}_{\mu[AB]} \\ \mathcal{W}_{[\mu\nu][AB]} \end{array} \right\}(x) &\rightarrow \left\{ \begin{array}{l} \mathcal{W}_\mu \\ \mathcal{W}_{[\mu\nu]} \end{array} \right\}(x) \\ \mathcal{W}_\mu^\Omega(x) = \Omega(x)\partial_\mu\Omega^{-1}(x) + \Omega(x)\mathcal{W}_\mu(x)\Omega^{-1}(x) & \\ \mathcal{W}_{[\mu\nu]}^\Omega(x) = \Omega(x)\mathcal{W}_{[\mu\nu]}(x)\Omega^{-1}(x).\end{aligned}\tag{118}$$

Lie cohomology and de Rham cohomology

With connection and curvature we associate the Lie algebra valued one and two forms, as defined in eqs. (112) - (117)

$$\begin{aligned}\left(\begin{array}{l} \mathcal{W}^{(1)} \equiv dx^\mu \mathcal{W}_\mu \\ \mathcal{W}^{(2)} \equiv \frac{1}{2}dx^\mu \wedge dx^\nu \mathcal{W}_{[\mu\nu]} \end{array} \right)(x, [AB]) & \\ \mathcal{W}^{(2)} = d\mathcal{W}^{(1)} + \mathcal{W}^{(1)} \circ \mathcal{W}^{(1)} \equiv D\mathcal{W}^{(1)}.\end{aligned}\tag{119}$$

In Eq. (119), the symbol \circ denotes normal matrix multiplication **to be distinguished** from the Lie product denoted below by \odot .

It is the antisymmetric nature of the wedge product $dx^\mu \wedge dx^\nu$ which renders the \circ product equivalent to a Lie algebra product \odot

$$\mathcal{W}^{(1)} \circ \mathcal{W}^{(1)} = \frac{1}{2}\mathcal{W}^{(1)} \odot \mathcal{W}^{(1)}.\tag{120}$$

We shall verify Eq. (120) by components

$$\begin{aligned}\mathcal{W}^{(1)} \circ \mathcal{W}^{(1)}(x, [AB]) &= dx^\mu \wedge dx^\nu \mathcal{W}_{\mu[AA']}\mathcal{W}_{\nu[A'B]} \rightarrow \\ &= \frac{1}{2}dx^\mu \wedge dx^\nu \left[\begin{array}{l} \mathcal{W}_{\mu[AA']}\mathcal{W}_{\nu[A'B]} - \\ -\mathcal{W}_{\nu[AA']}\mathcal{W}_{\mu[A'B]} \end{array} \right] \\ &= \frac{1}{2}dx^\mu \wedge dx^\nu \left[\mathcal{W}_\mu \odot \mathcal{W}_\nu \right]_{[AB]}\end{aligned}\tag{121}$$

$$\mathcal{W}_\mu \odot \mathcal{W}_\nu = [\mathcal{W}_\mu, \mathcal{W}_\nu] \equiv \mathcal{W}_\mu \circ \mathcal{W}_\nu - \mathcal{W}_\nu \circ \mathcal{W}_\mu.$$

Eq. (119) yields the first relation in the *adaptive* Lie cohomology chain, generated by the sequence of operations $D \rightarrow D' \neq D$

$$\begin{aligned} \mathcal{W}^{(2)} = D \mathcal{W}^{(1)} \quad \rightarrow \quad \mathcal{W}^{(3)} = D' \mathcal{W}^{(2)} = 0 \\ \hline D \quad : \quad \mathcal{W}^{(2)} = d\mathcal{W}^{(1)} + \frac{1}{2} \mathcal{W}^{(1)} \odot \mathcal{W}^{(1)} \\ D' \quad : \quad \mathcal{W}^{(3)} = d\mathcal{W}^{(2)} + \mathcal{W}^{(1)} \odot \mathcal{W}^{(2)} = 0. \end{aligned} \quad (122)$$

The termination of the *adaptive* $D \rightarrow D'$ sequence follows from the antisymmetry of the wedge product *and* the Jacobi identity of cyclic double commutators

$$\begin{aligned} \mathcal{W}^{(3)} = \left\{ \begin{aligned} & d \left((\mathcal{W}^{(1)} \circ)^2 \right) + \mathcal{W}^{(1)} \odot d\mathcal{W}^{(1)} \\ & + \mathcal{W}^{(1)} \odot (\mathcal{W}^{(1)} \circ)^2 \end{aligned} \right\} \\ (\mathcal{W}^{(1)} \circ)^n = \mathcal{W}^{(1)} \circ (\mathcal{W}^{(1)} \circ)^{n-1}, \dots \end{aligned} \quad (123)$$

Expressing the \odot product in Eq. (123) in \circ products, it follows

$$\mathcal{W}^{(3)} = \left\{ \begin{aligned} & d \left((\mathcal{W}^{(1)} \circ)^2 \right) \\ & + \mathcal{W}^{(1)} \circ (d\mathcal{W}^{(1)}) - (d\mathcal{W}^{(1)}) \circ \mathcal{W}^{(1)} \\ & + \mathcal{W}^{(1)} \circ \left((\mathcal{W}^{(1)} \circ)^2 \right) - \left((\mathcal{W}^{(1)} \circ)^2 \right) \circ \mathcal{W}^{(1)} \end{aligned} \right\}. \quad (124)$$

The contribution cubic in $\mathcal{W}^{(1)}$ vanishes on the ground of the associative product \circ , while the first three cancel due to the identity

$$d \left((\mathcal{W}^{(1)} \circ)^2 \right) = (d\mathcal{W}^{(1)}) \circ \mathcal{W}^{(1)} - \mathcal{W}^{(1)} \circ (d\mathcal{W}^{(1)}). \quad (125)$$

Loops of parallel transports, local holonomy groups

In the inverse of the differential Lie cohomology chain the parallel transport matrices

$$U(x, y; \xrightarrow{\mathcal{C}}) = P \exp \left(- \int_y^x \Big|_{\mathcal{C}} dz^\mu \mathcal{W}_\mu \right), \quad (126)$$

defined in Eqs. (96)–(97) can be combined to form a closed curve starting and ending at y ,

$$U(y, y; \mathcal{CL}) \curvearrowright_{AB} \rightarrow U(y, y; \mathcal{CL}). \quad (127)$$

The quantities $U(x, y; \xrightarrow{\mathcal{C}})$, called adjoint strings here, are rarely used in lattice discretized Yang-Mills theory. The associated fundamental strings, projected on the fundamental representation of the local gauge group (the triplet strings for $SU3_c$), are the dynamical *link* variables therein [34]. The quantities $U(y, y; \mathcal{CL})$, defined in Eq. (127) we shall call closed adjoint (octet) strings. Their counterparts, projected on the fundamental (triplet) representation, assigned to a minimal closed lattice loop, a plaquette, are used to generate the lattice action.

Closed loop matrices or operators are widely studied in their own right. For the fundamental representation they are called Wilson loops ($W(\mathcal{C})$) within Yang-Mills theories [35].

We continue to focus on open and closed adjoint strings here. Nevertheless, it is tacitly assumed that the configurations obey the regularity requirements of extensions of these strings to *all* representations of the gauge group. This framework is called the universal bundle in the mathematical literature.

The gauge transformation properties of open and closed (adjoint) strings in Eqs. (126) and (127) follow from Eqs. (108) and (109)

$$\begin{aligned} U^\Omega(x, y; \overset{\mathcal{C}}{\rightarrow}) &= \Omega(x) U(x, y; \overset{\mathcal{C}}{\rightarrow}) \Omega^{-1}(y) \rightarrow \\ U^\Omega(y, y; \mathcal{C}\mathcal{L}) &= \Omega(y) U(y, y; \mathcal{C}\mathcal{L}) \Omega^{-1}(y). \end{aligned} \quad (128)$$

The closed curve $\mathcal{C}\mathcal{L}$ is still punctuated at its beginning and ending. Yet the gauge transformation acts *locally* at this point. However, the simply connected closed loop can be repeatedly transcurred, leading to the multiple positive as well as negative powers, all transforming the same way under gauge transformations

$$\begin{aligned} U^n(y, y; \mathcal{C}\mathcal{L}) &= U(y, y; \mathcal{C}\mathcal{L}^{(n)}) \quad , \quad n = 0, \pm 1, \dots \\ U^\Omega(y, y; \mathcal{C}\mathcal{L}^{(n)}) &= \Omega(y) U(y, y; \mathcal{C}\mathcal{L}^{(n)}) \Omega^{-1}(y). \end{aligned} \quad (129)$$

The closed curve $\mathcal{C}\mathcal{L}^{(n)}$ shall represent the n -fold transcurred simple curve $\mathcal{C}\mathcal{L}$, whereby negative powers mean to reverse the orientation, say from clockwise to anticlockwise. Gauge invariant quantities are thus all (adjoint) traces

$$W_{(n)}(\mathcal{C}\mathcal{L}) = \text{tr}[U^n(y, y; \mathcal{C}\mathcal{L})] = \sum_{\{\lambda\}} \lambda^n (U(y, y; \mathcal{C}\mathcal{L})). \quad (130)$$

In Eq. (130), λ runs over all eigenvalues of the (real orthogonal) matrix $U(y, y; \mathcal{C}\mathcal{L})$. The quantities $W_{(n)}(\mathcal{C}\mathcal{L})$ in Eq. (130) do depend on the shape of the simply laced curve $\mathcal{C}\mathcal{L}$, but they are the same for all points along $\mathcal{C}\mathcal{L}$, when adopted as alternative starting and ending points. They represent the adjoint characters of the (self covering) Lie group, dependent only on the angles of the Cartan subalgebra. Thus they depend, for a simple gauge group with rank r ($r = 2$ for $SU3_c$) on the r Cartan subalgebra angles, characterising any of the representatives $U(y', y'; \mathcal{C}\mathcal{L})$ with y' anywhere on the curve $\mathcal{C}\mathcal{L}$. The characteristic coefficients are determined from the roots of the Lie algebra and, through its universal extension to all representations, from its r fundamental weights. For $SU3_c$, these are the weights of the 3 and $\bar{3}$ fundamental representations.

For $SU3_c$ let the two Cartan algebra angles be $\phi \leftrightarrow I_3$ and $\psi \leftrightarrow Y/(2\sqrt{3})$, using standard weight normalization, where I_3 and Y denote isospin and hypercharge respectively.

The 3 and $\bar{3}$ Cartan matrices shall be u and \bar{u} respectively, $u = u(\phi, \psi)$. The two fundamental characters thus become

$$\begin{aligned} \chi &= \chi(u) \rightarrow \chi(\phi, \psi) \quad \text{and} \quad \bar{\chi} \\ \chi &= \sum_{k=1}^3 \exp\left(\frac{1}{i} \kappa_k\right) \quad ; \quad \kappa_3 = -\kappa_1 - \kappa_2 \\ \kappa_1 &= \frac{1}{2} \phi + \frac{1}{2\sqrt{3}} \psi \quad , \quad \kappa_2 = -\frac{1}{2} \phi + \frac{1}{2\sqrt{3}} \psi. \end{aligned} \quad (131)$$

Then for a reducible direct product representation $D_{\text{red}; M, N}$ of M copies of u and N copies of \bar{u} , the character is multiplicative

$$\chi_{\text{red}; M, N} = \chi^M \bar{\chi}^N = \bar{\chi}_{\text{red}; N, M}. \quad (132)$$

From $D_{\text{red}; M, N}$, the characters of all irreducible representations of the gauge group can be derived. We only give the lowest characters for the $3, \bar{3}, 6, \bar{6}, 10, \bar{10}$ and adjoint (8) representations of $SU3_c \rightarrow SU3_.$, with the association

$$\begin{aligned}
3 &= D_{\text{ird}; 1, 0} & cc & \bar{3} &= D_{\text{ird}; 0, 1} \\
6 &= D_{\text{ird}; 2, 0} & cc & \bar{6} &= D_{\text{ird}; 0, 2} \\
10 &= D_{\text{ird}; 3, 0} & cc & \bar{10} &= D_{\text{ird}; 0, 3} \\
8 &= D_{\text{ird}; 1, 1} & \text{real} & & \\
\chi_{1,0}^{\text{ird}} &= \chi & cc & \chi_{0,1}^{\text{ird}} &= \bar{\chi} \\
\chi_{2,0}^{\text{ird}} &= \chi^2 - \bar{\chi} & cc & \chi_{0,2}^{\text{ird}} &= \bar{\chi}^2 - \chi \\
\chi_{3,0}^{\text{ird}} &= \begin{pmatrix} \chi^3 - 2|\chi|^2 \\ +1 \end{pmatrix} & cc & \chi_{0,3}^{\text{ird}} &= \begin{pmatrix} \bar{\chi}^3 - 2|\chi|^2 \\ +1 \end{pmatrix} \\
\chi_{1,1}^{\text{ird}} &= |\chi|^2 - 1 & \text{real} & & \\
(\chi, \bar{\chi}) &= (\chi, \bar{\chi}) (\phi, \psi).
\end{aligned} \tag{133}$$

In our case, the quantities $U(y, y; \mathcal{CL})$ in Eq. (127) are in the adjoint representation, i.e. in $D_{\text{ird}; 1, 1}$. Hence all equivalent representatives $U^n(y', y'; \mathcal{CL})$ with y' anywhere on \mathcal{CL} are characterized by the two Cartan subalgebra angles

$$U^n(y', y'; \mathcal{CL}) \rightarrow (n\phi, n\psi) \{ \mathcal{CL} \}. \tag{134}$$

The invariant quantities $W_{(n)}(\mathcal{CL})$ in Eq. (130) are thus given by

$$\begin{aligned}
W_{(n)}(\mathcal{CL}) &= |\chi_n \{ \mathcal{CL} \}|^2 - 1 \\
\chi_n \{ \mathcal{CL} \} &= \chi(n\phi, n\psi) \{ \mathcal{CL} \} \\
n &= 0, \pm 1 \dots ; \quad W_{(0)}(\mathcal{CL}) = 8.
\end{aligned} \tag{135}$$

Because the fundamental $SU3_.$ matrices u (and \bar{u}) are three dimensional, with determinant 1, only two out of the infinite n sequence of *fundamental* characters $\chi_n \{ \mathcal{CL} \}$: ($n = 1, 2 \bmod 3$) are independent of each other. The fundamental characters of any element u of the 3 representation of $SU3_.$ obey the *elementary* generating identity, expressing in terms of fundamental characters the fundamental polynomial $P_3(\mu; u) = \text{Det}(\mathbf{1} - \mu u)$,

$$\begin{aligned}
P_3(\mu; u) &= \text{Det}(\mathbf{1} - \mu u) = 1 - p_1 \mu + p_2 \mu^2 - \mu^3 \\
E(\mu; u) &= \exp\left(-\sum_{n=1}^{\infty} \mu^n \chi_n / n\right) \\
E(\mu; u) - P_3(\mu; u) &= 0 \quad \forall \mu
\end{aligned}$$

$$\begin{aligned}
p_k &= p_k(u); \quad k = 1, 2 \quad \leftrightarrow \quad \chi_n = \text{tr} u^n = \chi_n(u) \\
\Pi_k &= p_k(u = \mathbf{1}) \\
p_1 &= \chi_1 \quad , \quad p_2 = \frac{1}{2}(\chi_1^2 - \chi_2) \\
\chi_{-n} &= \bar{\chi}_n, \chi_0 = 3 \quad ; \quad \Xi_n = \chi_n(u = \mathbf{1}) = 3 \quad \forall n \\
\Xi_n &= \Xi \quad ; \quad \Pi_k = \Xi.
\end{aligned} \tag{136}$$

The first of the reducing identities is

$$\begin{aligned} P_3(\mu = u; u) = 0 &\rightarrow \chi_3 = \chi_0 - p_1 \chi_1 + p_2 \chi_2 \quad ; \quad \dots \\ &\rightarrow \chi_3 = \chi_0 - \chi_1^2 + \frac{1}{2}(\chi_1^2 \chi_2 - \chi_2^2). \end{aligned} \quad (137)$$

Substituting $\chi_{M,N}^{ird}(\chi, \bar{\chi})$ the values for $u = \mathbf{1}$, we obtain the dimension of the associated irreducible representation (Eq. (133))

$$\dim(D_{ird;M,N}) = \chi_{M,N}^{ird}(\Xi, \Xi) \quad ; \quad \Xi = 3. \quad (138)$$

All this notwithstanding, the adjoint matrices $U(y, y; \mathcal{CL})$ represent the holonomy group at the point y mapping through \mathcal{CL} parallel transport all adjoint tangent space into itself.

The entire range of adjoint matrices forms the group $SU3./Z_3$. The mapping

$$\begin{aligned} u &\longrightarrow U \\ \in D_{ird;1,0} &\quad \in D_{ird;1,1} \\ (uz_0, uz_1, uz_2) &\rightarrow U \end{aligned} \quad (139)$$

is covering the adjoint representation $D_{ird;1,1}$ three times. In Eq. (139), z_s , $s = 0, 1, 2$ denote the elements forming the center Z_3 of $SU3$.

But there is no loss of information in considering only $U(y, y; \mathcal{CL})$, assuming the analytic extension of the underlying Lie group to be implementable in the classical field configurations, which resolves the above threefold covering through the analytic extension inherent to the Lie algebra leading from $SU3./Z_3 \rightarrow SL3C \rightarrow SU3$. This is in accordance with the universal fibre bundle structure.

At the end of this Appendix we shall go back to $U(y, y; \mathcal{CL})$, as defined in Eq. (127) and state the nonabelian Stokes relation [36]:

$$\begin{aligned} U(y, y; \mathcal{CL} \curvearrowright)_{AB} &= \\ &= \left(U(y, x; \xrightarrow{c}) \right)_{AG} \\ &\quad \times \left(P_2^\Omega \exp \left(- \int_{S_x} \mathcal{W}^{(2)} \right) \right)_{GH} \left(U(x, y; \xrightarrow{c}) \right)_{HB}, \quad (140) \\ (U_{(2)}(x; P_2^\Omega | \mathcal{CL} = \partial S))_{GH} &\rightarrow U_{(2)}^\Omega(x; \mathcal{CL} = \partial S) \\ &= \left(P_2^\Omega \exp \left(- \int_{S_x} \mathcal{W}^{(2)} \right) \right)_{GH}. \end{aligned}$$

In Eq. (140), $U_{(2)}(x; P_2^\Omega | \mathcal{CL} = \partial S) \rightarrow U_{(2)}^\Omega(x; \mathcal{CL} = \partial S)$ denotes the Stokes surface integral proper, punctuated at an internal point x and oriented in a coil-like wiring fashion, denoted by P_2^Ω .

The P_2^Ω ordering for four coils and two wiring layers is shown in Fig. 7 below. The ordering P_2^Ω for the segments at fixed distance from the base point x converges to a flagpole path, shown in the lower-right corner of Fig. 7. This path, denoted \mathfrak{h} , starts and ends at the base point x and turns around the plaquette at the point z on the surface \mathcal{S} . Its contribution inside the ordering P_2^Ω is

$$\mathfrak{h} = U(x, z; \xrightarrow{c}) P_2^{\Omega|z} \exp \left(- \int_{S_x} \mathcal{W}^{(2)} \right) U(z, x; \xrightarrow{c}). \quad (141)$$

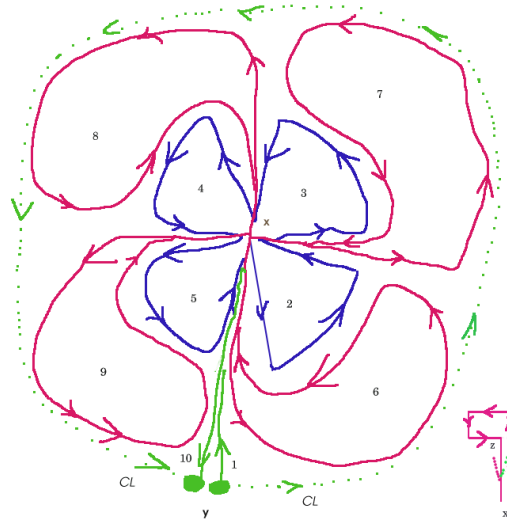


Fig. 7. The surface coil-wiring ordering surface integration. Both number of coils and number of wirings, here 4 and 2, are to be increased, refining the surface covering.

The superscript Ω characterizing the surface ordering P_2^Ω is chosen to associate a local gauge transformation with the surface \mathcal{S} . This follows from the similarity transformation induced on the flagpole path \natural as defined in Eq. (141).

To make this explicit, we rename the parallel transport matrix $U(z, x; \xrightarrow{c})$ associated with the fixed base point x and the point z varying over the entire surface \mathcal{S}

$$\begin{aligned}
 U(z, x; \xrightarrow{c}) &\longrightarrow \omega_x(z) \longrightarrow \\
 \natural &= (\omega_x(z))^{-1} P_2^{\Omega|z} \exp\left(-\int_{S_x} \mathcal{W}^{(2)}\right) \omega_x(z) \quad (142) \\
 \omega_x(z) &= \omega_x(z)|_c.
 \end{aligned}$$

The last line in Eq. (142) shall make it explicit that the parallel transport matrices $\omega_x(z)$ are not local functions of the surface point z . They rather depend on the path, one each from x to z .

The *family* of similarity transformations $\{\omega_x(z)\}$ induced on the *local* field strength differential $\mathcal{W}^{(2)} = \mathcal{W}^{(2)}(z)$ reflects the nested structure of the weaving pattern defining P_2^Ω as a whole¹. Looking at the structure of the similarity transformations forming the *nonlocal* structure \natural in Eq. (142) the question arises, whether there exists a local gauge transformation $\widehat{\Omega}$ - *adapted* to \mathcal{S} - which would

¹Nachtmann [36] compares the repetitious return of the weaving pattern to the base point x with the way a spider weaves its *fan-type anchoring part* of the net.

render the gauge transformed set $\left\{ \omega_x^{\widehat{\Omega}}(z) \right\}$ trivial

$$\omega_x^{\widehat{\Omega}} = \widehat{\Omega}(z) \omega_x \left(\widehat{\Omega}(x) \right)^{-1} \Big|_{\mathcal{C}} = \mathbf{1}, \quad \forall z \in \mathcal{S} \quad (143)$$

$\widehat{\Omega} \rightarrow$ Riemann normal gauge.

Indeed, the gauge transformation with the requirements in Eq. (143) exists and can be found *together* with a coordinate transformation of local coordinates on \mathcal{S} and the original contour $\mathcal{C}\mathcal{L}$ such that \mathcal{S} becomes the inner part of a bounding circle. The latter forms in the new coordinates the closed contour $\mathcal{C}\mathcal{L}$ and the family of curves from the base point x to z becomes the family of straight *radial* lines. The point y punctuating the contour $\mathcal{C}\mathcal{L}$ then can be mapped on the south pole of the bounding circle (to be definite).

The transformed variables are well known in the analogous situation, where gauge transformations refer to coordinate transformations, i.e. the tangent space (universal) spin bundle. The respective coordinates are called Riemann normal coordinates. The gauge equivalent we shall call the Riemann normal gauge as indicated in Eq. (143). The Riemann normal gauge is also known as radial gauge, at least in the case of an Abelian gauge group.

It is precisely in the Riemann normal gauge where the $P_2^\Omega \rightarrow P_2^{\widehat{\Omega}}$ ordering becomes ‘normal’: Transforming to the Riemann normal gauge *R.n.g.* (\mathcal{S}), we have

$$\begin{aligned} \text{R.n.g.}(\mathcal{S}) : \\ \omega_x(z)|_{\mathcal{C}} &\rightarrow \omega_x^{\widehat{\Omega}}(z)|_{\mathcal{C}} \equiv \mathbf{1} \\ P_2^\Omega &\rightarrow P_2^{\widehat{\Omega}} \\ \mathcal{W}^{(2)}(z) &\rightarrow \mathcal{W}^{(2)\widehat{\Omega}}(z) = \widehat{\Omega}(z) \mathcal{W}^{(2)}(z) \left(\widehat{\Omega}(z) \right)^{-1}. \end{aligned} \quad (144)$$

Using the transformed quantities on the right-hand side of Eq. (144), we undo first the flagpole sequence \natural in Eq. (142)

$$\begin{aligned} \natural &= (\omega_x(z))^{-1} P_2^\Omega|_z \exp \left(- \int_{S_x} \mathcal{W}^{(2)} \right) \omega_x(z) \rightarrow \natural^{\widehat{\Omega}} \\ \natural^{\widehat{\Omega}} &= P_2^{\widehat{\Omega}}|_z \exp \left(- \int_{S_x} \mathcal{W}^{(2)\widehat{\Omega}} \right). \end{aligned} \quad (145)$$

Next, Eq. (140) becomes

$$\begin{aligned} U^{\widehat{\Omega}}(y, y; \mathcal{C}\mathcal{L} \xrightarrow{\text{flagpole}})_{AB} &= \\ &= \left(P_2^{\widehat{\Omega}} \exp \left(- \int_{S_x} \mathcal{W}^{(2)\widehat{\Omega}} \right) \right)_{AB} \\ \hline &\left(U_{(2)}(x; P_2^{\widehat{\Omega}} | \mathcal{C}\mathcal{L} = \partial S) \right)_{AB} \rightarrow U_{(2)}^{\widehat{\Omega}}(x; \mathcal{C}\mathcal{L} = \partial S) \\ &= \left(P_2^{\widehat{\Omega}} \exp \left(- \int_{S_x} \mathcal{W}^{(2)\widehat{\Omega}} \right) \right)_{AB}. \end{aligned} \quad (146)$$

At this stage, although implicit in the original definition of the general P_2^Ω ordering, it remains to indicate the (or a) simplified ordering in the Riemann normal gauge. This is shown in Fig. 8. In the Riemann normal gauge the repeated intermediate returns to the base point x are no more necessary².

An interesting shortcut is shown in an actual spiderweb in Fig. 9.

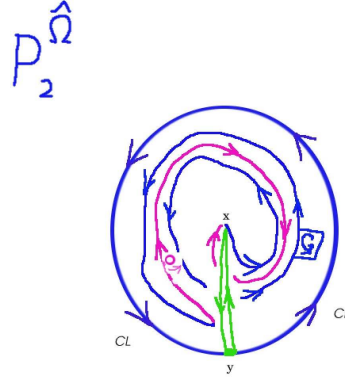


Fig. 8. The abridged ordering of plaquettes in the Riemann normal gauge. It follows a double spiral pattern from the base point x and back.

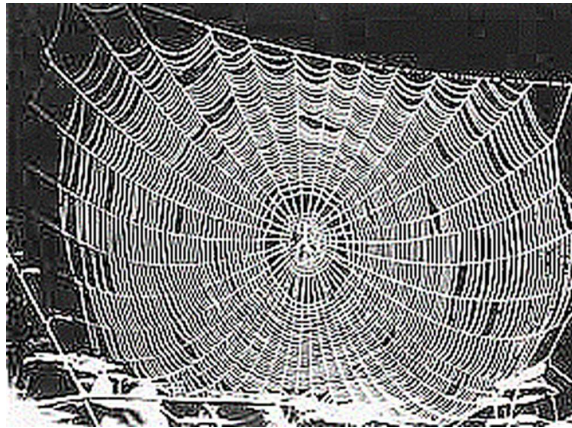


Fig. 9. The abridged ordering in an actual spider web. It follows an abridged double spiral pattern from the base point x and back. The figure is adapted from a Lui Bernard photograph [38].

Several remarks conclude this discussion :

i) Back to the original gauge .

In Eq. (146) we have to transform back from Riemann normal gauge on the

²This also is the spiders path, in the second stage: the scaffolding spiral [37, 38] .

surface $\mathcal{S}_{x|y}$ to the original gauge

$$\begin{aligned} U(y, y; \mathcal{C}\mathcal{L} \curvearrowright)_{AB} &= \\ &= \left(\left(\widehat{\Omega}(y) \right)^{-1} U^{\widehat{\Omega}}(y, y; \mathcal{C}\mathcal{L} \curvearrowright) \widehat{\Omega}(y) \right)_{AB}. \end{aligned} \quad (147)$$

ii) Cut the edges of the contour $\mathcal{C}\mathcal{L}$.

In order to transform the map of the contour $\mathcal{C}\mathcal{L}$ continuously into a circle, the edges marked in the corresponding symbol in eqs. (127), (140), (146) and (147) need to be cut

$$\curvearrowright \rightarrow \bigcirc. \quad (148)$$

iii) The full collection of surfaces and Riemann normal gauges.

As indicated in point i), the meaning of Stokes relations summarized in Eqs. (146) and (147) is to consider *all* surfaces with boundary $\mathcal{C}\mathcal{L}(y)$, the latter punctuated at the point y , the former with base point x , inheriting the point y , *and* the associated Riemann normal gauges $\widehat{\Omega}(x)$. The collection of surfaces and associated Riemann normal gauges shall be denoted

$$\left\{ \mathcal{S}_{x|y}; \widehat{\Omega}(x) \right\}. \quad (149)$$

iv) The Stokes relations proper.

Stokes relations in Eq. (146) in Riemann normal gauges take the form

$$\begin{aligned} U^{\widehat{\Omega}_x}(y, y; \mathcal{C}\mathcal{L}(y) \bigcirc)_{AB} &= \\ &= \left(P_2^{\widehat{\Omega}_x} \exp \left(- \int_{\mathcal{S}_{x|y}} \mathcal{W}^{(2)\widehat{\Omega}_x} \right) \right)_{AB} \\ &\forall \left\{ \mathcal{S}_{x|y}; \widehat{\Omega}_x \right\}. \end{aligned} \quad (150)$$

The true form of Stokes relations returns to a general *common* gauge, combining Eqs. (147) and (150)

$$\begin{aligned} U(y, y; \mathcal{C}\mathcal{L}(y) \bigcirc)_{AB} &= \\ &= \left(\begin{array}{c} \left(\widehat{\Omega}_x(y) \right)^{-1} \\ \times P_2^{\widehat{\Omega}_x} \exp \left(- \int_{\mathcal{S}_{x|y}} \mathcal{W}^{(2)\widehat{\Omega}_x} \right) \\ \times \widehat{\Omega}_x(y) \end{array} \right)_{AB} \\ &\forall \left\{ \mathcal{S}_{x|y}; \widehat{\Omega}_x \right\}. \end{aligned} \quad (151)$$

The closed contour $\mathcal{C}\mathcal{L}(y)$ integral $U(y, y; \mathcal{C}\mathcal{L}(y) \bigcirc)$ on the left-hand side of Eq. (151) is dependent on the point y , where the contour begins and

ends, but *not* on any surface and associated Riemann normal gauge forming the collection $\left\{ \mathcal{S}_{x|y}; \widehat{\Omega}_x \right\}$.

v) The surface integral proper in Riemann normal gauge.

The main ingredient in the Stokes relations in Eq. (151) is – selecting a surface and a Riemann normal gauge out of the collection $\left\{ \mathcal{S}_{x|y}; \widehat{\Omega}_x \right\}$ – the surface integral proper as summarized in Eq. (150)

$$\begin{aligned} U^{\widehat{\Omega}_x} \left(y, y; \mathcal{CL}(y) \quad \bigcirc \right)_{AB} &= \\ &= \left(P_2^{\widehat{\Omega}_x} \exp \left(- \int_{\mathcal{S}_{x|y}} \mathcal{W}^{(2)\widehat{\Omega}_x} \right) \right)_{AB}. \end{aligned} \quad (152)$$

The surface integral on the right hand side of Eq. (152) – *in Riemann normal gauge* – involves the ordering, denoted $P_2^{\widehat{\Omega}_x}$, of products of *local* surface differentials $\mathcal{W}^{(2)\widehat{\Omega}_x}$. By this local property the surface ‘integral’ is indeed an integral.

In any gauge other than a Riemannian normal one, the corresponding differentials are *not* local functions of the plaquette differentials, rather they depend on the entire set of flagpole paths, described in Fig. 7 and Eqs. (141) and (142).

vi) The ordering of surface elements in Riemann normal gauge.

The path ordering $P_2^{\widehat{\Omega}_x}$ of the – matrix valued – surface elements is very special to Riemann normal gauges. It derives from two steps, starting in a general (original) gauge. They are described in the text following Eq.(140) and in Figs. 7 and 8.

An appropriate name for $P_2^{\widehat{\Omega}_x}$ is ‘spider-web ordering’ illustrated in Fig. 8a, [38].

Appendix A.4 Spin projection operations on adjoint string operators

The adjoint string operators forming binary gluonic mesons are introduced in Eq. (14), repeated below

$$\begin{aligned} B_{[\mu_1 \nu_1], [\mu_2 \nu_2]}(x_1, x_2) &= \\ F_{[\mu_1 \nu_1]}(x_1; A) U(x_1, A; x_2, B) F_{[\mu_2 \nu_2]}(x_2; B) & \quad (153) \\ A, B, \dots &= 1, \dots, 8. \end{aligned}$$

The Lorentz invariant tensors K^\pm are introduced in Eq. (23), repeated below

$$\begin{aligned} \tilde{t}_{\pm; I^\pm}(z, p, J^{\pm+}; \cdot) &= \left(\begin{array}{c} (K^\pm)_{[\mu_1 \nu_1][\mu_2 \nu_2]} \\ \times \tilde{t}_{I^\pm}(z, p, J^{\pm+}; \cdot) \end{array} \right) \\ (K^+)_{[\mu_1 \nu_1][\mu_2 \nu_2]} &= g_{\mu_1 \mu_2} g_{\nu_1 \nu_2} - g_{\mu_1 \nu_2} g_{\mu_2 \nu_1} \\ (K^-)_{[\mu_1 \nu_1][\mu_2 \nu_2]} &= \varepsilon_{\mu_1 \mu_2 \nu_1 \nu_2}. \end{aligned} \quad (154)$$

We perform the associated projections

$$B_{[\mu_1 \nu_1], [\mu_2 \nu_2]} = \left(\begin{array}{c} K_{[\mu_1 \nu_1][\mu_2 \nu_2]}^+ B^{(+)} \\ + K_{[\mu_1 \nu_1][\mu_2 \nu_2]}^- B^{(-)} \\ + B'_{[\mu_1 \nu_1], [\mu_2 \nu_2]} \end{array} \right). \quad (155)$$

The decomposition according to Eq. (155) is the same for the Riemann curvature tensor, where $B^{(+)}$ relates to the curvature scalar, B' to the Ricci and Weyl tensors and $B^{(-)} = 0$, unlike here.

So we form the metric (Ricci-) contraction

$$\begin{aligned} g^{\mu_1 \mu_2} B_{[\mu_1 \nu_1], [\mu_2 \nu_2]} &= R_{\nu_1 \nu_2} \\ R_{\nu_1 \nu_2} &= \left(\begin{array}{c} 3g_{\nu_1 \nu_2} B^{(+)} \\ + g^{\mu_1 \mu_2} B'_{[\mu_1 \nu_1], [\mu_2 \nu_2]} \end{array} \right) \\ R_{\nu_1 \nu_2} &= \varrho_{\nu_1 \nu_2} + \frac{1}{4} g_{\nu_1 \nu_2} R \quad ; \quad R = g^{\nu_1 \nu_2} R_{\nu_1 \nu_2} \\ \varrho_{\nu_1 \nu_2} &= R_{\nu_1 \nu_2} - \frac{1}{4} g_{\nu_1 \nu_2} R. \end{aligned} \quad (156)$$

It follows from Eq. (156)

$$\begin{aligned} \varrho_{\nu_1 \nu_2} &= g^{\mu_1 \mu_2} B'_{[\mu_1 \nu_1], [\mu_2 \nu_2]} \rightarrow \\ g^{\mu_1 \mu_2} g^{\nu_1 \nu_2} B'_{[\mu_1 \nu_1], [\mu_2 \nu_2]} &= 0 \quad \rightarrow \quad R = 12 B^{(+)}. \end{aligned} \quad (157)$$

The quantity B' with the trace condition in Eq. (157) forms the irreducible *relativistic* spin two part $S_{12}^+ = 2$ as defined in Eqs. (21) and (22) in the main text. Here we concentrate on the projection on $B^{(\pm)}$.

From Eq. (157) we obtain

$$\begin{aligned} B^{(+)}(x_1, x_2) &= \\ &= \frac{1}{12} F_{[\alpha \beta]}(x_1; A) U(x_1, A; x_2, B) F^{[\alpha \beta]}(x_2; B). \end{aligned} \quad (158)$$

The projection on $B^{(-)}$ proceeds in a similar way

$$\begin{aligned} \varepsilon^{\mu_1 \mu_2 \nu_1 \nu_2} B_{[\mu_1 \nu_1], [\mu_2 \nu_2]} &= -24 B^{(-)} + \\ &\quad + \varepsilon^{\mu_1 \mu_2 \nu_1 \nu_2} B'_{[\mu_1 \nu_1], [\mu_2 \nu_2]} \rightarrow \\ \varepsilon^{\mu_1 \mu_2 \nu_1 \nu_2} B'_{[\mu_1 \nu_1], [\mu_2 \nu_2]} &= 0. \end{aligned} \quad (159)$$

The structure of $B^{(-)}$ follows similarly as for $B^{(+)}$ in Eq. (158). We thus give both expressions together below

$$\begin{aligned}
& B^{(+)}(x_1, x_2) \\
& \quad = \frac{1}{12} F_{[\alpha\beta]}(x_1; A) U(x_1, A; x_2, B) F^{[\alpha\beta]}(x_2; B) \\
\hline
& B^{(-)}(x_1, x_2) \\
& \quad = -\frac{1}{12} F_{[\alpha\beta]}(x_1; A) U(x_1, A; x_2, B) \tilde{F}^{[\alpha\beta]}(x_2; B) \\
& \quad = -\frac{1}{12} \tilde{F}_{[\alpha\beta]}(x_1; A) U(x_1, A; x_2, B) F^{[\alpha\beta]}(x_2; B) \\
\hline
& \tilde{F}_{[\alpha\beta]}(x_2; B) = \frac{1}{2} \varepsilon_{\alpha\beta\gamma\delta} F^{[\gamma\delta]}(x_2; B) \\
& \text{and } (x_2; B) \leftrightarrow (x_1; A).
\end{aligned} \tag{160}$$

Appendix A.5 Spin projection operations on adjoint string operators - extended

We continue the projection operations carried out in Appendix A.4 in order to extend them to the remaining gb spectral series of type II^+ . This is related to the quantities $B'_{[\mu_1\nu_1],[\mu_2\nu_2]}$ defined in Eq. (24) and refined in Appendix A.4 (Eq. (155)).

To that end we perform the *full* decomposition of the tensorial structure of the octet string operators introduced in Eq. (14) and rewritten in Eq. (153)

$$B_{[\mu_1\nu_1],[\mu_2\nu_2]}(x_1, x_2) \rightarrow B_{[\mu_1\nu_1],[\mu_2\nu_2]}, \tag{161}$$

which is analogous to that of the Riemann curvature tensor, without the metric constraints of the latter.

The Ricci contraction introduced in Eq. (156) yields the following structure

$$\begin{aligned}
& B_{[\mu_1\nu_1],[\mu_2\nu_2]} = w_{[\mu_1\nu_1],[\mu_2\nu_2]} + \Delta B_{[\mu_1\nu_1],[\mu_2\nu_2]} \\
& \Delta B_{[\mu_1\nu_1],[\mu_2\nu_2]} = \frac{1}{2} \begin{pmatrix} g_{\mu_1\mu_2} R_{\nu_1\nu_2} - g_{\nu_1\nu_2} R_{\mu_1\mu_2} \\ -g_{\mu_1\nu_2} R_{\nu_1\mu_2} + g_{\nu_1\nu_2} R_{\mu_1\mu_2} \end{pmatrix} \\
& \quad - \frac{1}{6} K^+_{[\mu_1\nu_1],[\mu_2\nu_2]} R
\end{aligned} \tag{162}$$

with : $g^{\mu_1\mu_2} w_{[\mu_1\nu_1],[\mu_2\nu_2]} = 0$

$$g^{\mu_1\mu_2} B_{[\mu_1\nu_1],[\mu_2\nu_2]} = g^{\mu_1\mu_2} \Delta B_{[\mu_1\nu_1],[\mu_2\nu_2]} = R_{\nu_1\nu_2}$$

$$R = g^{\nu_1\nu_2} R_{\nu_1\nu_2} = 12 B^{(+)}.$$

Before proceeding, let's express the Ricci bilinear in terms of the base octet string operators $B_{[\mu_1\nu_1],[\mu_2\nu_2]}$

$$\begin{aligned}
& R_{\nu_1\nu_2} = \\
& \quad = -F_{\nu_1\alpha}(x_1; A) U(x_1, A; x_2, B) F^\alpha_{\nu_2}(x_2; B).
\end{aligned} \tag{163}$$

In order to simplify notation, we shall suppress the position arguments and use chromoelectric and -magnetic fields for the field strength tensor.

$$\begin{aligned}
 -R_{\nu_1\nu_2} &= \begin{pmatrix} \vec{E}^A \vec{E}^D & \vec{S}^{kAD} \\ \vec{S}^{iAD} & -\vec{E}^{iA} \vec{E}^{kD} - \vec{B}^{iA} \vec{B}^{kD} \\ & + \delta_{ik} \vec{B}^A \vec{B}^D \end{pmatrix} U_{AD} \\
 R &= 2 \left(\vec{B}^A \vec{B}^D - \vec{E}^A \vec{E}^D \right) U_{AD} \quad ; \quad \vec{S}^{AD} = \vec{E}^A \wedge \vec{B}^D \\
 \vec{E}^{iA} &= F^{0iA} \quad , \quad \vec{B}^{iA} = \frac{1}{2} \varepsilon_{ikl} F^{klA} .
 \end{aligned} \tag{164}$$

In Eq. (164) we recognize the Maxwell energy momentum like (bilinear) expression, where \vec{S}^{AD} shall be called the bilinear Poynting vector.

Next we substitute the traceless part of the Ricci bilinear (Eq. (156)) in Eq. (162)

$$\begin{aligned}
 -\varrho^{\mu\nu} &= -R^{\mu\nu} + \frac{1}{4} g^{\mu\nu} R = \vartheta_{cl}^{\mu\nu} \\
 &= \begin{pmatrix} \frac{1}{2} \left(\vec{E}^A \vec{E}^D + \vec{B}^A \vec{B}^D \right) & -\vec{S}^{kAD} \\ -\vec{S}^{iAD} & -\vec{E}^{iA} \vec{E}^{kD} - \vec{B}^{iA} \vec{B}^{kD} \\ & + \frac{1}{2} \delta_{ik} \left(\vec{E}^A \vec{E}^D + \vec{B}^A \vec{B}^D \right) \end{pmatrix} U_{AD} .
 \end{aligned} \tag{165}$$

In Eq. (165) we recognize the bilinear with the structure of the classical (traceless) Maxwell energy momentum tensor of nonabelian gauge field strengths.

Equation (162) becomes decomposed into positive parity irreducible parts

$$\begin{aligned}
 B_{[\mu_1\nu_1],[\mu_2\nu_2]} &= w_{[\mu_1\nu_1],[\mu_2\nu_2]} + \Delta B_{[\mu_1\nu_1],[\mu_2\nu_2]} \\
 \Delta B_{[\mu_1\nu_1],[\mu_2\nu_2]} &= \frac{1}{2} \begin{pmatrix} g_{\mu_1\mu_2} \varrho_{\nu_1\nu_2} - g_{\nu_1\nu_2} \varrho_{\mu_1\mu_2} \\ -g_{\mu_1\nu_2} \varrho_{\nu_1\mu_2} + g_{\nu_1\nu_2} \varrho_{\mu_1\mu_2} \end{pmatrix} \\
 &\quad + \frac{1}{12} K_{[\mu_1\nu_1],[\mu_2\nu_2]}^+ R
 \end{aligned} \tag{166}$$

$$\text{with : } g^{\mu_1\mu_2} w_{[\mu_1\nu_1],[\mu_2\nu_2]} = 0$$

$$g^{\mu_1\mu_2} B_{[\mu_1\nu_1],[\mu_2\nu_2]} = g^{\mu_1\mu_2} \Delta B_{[\mu_1\nu_1],[\mu_2\nu_2]} = R_{\nu_1\nu_2}$$

$$R = g^{\nu_1\nu_2} R_{\nu_1\nu_2} = 12 B^{(+)} .$$

As a side remark to the (Lorentz-) tensorial reduction of the bilinear quantities $B_{[\mu_1\nu_1],[\mu_2\nu_2]}$, it is necessary to include the spatio-temporal *nonlocal* parallel transport matrices pertaining to a general connection and metric $\Gamma_{\sigma}^{\mu}{}_{\nu}$ and $g_{\mu\nu}$. This is necessary to render $B_{[\mu_1\nu_1],[\mu_2\nu_2]}$ a true *nonlocal* Lorentz-tensor. We do not do this here. In globally flat Minkowski space coordinates, this parallel transport is trivial.

The sequence of projections on first Lorentz spin ($\underline{\cdot}$) and second on rotational spin ($\dot{\cdot}$), needs two steps, rearranging the structure of $-\varrho^{\mu\nu}$ in Eq. (165)

$$\begin{aligned}
-\varrho^{\mu\nu} &= \vartheta_{cl}^{\mu\nu} = \\
&= \begin{pmatrix} \frac{1}{2} \begin{pmatrix} \vec{E}^A \vec{E}^D \\ + \vec{B}^A \vec{B}^D \end{pmatrix} & -\vec{S}^k{}_{AD} \\ -\vec{S}^i{}_{AD} & \begin{pmatrix} -\vec{E}^{iA} \vec{E}^{kD} - \vec{B}^{iA} \vec{B}^{kD} \\ + \frac{1}{3} \delta_{ik} \begin{pmatrix} \vec{E}^A \vec{E}^D \\ + \vec{B}^A \vec{B}^D \end{pmatrix} \\ + \frac{1}{6} \delta_{ik} \begin{pmatrix} \vec{E}^A \vec{E}^D \\ + \vec{B}^A \vec{B}^D \end{pmatrix} \end{pmatrix} \end{pmatrix} \times U_{AD}. \tag{167}
\end{aligned}$$

The tensor structure of $\vartheta_{cl}^{\mu\nu}$ in Eq. (167) follows the hydrodynamic nomenclature

$$\begin{aligned}
-\varrho^{\mu\nu} &= \vartheta_{cl}^{\mu\nu} = \begin{pmatrix} \varrho_e & -\vec{S}^k \\ -\vec{S}^i & \begin{pmatrix} \pi_{ik} \\ + \delta_{ik} p \end{pmatrix} \end{pmatrix} \\
\varrho_e &= 3p = \frac{1}{2} \left(\vec{E}^A \vec{E}^D + \vec{B}^A \vec{B}^D \right) U_{AD} \\
\pi_{ik} &= 2p \delta_{ik} - \left(\vec{E}^{iA} \vec{E}^{kD} + \vec{B}^{iA} \vec{B}^{kD} \right) U_{AD} \\
\sum_i \pi_{ii} &= 0, \tag{168}
\end{aligned}$$

with the identifications given in Eq. (168).

The chain of irreducible components of $\Delta B_{\dot{\cdot}}$ is shown in Eq. (169) below

step	name	# comp.	L.-spin	R.-spin
1	$\Delta B_{\dot{\cdot}}$	10	mixed	mixed
2	$B^{(+)\dot{\cdot}}$	1	1	1
2	$\varrho^{\dot{\cdot}}$	9	$D^{1, \bar{1}}$	mixed
3	ϱ_e	1	—	1
3	$\vec{S}^{\dot{\cdot}}$	3	—	D^1
3	$\pi_{\dot{\cdot}}$	5	—	D^2

(169)

It is the last term in Eq. (169) π_{ik} as displayed in Eq. (168) which characterizes the $S_{12}^+ = 2$ spectral series of binary gluonic mesons. The R-spin 2 tensor π_{ik} is related to the corresponding components of the Weyl bilinear $w_{[\mu_1 \nu_1][\mu_2 \nu_2]}$ introduced in Eq. (162), which represents the traceless part of the bilinear Riemann like tensor $B_{[\mu_1 \nu_1], [\mu_2 \nu_2]}$, to which we turn next.

Weyl bilinear and circular polarization basis for gauge field strengths

We recall the right and left chiral spin matrices defined in Appendix A.1 (Eqs. (62) and (63)) reproduced below, first for the right-circular part. Here the notion

right (left) circular refers to a fixed spin axis and *not* to the individual momenta of the two gauge bosons at the end of the octet string, in question. The spin axis is common to both and an axial vector.

$$\begin{aligned}
(\sigma_{\mu\nu})_{\alpha}^{\beta} &\leftrightarrow P_R \frac{i}{2} [\gamma_{\mu}, \gamma_{\nu}] P_R \quad ; \quad P_R = \frac{1}{2} (1 + \gamma_{5R}) \\
\gamma_{5R} &= \frac{1}{i} \gamma_0 \gamma_1 \gamma_2 \gamma_3 \\
(\sigma_{\mu\nu})_{\alpha}^{\beta} &= \begin{pmatrix} -i \Sigma_k \\ \varepsilon_{mnr} \Sigma_r \end{pmatrix}_{\alpha}^{\beta} \quad \begin{array}{l} \text{for } \mu = 0, \nu = k = 1, 2, 3 \\ \text{for } \mu = m, \nu = n; \\ \quad \quad \quad \quad \quad \quad \quad \quad m, n, r = 1, 2, 3 \end{array} \quad (170) \\
(\sigma_{\mu\nu})_{\alpha}^{\beta} &\rightarrow \sigma_{\mu\nu}^R \quad ; \quad \sigma_{\mu\nu}^R = -i \frac{1}{2} \varepsilon_{\mu\nu\varrho\tau} \sigma^{\varrho\tau R}.
\end{aligned}$$

The right-circular spinor basis in Eq. (170) yields the projection on the gauge field strengths

$$\begin{aligned}
\frac{1}{2} \sigma_{\mu\nu}^R F^{[\mu\nu]}(x; A) &= \Sigma_r \vec{C}^{rA}(x) \\
\vec{C}^{rA}(x) &= \left(\vec{B} - i \vec{E} \right)^{rA}(x) \quad \rightarrow \quad \vec{C}^{rA} \quad (171) \\
r &= 1, 2, 3.
\end{aligned}$$

The right circular quantities \vec{C}^{rA} in Eq. (171) are complex combinations of the hermitian field strengths $F^{[\mu\nu]A}$ in the adjoint representation of $SU3_c$.

We note the right circular identity, following from Eq. (170)

$$\begin{aligned}
\frac{1}{2} \sigma_{\mu\nu}^R F^{[\mu\nu]A} &\equiv \frac{1}{2} \sigma_{\mu\nu}^R (F^R)^{[\mu\nu]A} \\
(F^R)^{[\mu\nu]A} &= \frac{1}{2} \left(F^{[\mu\nu]A} - i \tilde{F}^{[\mu\nu]A} \right) \quad (172) \\
\tilde{F}_{[\mu\nu]}^A &= \frac{1}{2} \varepsilon_{\mu\nu\sigma\tau} F^{[\sigma\tau]A}.
\end{aligned}$$

When the space-time component r in \vec{C}^{rA} is explicitly denoted, the vector symbol of \vec{C} shall be omitted for simplicity.

Now we recall the left chiral spinor matrices defined in Eqs. (81) and (82) in Appendix A.1

$$\begin{aligned}
(\sigma_{\mu\nu})_{\dot{\delta}}^{\dot{\gamma}} &\leftrightarrow P_L \frac{i}{2} [\gamma_{\mu}, \gamma_{\nu}] P_L \quad ; \quad P_L = \frac{1}{2} (1 - \gamma_{5R}) \\
\gamma_{5R} &= \frac{1}{i} \gamma_0 \gamma_1 \gamma_2 \gamma_3 \\
(\sigma_{\mu\nu})_{\dot{\delta}}^{\dot{\gamma}} &= \begin{pmatrix} i \Sigma_k \\ \varepsilon_{mnr} \Sigma_r \end{pmatrix}_{\dot{\delta}}^{\dot{\gamma}} \quad \begin{array}{l} \text{for } \mu = 0, \nu = k = 1, 2, 3 \\ \text{for } \mu = m, \nu = n; \\ \quad \quad \quad \quad \quad \quad \quad \quad m, n, r = 1, 2, 3 \end{array} \quad (173) \\
(\sigma_{\mu\nu})_{\dot{\delta}}^{\dot{\gamma}} &\rightarrow \sigma_{\mu\nu}^L \quad ; \quad \sigma_{\mu\nu}^L = +i \frac{1}{2} \varepsilon_{\mu\nu\varrho\tau} \sigma^{\varrho\tau L}.
\end{aligned}$$

Correspondingly to Eq. (170), the left-circular spinor basis in Eq. (173) yields the projection on the left-circular gauge field strengths, completing the right-

circular one in Eq. (171)

$$\begin{aligned} \frac{1}{2} \sigma_{\mu\nu}^L F^{[\mu\nu]}(x; A) &= \Sigma_r \vec{G}^{rA}(x) \\ \vec{G}^{rA}(x) &= \left(\vec{B} + i\vec{E} \right)^{rA}(x) \rightarrow \vec{G}^{rA} \\ r &= 1, 2, 3. \end{aligned} \quad (174)$$

Analogous to the right-circular identity in Eq. (172) is the left-circular one, displayed together in Eq. (175) below

$$\begin{aligned} \frac{1}{2} \sigma_{\mu\nu}^R F^{[\mu\nu]A} &\equiv \frac{1}{2} \sigma_{\mu\nu}^R (FR)^{[\mu\nu]A} \\ (FR)^{[\mu\nu]A} &= \frac{1}{2} \left(F^{[\mu\nu]A} - i\tilde{F}^{[\mu\nu]A} \right) \\ \tilde{F}_{[\mu\nu]}^A &= \frac{1}{2} \varepsilon_{\mu\nu\sigma\tau} F^{[\sigma\tau]A} \\ \sigma_{\mu\nu}^L F^{[\mu\nu]A} &\equiv \frac{1}{2} \sigma_{\mu\nu}^L (FL)^{[\mu\nu]A} \\ (FL)^{[\mu\nu]A} &= \frac{1}{2} \left(F^{[\mu\nu]A} + i\tilde{F}^{[\mu\nu]A} \right). \end{aligned} \quad (175)$$

As long as we remain within the real Lorentz group, as discussed in Appendix A.1, the three vector quantities \vec{C}^A and \vec{G}^A are relative hermitian conjugates of each other. They transform according to the $D^{1,0}$ and $D^{0,1}$ representations of the $spin(1, 3; \mathfrak{R}) \simeq SL2C$ group, as defined in eqs. (80) and (81) in Appendix A.2.

$$\begin{aligned} \vec{C}^A &= \left(\vec{G}^A \right)^* \rightarrow \\ D^{1,0} : C^{rA} &\rightarrow R_{rs} C^{sA} ; \quad D^{0,1} : G^{rA} \rightarrow L_{rs} G^{sA} \\ R_{rs} &= R_{rs}(\mathcal{A}) , \quad L_{rs} = L_{rs}(\mathcal{B}) \\ R_{rs} &= \bar{L}_{rs} \quad \text{within } spin(1, 3; \mathfrak{R}). \end{aligned} \quad (176)$$

The three by three matrices R_{rs} and L_{rs} are complex orthogonal with determinant 1, forming the group $SO3C \simeq SL2C / Z_2$, where Z_2 denotes the center of $SL2C$.

We are now ready to decompose the Weyl bilinear $w_{[\mu_1 \nu_1][\mu_2 \nu_2]}$ in Eq. (162), into its irreducible parts.

$$\begin{aligned} w_{[\mu_1 \nu_1][\mu_2 \nu_2]} &= \left(\begin{array}{c} \left(P^{RR} \left(\vec{C} \otimes \vec{C} \right) \right)_{[\mu_1 \nu_1][\mu_2 \nu_2]} \\ + \left(P^{LL} \left(\vec{G} \otimes \vec{G} \right) \right)_{[\mu_1 \nu_1][\mu_2 \nu_2]} \\ + B^{(-)} \left(K^- \right)_{[\mu_1 \nu_1][\mu_2 \nu_2]} \end{array} \right) \\ \left(K^- \right)_{[\mu_1 \nu_1][\mu_2 \nu_2]} &= \varepsilon_{\mu_1 \mu_2 \nu_1 \nu_2}. \end{aligned} \quad (177)$$

In Eq. (177), the quantities $B^{(-)}$ and (K^-) are defined in Eqs. (23)–(25). The projections denoted $P^{RR} \left(\vec{C} \otimes \vec{C} \right)$ and $P^{LL} \left(\vec{G} \otimes \vec{G} \right)$, operate on the doubly right- and left-circular, direct product combinations indicated as respective arguments in Eq. (177). Omitting the explicit dependence on the Lorentz indices

$[\mu_1 \nu_1] [\mu_2 \nu_2]$ for simplicity, they are of the form

$$\begin{aligned} P^{RR} \left(\vec{C} \otimes \vec{C} \right) &= \pi_{rs}^{(2)} \left(C^{rA} C^{sD} - \frac{1}{3} \delta^{rs} \vec{C}^A \vec{C}^D \right) U_{AD} \\ P^{LL} \left(\vec{G} \otimes \vec{G} \right) &= \pi_{rs}^{(2)} \left(G^{rA} G^{sD} - \frac{1}{3} \delta^{rs} \vec{G}^A \vec{G}^D \right) U_{AD}. \end{aligned} \quad (178)$$

We thus introduce the abbreviations following Eq. (178)

$$\begin{aligned} P^{RR} \left(\vec{C} \otimes \vec{C} \right) &\rightarrow w_{\dot{\cdot}}^{RR} \\ P^{LL} \left(\vec{G} \otimes \vec{G} \right) &\rightarrow w_{\dot{\cdot}}^{LL} \\ w_{\dot{\cdot}}^{RR} &= \left(C^{rA} C^{sD} - \frac{1}{3} \delta^{rs} \vec{C}^A \vec{C}^D \right) U_{AD} \\ w_{\dot{\cdot}}^{LL} &= \left(G^{rA} G^{sD} - \frac{1}{3} \delta^{rs} \vec{G}^A \vec{G}^D \right) U_{AD} \\ \hline w_{\dot{\cdot}}^{LL} &= \left(w_{\dot{\cdot}}^{RR} \right)^*. \end{aligned} \quad (179)$$

The bilinears $w_{\dot{\cdot}}^{RR}$ and $w_{\dot{\cdot}}^{LL}$ defined in Eq. (179) transform according to the complex representations $D^{2,0}$ and $D^{0,\dot{2}}$ of $spin(1, 3; \mathbb{R}) \simeq SL_2C$, respectively. These two representations are complex conjugate to each other.

As in the case of the Lorentz tensor $\varrho^{\mu\nu}$ in Eqs. (165), (167) and (168), the space time indices rs for the quantities $w_{\dot{\cdot}}^{LL}$ and $w_{\dot{\cdot}}^{RR}$ in Eq. (179) are understood to be symmetrized.

This completes the decomposition of the Weyl bilinear. We compare the structure of the irreducible components $w_{\dot{\cdot}}$ with that of $\Delta B_{\dot{\cdot}}$, as shown in Eq. (169) reproduced below

step	name	# comp.	L.-spin	R.-spin
1	$\Delta B_{\dot{\cdot}}$	10	mixed	mixed
2	$B^{(+)}$	1	1	1
2	$\varrho_{\dot{\cdot}}$	9	$D^{1,\bar{1}}$	mixed
3	ϱ_e	1	—	1
3	\vec{S}	3	—	D^1
3	$\pi_{\dot{\cdot}}$	5	—	D^2

(180)

The corresponding structure of the Weyl bilinears is displayed in Eq. (181)

step	name	# comp.	L.-spin	R.-spin
1	$w_{\dot{\cdot}}$	11	mixed	mixed
2	$B^{(-)}$	1	1	1
2	w^{RR}	5	$D^{2,0}$	D^2
2	$w_{\dot{\cdot}}^{LL}$	$\bar{5}$	$D^{0,\dot{2}}$	D^2

(181)

Comparing the counting in the two tables (Eqs. (180) and (181)), we should keep in mind that the columns labeled $\# \text{ comp.}$ are based on counting independent *hermitian operators* among the bilinears B_{\pm} .

In this respect we verify the correctness of the counting: the Riemann tensor like bilinears have $6 \times 7/2 = 21$ hermitian components, which combine into 10 for the Ricci tensor-like quantities, further decomposed according to Eq. (180), and 11 for the Weyl tensor-like in Eq. (181).

For the Ricci tensor the decomposition into $B^{(+)}$ corresponding to the curvature scalar and the traceless part, called ϱ^{\pm} here, is straightforward.

For the Weyl tensor the splitting into $10 + 1$ hermitian components, corresponding to the pseudoscalar $B^{(-)}$ and the right- and left circular bilinears w_{\pm}^{RR} and w_{\pm}^{LL} , with together 10 *hermitian* components is also quite clear.

What appears impossible, is to find a common contribution to the so defined irreducibles: ϱ^{\pm} with 9 hermitian components on one hand and w_{\pm}^{RR} and w_{\pm}^{LL} with 10 on the other. It follows from the discussion below, that this is indeed impossible.

In this connection, we have to remember that we are considering matrix elements of the form defined in Eq. (17)

$$\langle \emptyset | B_{[\mu_1 \nu_1], [\mu_2 \nu_2]}(x_1, x_2) | gb(J^{PC}); p, \{spin\} \rangle \rightarrow e^{-ipX} \tilde{t}_{\pm}(z, p, J^{PC}; \cdot), \quad (182)$$

where hermitian bilinears induce *complex* amplitudes.

Next we focus on the continuity equation for the classical energy-momentum tensor pertaining to the field strengths, extended to the nonlocal situation, conditioned by the c.m. four momentum p . This follows the relations in Eqs. (167) and (168)

$$-\varrho^{\mu\nu} = \vartheta_{cl}^{\mu\nu}(X; z) \rightarrow \partial_{X\mu} \vartheta_{cl}^{\mu\nu}(X; z) = 0. \quad (183)$$

Equation (183) is valid for classical field configurations and follows from the analogous classical treatment of the Stokes relation discussed in Appendix A.3. It is not straightforward for quantized local gauge fields. In the latter case, the identical relation is not sufficiently established and deserves further study. Nevertheless, we use it here for consistency. Thus it follows that the quantities ϱ_e and \vec{S} defined in Eq. (168) do not contribute to the amplitudes associated with the classical energy-momentum tensor $\vartheta_{cl}^{\mu\nu}(X; z)$.

Thus we associate each bilinear irreducible to the (family of) wave functions, following the notation introduced in Eq. (17) and repeated in Eq. (182). Hereby the complete family of wave functions is accordingly projected

$$\begin{aligned} \varrho^{\pm} &\leftrightarrow \tilde{t}_{\pm}(\{\varrho\}; z, p, J^{PC}; \cdot) &\rightarrow \tilde{t}(\{\varrho\}) \\ w_{\pm} &\leftrightarrow \tilde{t}_{\pm}(\{w\}; z, p, J^{PC}; \cdot) &\rightarrow \tilde{t}(\{w\}) \\ w_{\pm}^{RR} &\leftrightarrow \tilde{t}_{\pm}(\{w^{RR}\}; z, p, J^{PC}; \cdot) &\rightarrow \tilde{t}(\{w^{RR}\}) \\ w_{\pm}^{LL} &\leftrightarrow \tilde{t}_{\pm}(\{w^{LL}\}; z, p, J^{PC}; \cdot) &\rightarrow \tilde{t}(\{w^{LL}\}). \end{aligned} \quad (184)$$

The bilinears $B^{(\pm)}$ are already fully characterized. They do not contribute to the wave functions of the II^+ , i.e. $S_{12}^+ = 2$ spectral type, and thus we will not discuss them any further here.

The tables in Eqs. (180) and (181) are thus reduced and adapted to the wave functions \tilde{t} defined in Eq. (184)

step	name	# comp.	L.-spin	R.-spin
2	$\tilde{t}(\{\varrho\})$	9	$D^{1,\bar{1}}$	D^2
3	$\tilde{t}(\{\varrho_e\})$	0	–	–
3	$\tilde{t}(\{\vec{S}\})$	0	–	–
3	$\tilde{t}(\{\pi\})$	5	–	D^2
2	$\tilde{t}(\{w^{RR}\})$	5	$D^{2,0}$	D^2
2	$\tilde{t}(\{w^{LL}\})$	5	$D^{0,2}$	D^2

(185)

The wave functions denoted $\tilde{t}(\{\varrho_e\})$ and $\tilde{t}(\{\vec{S}\})$ in Eq. (185) vanish, as a consequence of the continuity equation in Eq. (183).

Thus the table in Eq. (185) reduces to

step	name	# comp.	L.-spin	R.-spin
2	$\tilde{t}(\{\varrho\})$	9	$D^{1,\bar{1}}$	D^2
3	$\tilde{t}(\{\pi\})$	5	–	D^2
2	$\tilde{t}(\{w^{RR}\})$	5	$D^{2,0}$	D^2
2	$\tilde{t}(\{w^{LL}\})$	5	$D^{0,2}$	D^2

(186)

In the tables (Eqs. (185) and (186)), the column labelled # comp. refers to wave function components over the complex numbers.

The entries and properties displayed in Eq. (186) look more coherent than in the tables in Eqs. (180) and (181), but the puzzle of 5 versus 10 components for $\tilde{t}(\{\varrho\})$ compared to $\tilde{t}(\{w^{RR}\})$ and $\tilde{t}(\{w^{LL}\})$ remains.

To understand this difference, we compare the structure of the bilinears associated with $\tilde{t}(\{\pi\})$ (Eq. (168)) with the one pertaining to $\tilde{t}(\{w^{RR}\})$ and $\tilde{t}(\{w^{LL}\})$ ((178)). To this end we use the relations in Eqs. (171) defining the

quantities \vec{C}^A and (174) for \vec{G}^A , respectively.

$$\begin{aligned}
& -\varrho^{\mu\nu} = \vartheta_{cl}^{\mu\nu} \rightarrow \\
& \pi_{ik} = \left(\begin{array}{c} \frac{1}{3} \delta_{ik} \left(\vec{E}^A \vec{E}^D + \vec{B}^A \vec{B}^D \right) \\ - \left(\vec{E}^{iA} \vec{E}^{kD} + \vec{B}^{iA} \vec{B}^{kD} \right) \end{array} \right) U_{AD} \\
\hline
& P^{RR} \left(\vec{C} \otimes \vec{C} \right) \rightarrow \\
& \left(\pi^{RR} \right)^{rs} = \left(C^{rA} C^{sD} - \frac{1}{3} \delta^{rs} \vec{C}^A \vec{C}^D \right) U_{AD} \\
\hline
& P^{LL} \left(\vec{G} \otimes \vec{G} \right) \rightarrow \\
& \left(\pi^{LL} \right)^{rs} = \left(G^{rA} G^{sD} - \frac{1}{3} \delta^{rs} \vec{G}^A \vec{G}^D \right) U_{AD} \\
\hline
& \vec{C}^{rA}(x) = \left(\vec{B} - i\vec{E} \right)^{rA}(x) \\
& \vec{G}^{rA}(x) = \left(\vec{B} + i\vec{E} \right)^{rA}(x) \\
& \sum_i \pi_{ii} = 0 \quad ; \quad \sum_r \left(\pi^{RR} \right)^{rr} = \sum_r \left(\pi^{LL} \right)^{rr} = 0.
\end{aligned} \tag{187}$$

In Eq. (187), the 21 complex components of the octet string bilinear wave functions are reduced to 3 complex, traceless and symmetric 3×3 matrices, denoted π , π^{RR} and π^{LL} , respectively. There is at this stage an essential ingredient missing. The property distinguishing the above matrices is the spatial ‘Dreibein’ nature of chromoelectric-, chromomagnetic and orientation axis vectors [39].

In order to realize the ‘Dreibein’ property, we reduce the three quantities π , π^{RR} and π^{LL} in Eq. (87) to their common (chromo-) electric and magnetic components. This leaves π unchanged

$$\begin{aligned}
& \pi^{rs} = \left(\begin{array}{c} \frac{1}{3} \delta^{rs} \left(\vec{E}^A \vec{E}^D + \vec{B}^A \vec{B}^D \right) \\ - \left(\vec{E}^{rA} \vec{E}^{sD} + \vec{B}^{rA} \vec{B}^{sD} \right) \end{array} \right) U_{AD} \\
\hline
& \left(\pi^{RR} \right)^{rs} = a^{rs} - ib^{rs} \\
\hline
& \left(\pi^{LL} \right)^{rs} = a^{rs} + ib^{rs} \\
\hline
& a^{rs} = \left(\begin{array}{c} \frac{1}{3} \delta^{rs} \left(-\vec{E}^A \vec{E}^D + \vec{B}^A \vec{B}^D \right) \\ - \left(-\vec{E}^{rA} \vec{E}^{sD} + \vec{B}^{rA} \vec{B}^{sD} \right) \end{array} \right) U_{AD} \\
\hline
& b^{rs} = \left(\begin{array}{c} \frac{1}{3} \delta^{rs} \left(\vec{E}^A \vec{B}^D + \vec{B}^A \vec{E}^D \right) \\ - \left(\vec{E}^{rA} \vec{B}^{sD} + \vec{B}^{rA} \vec{E}^{sD} \right) \end{array} \right) U_{AD}.
\end{aligned} \tag{188}$$

The adjoint representation indices A, D and the position difference z make it necessary to symmetrize the above expressions with respect to the indices r, s taking

into account the dependence on the relative (Lorentz-) coordinate z , not explicitly shown in Eq. (188).

In order to retain the relevant degrees of freedom, we streamline the displayed indices and kinematic variables to the electromagnetic case. But in no way is this implying, that the nonabelian character of the underlying variables is sacrificed, to the contrary.

With this in mind, we introduce the abbreviated notation

$$\begin{aligned} (\vec{E}^A, \vec{B}^A) &\rightarrow (\vec{E}, \vec{B}) (\zeta) \rightarrow (\vec{E}, \vec{B})_+ \\ (\vec{E}^D, \vec{B}^D) &\rightarrow (\vec{E}, \vec{B}) (-\zeta) \rightarrow (\vec{E}, \vec{B})_- \\ U_{AD} &\rightarrow \cdot ; \quad \zeta = z/2. \end{aligned} \quad (189)$$

The trace parts proportional to δ^{rs} of the matrix π in Eq. (188) can be neglected. This follows from Eq. (183).

Thus Eq. (188) takes the form using the notation introduced in Eq. (189)

$$\begin{aligned} -\pi^{rs} &\sim \vec{E}_+^r \vec{E}_-^s + \vec{B}_+^r \vec{B}_-^s \\ a^{rs} &\sim \vec{E}_+^r \vec{E}_-^s - \vec{B}_+^r \vec{B}_-^s + (r \leftrightarrow s) \\ -b^{rs} &\sim \vec{E}_+^r \vec{B}_-^s + \vec{B}_+^r \vec{E}_-^s \end{aligned} \quad (190)$$

modulo trace parts.

Here we need the variable $\vec{e} = \vec{z}/r$ introduced in Eq. (39) in order to orient chromoelectric and -magnetic fields, in a radial gauge, where the parallel transport matrix $U_{AD} \rightarrow \delta_{AD}$. The chromomagnetic fields then become related to the -electric ones

$$\begin{aligned} \vec{B}_+ &= \vec{e} \wedge \vec{E}_+ ; \quad \vec{B}_- = -\vec{e} \wedge \vec{E}_- \\ \vec{e} \vec{E}_\pm &= \vec{e} \vec{B}_\pm = 0. \end{aligned} \quad (191)$$

Eq. (191) establishes the nonabelian ‘Dreibein’ form.

As the wave functions associated with the field strengths in Eqs. (191) and (191) are complex, we can choose the \vec{e} associated helicity basis. Choosing the z axis along \vec{e} , Eq. (191) takes the component form

$$\begin{aligned} \vec{E}_\pm &= (E_{x\pm}, E_{y\pm}, 0) \\ \vec{B}_+ &= (-E_{y+}, E_{x+}, 0) ; \quad \vec{B}_- = (E_{y-}, -E_{x-}, 0) \rightarrow \\ (\mathcal{E}, \mathcal{B})_+^R &= (E, B)_{x+} - i(E, B)_{y+} \\ (\mathcal{E}, \mathcal{B})_+^L &= (E, B)_{x+} + i(E, B)_{y+} \\ (\mathcal{E}, \mathcal{B})_-^R &= (E, B)_{x-} + i(E, B)_{y-} \\ (\mathcal{E}, \mathcal{B})_-^L &= (E, B)_{x-} - i(E, B)_{y-}. \end{aligned} \quad (192)$$

The (complex) components $(\mathcal{E}, \mathcal{B})_{\pm}^{R(L)}$ in Eq. (192)³ define the sought helicity basis, where Eq. (192) takes the form

$$\mathcal{B}_{\pm}^R = (-i) \mathcal{E}_{\pm}^R ; \quad \mathcal{B}_{\pm}^L = (i) \mathcal{E}_{\pm}^L . \quad (193)$$

The spin component associated with the operation

$$\widehat{S}_{\vec{e}} = i \vec{e} \wedge , \quad (194)$$

which represents an infinitesimal rotation around the \vec{e} - axis (i.e., its derivative with respect to the rotation angle), takes the eigenvalues implied by the R, L components in Eq. (193)

$$\begin{aligned} \widehat{S}_{\vec{e}} (\mathcal{E}_+^R, \mathcal{B}_+^R) &= +1 , & \widehat{S}_{\vec{e}} (\mathcal{E}_-^L, \mathcal{B}_-^L) &= +1 \\ \widehat{S}_{\vec{e}} (\mathcal{E}_+^L, \mathcal{B}_+^L) &= -1 , & \widehat{S}_{\vec{e}} (\mathcal{E}_-^R, \mathcal{B}_-^R) &= -1 . \end{aligned} \quad (195)$$

Hence the direct product components $R_+ R_- , R_+ L_- , L_+ R_-$ and $L_+ L_-$ describe four $S_{\vec{e}12}$ spin states

Δ helicity components	$S_{\vec{e}12}$
$(\mathcal{E}_+^R, \mathcal{B}_+^R) \otimes (\mathcal{E}_-^R, \mathcal{B}_-^R)$	0
$(\mathcal{E}_+^L, \mathcal{B}_+^L) \otimes (\mathcal{E}_-^L, \mathcal{B}_-^L)$	0
$(\mathcal{E}_+^R, \mathcal{B}_+^R) \otimes (\mathcal{E}_-^L, \mathcal{B}_-^L)$	2
$(\mathcal{E}_+^L, \mathcal{B}_+^L) \otimes (\mathcal{E}_-^R, \mathcal{B}_-^R)$	-2

(196)

For clarity let us associate a pair of complex, transverse three vectors $(\vec{v}, \vec{w})^4$ with the two sides of the octet string denoted by + and -

$$\begin{aligned} \vec{v} &\leftrightarrow \left(\vec{E}, \vec{B} \right)_+ , & \vec{w} &\leftrightarrow \left(\vec{E}, \vec{B} \right)_- \\ \vec{e} \vec{v} &= 0 , & \vec{e} \vec{w} &= 0 \\ v^R &= v_x - i v_y , & w^R &= w_x + i w_y \\ v^L &= v_x + i v_y , & w^L &= w_x - i w_y . \end{aligned} \quad (197)$$

Using the components R, L as defined in Eqs. (192) and (197), the (complex orthogonal) scalar product takes the form

$$u \cdot v = u_x v_x + u_y v_y = \frac{1}{2} (u^R w^R + u^L w^L) . \quad (198)$$

We adapt the tensor structure of the symmetric matrices π, a, b in Eq. (190) to the RR, RL, LR and LL basis defined in Eq. (192)

$$\pi^{\widetilde{rs}} \sim \begin{pmatrix} \pi^{RR} & \pi^{RL} \\ \pi^{LR} & \pi^{LL} \end{pmatrix} + (r \leftrightarrow s) ; \quad \text{and } \pi \rightarrow a, b \quad (199)$$

modulo trace parts .

³The helicity basis components \mathcal{B} shall not be confused with the SL2C matrix \mathcal{B} defined in Appendix A.1 .

⁴The auxiliary vector \vec{w} introduced here shall not be confused with the Weyl bilinears w_{\pm}^{RR} and w_{\pm}^{RL} in Eqs. (177) and (179) .

It follows from Eqs. (198) and (199) that the trace part remains valid in the specific $\tilde{r}\tilde{s}$ assignment chosen. However, symmetrization with respect to the indices $r s$ is not equivalent to symmetrization with respect to $\tilde{r}\tilde{s}$

$$(r \leftrightarrow s) \equiv \left(\begin{array}{c} \pi^{RR} \leftrightarrow \pi^{LL} \\ \pi^{RL} \rightarrow \pi^{RL} \text{ and } \pi^{LR} \rightarrow \pi^{LR} \end{array} \right) \quad (200)$$

modulo trace parts and $\pi \rightarrow a, b$.

Equation (200) implies for the symmetrized matrices π, a, b

$$\pi^{\tilde{r}\tilde{s}} \sim \left(\begin{array}{cc} \frac{1}{2} (\pi^{RR} + \pi^{LL}) & \pi^{RL} \\ \pi^{LR} & \frac{1}{2} (\pi^{RR} + \pi^{LL}) \end{array} \right) \quad (201)$$

modulo trace parts and $\pi \rightarrow a, b$.

Now taking the traceless parts simply removes the RR and LL components

$$\pi^{\tilde{r}\tilde{s}} \sim \left(\begin{array}{cc} 0 & \pi^{RL} \\ \pi^{LR} & 0 \end{array} \right) \text{ and } \pi \rightarrow a, b. \quad (202)$$

Now we cast π, a, b in Eq. (190) into the $\tilde{r}\tilde{s}$ basis

$$\begin{aligned} -\pi^{RL} &\sim \mathcal{E}_+^R \mathcal{E}_-^L + \mathcal{B}_+^R \mathcal{B}_-^L, & -\pi^{LR} &\sim \mathcal{E}_+^L \mathcal{E}_-^R + \mathcal{B}_+^L \mathcal{B}_-^R \\ a^{RL} &\sim \mathcal{E}_+^R \mathcal{E}_-^L - \mathcal{B}_+^R \mathcal{B}_-^L, & a^{LR} &\sim \mathcal{E}_+^L \mathcal{E}_-^R - \mathcal{B}_+^L \mathcal{B}_-^R \\ -b^{RL} &\sim \mathcal{E}_+^R \mathcal{B}_-^L + \mathcal{B}_+^R \mathcal{E}_-^L, & -b^{LR} &\sim \mathcal{E}_+^L \mathcal{B}_-^R + \mathcal{B}_+^L \mathcal{E}_-^R. \end{aligned} \quad (203)$$

We substitute the relations in Eq. (193) in Eq. (203)

$$\mathcal{B}_\pm^R = (-i) \mathcal{E}_\pm^R; \quad \mathcal{B}_\pm^L = (i) \mathcal{E}_\pm^L \rightarrow, \quad (204)$$

with the result that *all contributions from the spin 2 Weyl bilinear vanish*, as a consequence of the ‘Dreibein’ conditions

$$\begin{aligned} -\pi^{RL} &\sim 2 \mathcal{E}_+^R \mathcal{E}_-^L, & -\pi^{LR} &\sim 2 \mathcal{E}_+^L \mathcal{E}_-^R \\ \hline (a^{RL}, a^{LR}) &\sim 0, & (b^{RL}, b^{LR}) &\sim 0. \end{aligned} \quad (205)$$

Comparing with the helicity structure in Eq. (196), we find

Δ helicity components	$S_{\vec{e}_{12}}$
$-\frac{1}{2} \pi^{RL} = \mathcal{E}_+^R \mathcal{E}_-^L$	2
$-\frac{1}{2} \pi^{LR} = \mathcal{E}_+^L \mathcal{E}_-^R$	-2
$a = b = 0$	0

(206)

Summary remarks on the construction of the II^+ spectral gb series

i) Decomposition of adjoint string bilinears and their associated wave functions

We reproduce here the structure of the adjoint string bilinears introduced in Eq. (14)

$$\begin{aligned} B_{[\mu_1 \nu_1], [\mu_2 \nu_2]}(x_1, x_2) &= \\ &F_{[\mu_1 \nu_1]}(x_1; A) U(x_1, A; x_2, B) F_{[\mu_2 \nu_2]}(x_2; B) \\ A, B, \dots &= 1, \dots, 8. \end{aligned} \quad (207)$$

The bilinear quantities in Eq. (207) yield the gb wave functions in the three spectral series I^+ , I^- and II^+ introduced in Eqs. (21)–(23), summarized in Eq. (208) below

$$\begin{aligned} \tilde{t}_{\pm}(z, p, J^{P+}; \cdot) &\rightarrow \tilde{t}_{\pm; S_{12}^{\pm}}(z, p, J^{\pm+}; \cdot) \\ \tilde{t}_{\pm; S_{12}^{\pm}}(z, p, J^{\pm+}; \cdot) &\begin{cases} \nearrow \tilde{t}_{\pm; II^+}(z, p, J^{++}; \cdot) \\ \rightarrow \tilde{t}_{\pm; I^+}(z, p, J^{++}; \cdot) \\ \searrow \tilde{t}_{\pm; I^-}(z, p, J^{-+}; \cdot) \end{cases} \\ \pm; S_{12}^{\pm} \rightarrow \pm &\rightarrow [\mu_1 \nu_1], [\mu_2 \nu_2]. \end{aligned} \quad (208)$$

The decomposition of the adjoint string bilinears, introduced in Eq. (24), is repeated below

$$\begin{aligned} B_{[\mu_1 \nu_1], [\mu_2 \nu_2]}(x_1, x_2) &= \begin{pmatrix} (K^+)_{[\mu_1 \nu_1][\mu_2 \nu_2]} B^{(+)} \\ + (K^-)_{[\mu_1 \nu_1][\mu_2 \nu_2]} B^{(-)} \\ + B'_{[\mu_1 \nu_1], [\mu_2 \nu_2]} \end{pmatrix} \\ (K^+)_{[\mu_1 \nu_1][\mu_2 \nu_2]} &= g_{\mu_1 \mu_2} g_{\nu_1 \nu_2} - g_{\mu_1 \nu_2} g_{\mu_2 \nu_1} \\ (K^-)_{[\mu_1 \nu_1][\mu_2 \nu_2]} &= \varepsilon_{\mu_1 \mu_2 \nu_1 \nu_2}. \end{aligned} \quad (209)$$

In Eq. (209) K^{\pm} and the associated bilinears and their induced amplitudes denoted $B(\pm)$ project on the spectral types I^{\pm} according to Eq. (208), whereas $B'_{[\mu_1 \nu_1], [\mu_2 \nu_2]}$ refers to the projection on the II^+ spectral type. The unique projection of B' on the traceless part of the Ricci bilinear, identical to the classical energy momentum tensor pertaining to gauge bosons, is derived in this Appendix (A.5).

The general decomposition of $B_{[\mu_1 \nu_1], [\mu_2 \nu_2]}$ in Eq. (207) is introduced in Eq. (162) reproduced below

$$\begin{aligned} B_{[\mu_1 \nu_1], [\mu_2 \nu_2]} &= w_{[\mu_1 \nu_1][\mu_2 \nu_2]} + \Delta B_{[\mu_1 \nu_1], [\mu_2 \nu_2]} \\ \Delta B_{[\mu_1 \nu_1], [\mu_2 \nu_2]} &= \frac{1}{2} \begin{pmatrix} g_{\mu_1 \mu_2} R_{\nu_1 \nu_2} - g_{\nu_1 \mu_2} R_{\mu_1 \nu_2} \\ -g_{\mu_1 \nu_2} R_{\nu_1 \mu_2} + g_{\nu_1 \nu_2} R_{\mu_1 \mu_2} \end{pmatrix} \\ &\quad - \frac{1}{6} K^+_{[\mu_1 \nu_1][\mu_2 \nu_2]} R \end{aligned} \quad (210)$$

with: $g^{\mu_1 \mu_2} w_{[\mu_1 \nu_1][\mu_2 \nu_2]} = 0$

$$g^{\mu_1 \mu_2} B_{[\mu_1 \nu_1], [\mu_2 \nu_2]} = g^{\mu_1 \mu_2} \Delta B_{[\mu_1 \nu_1], [\mu_2 \nu_2]} = R_{\nu_1 \nu_2}$$

$$R = g^{\nu_1 \nu_2} R_{\nu_1 \nu_2} = 12 B^{(+)}.$$

In Eq. (210) we have denoted the still reducible parts in the following way

$$\begin{aligned} w_{[\mu_1 \nu_1][\mu_2 \nu_2]} &: \text{Weyl bilinear} \\ R_{\mu \nu} &: \text{Ricci bilinear.} \\ R &: \text{Riemann scalar bilinear} \end{aligned} \quad (211)$$

The decomposition in Eq. (210) into positive parity irreducible parts, leaving the Weyl bilinear reducible, is introduced in Eq. (166) repeated below

$$\begin{aligned}
B_{[\mu_1 \nu_1], [\mu_2 \nu_2]} &= w_{[\mu_1 \nu_1], [\mu_2 \nu_2]} + \Delta B_{[\mu_1 \nu_1], [\mu_2 \nu_2]} \\
\Delta B_{[\mu_1 \nu_1], [\mu_2 \nu_2]} &= \frac{1}{2} \begin{pmatrix} g_{\mu_1 \mu_2} \varrho_{\nu_1 \nu_2} - g_{\nu_1 \mu_2} \varrho_{\mu_1 \nu_2} \\ -g_{\mu_1 \nu_2} \varrho_{\nu_1 \mu_2} + g_{\nu_1 \nu_2} \varrho_{\mu_1 \mu_2} \end{pmatrix} \\
&\quad + \frac{1}{12} K^+_{[\mu_1 \nu_1], [\mu_2 \nu_2]} R
\end{aligned} \tag{212}$$

with : $g^{\mu_1 \mu_2} w_{[\mu_1 \nu_1], [\mu_2 \nu_2]} = 0$

$$g^{\mu_1 \mu_2} B_{[\mu_1 \nu_1], [\mu_2 \nu_2]} = g^{\mu_1 \mu_2} \Delta B_{[\mu_1 \nu_1], [\mu_2 \nu_2]} = R_{\nu_1 \nu_2}$$

$$R = g^{\nu_1 \nu_2} R_{\nu_1 \nu_2} = 12 B^{(+)}$$

In Eq. (212), the irreducible positive parity parts introduce the traceless part of the Ricci bilinear, i.e. the classical traceless energy momentum bilinear pertaining to gauge bosons. Thus the notations in Eq. (211) are extended, as shown in Eq. (165)

$$\begin{aligned}
w_{[\mu_1 \nu_1], [\mu_2 \nu_2]} &: \text{Weyl bilinear} \\
R_{\mu\nu} &: \text{Ricci bilinear} \\
R &: \text{Riemann scalar bilinear} \\
-\varrho^{\mu\nu} = -R^{\mu\nu} + \frac{1}{4} g^{\mu\nu} R &: \text{energy momentum} \\
\equiv \vartheta_{cl}^{\mu\nu} &: \text{bilinear.}
\end{aligned} \tag{213}$$

The structure of the energy-momentum bilinear introduced in Eq. (165) (and Eqs. 212–213) with respect to chromoelectric and -magnetic field strengths is reproduced in Eq. (214) below

$$\begin{aligned}
-\varrho^{\mu\nu} &= -R^{\mu\nu} + \frac{1}{4} g^{\mu\nu} R = \vartheta_{cl}^{\mu\nu} = \\
&= \begin{pmatrix} \frac{1}{2} \begin{pmatrix} \vec{E}^A \vec{E}^D \\ + \vec{B}^A \vec{B}^D \end{pmatrix} & -\vec{S}^{kAD} \\ -\vec{S}^{iAD} & -\vec{E}^{iA} \vec{E}^{kD} - \vec{B}^{iA} \vec{B}^{kD} \\ & + \frac{1}{2} \delta_{ik} \begin{pmatrix} \vec{E}^A \vec{E}^D \\ + \vec{B}^A \vec{B}^D \end{pmatrix} \end{pmatrix} U_{AD}.
\end{aligned} \tag{214}$$

The Weyl bilinear is decomposed into irreducible parts according to Eq. (177) repeated in Eq. (215) below

$$\begin{aligned}
w_{[\mu_1 \nu_1], [\mu_2 \nu_2]} &= \begin{pmatrix} \left(P^{RR} \left(\vec{C} \otimes \vec{C} \right) \right)_{[\mu_1 \nu_1], [\mu_2 \nu_2]} \\ + \left(P^{LL} \left(\vec{G} \otimes \vec{G} \right) \right)_{[\mu_1 \nu_1], [\mu_2 \nu_2]} \\ + B^{(-)} \left(K^- \right)_{[\mu_1 \nu_1], [\mu_2 \nu_2]} \end{pmatrix} \\
\left(K^- \right)_{[\mu_1 \nu_1], [\mu_2 \nu_2]} &= \varepsilon_{\mu_1 \mu_2 \nu_1 \nu_2}.
\end{aligned} \tag{215}$$

The irreducible parts ϱ , P^{RR} and P^{LL} representing the spin 2 parts of the energy momentum bilinear (ϱ) and the Weyl bilinear (P^{RR} , P^{LL}) are

identified with the wave functions of the II^+ spectral series in Eq. (184) repeated in Eq. (216) below

$$\begin{aligned}
\varrho^z &\leftrightarrow \tilde{t}_z(\{\varrho\}; z, p, J^{PC}; \cdot) \rightarrow \tilde{t}(\{\varrho\}) \\
w_z &\leftrightarrow \tilde{t}_z(\{w\}; z, p, J^{PC}; \cdot) \rightarrow \tilde{t}(\{w\}) \\
w_z^{RR} &\leftrightarrow \tilde{t}_z(\{w^{RR}\}; z, p, J^{PC}; \cdot) \rightarrow \tilde{t}(\{w^{RR}\}) \\
w_z^{LL} &\leftrightarrow \tilde{t}_z(\{w^{LL}\}; z, p, J^{PC}; \cdot) \rightarrow \tilde{t}(\{w^{LL}\}).
\end{aligned} \tag{216}$$

The *new* result, worked out in this Appendix (A.5), shows that the wave functions pertaining to P^{RR} and P^{LL} , i.e. to the spin 2 irreducible parts of the Weyl bilinear vanish.

In this sense we identify here the bilinear with its gb wave functions, keeping in mind that the full spin 2 Weyl bilinear operator does *not* vanish identically. This implies for the wave functions defined in Eq. (216)

$$\tilde{t}(\{w^{RR}\}) = \tilde{t}(\{w^{LL}\}) = 0. \tag{217}$$

Eq. (217) is the main result of this Appendix (A.5).

With the above identification, the full decomposition of the adjoint string bilinear in Eq. (212) becomes

$$B_{[\mu_1 \nu_1], [\mu_2 \nu_2]} = \left\{ \begin{array}{l} \frac{1}{2} \left(\begin{array}{l} g_{\mu_1 \mu_2} \varrho_{\nu_1 \nu_2} - g_{\nu_1 \mu_2} \varrho_{\mu_1 \nu_2} \\ -g_{\mu_1 \nu_2} \varrho_{\nu_1 \mu_2} + g_{\nu_1 \nu_2} \varrho_{\mu_1 \mu_2} \end{array} \right) \\ + K_{[\mu_1 \nu_1], [\mu_2 \nu_2]}^+ B^{(+)} \\ + K_{[\mu_1 \nu_1], [\mu_2 \nu_2]}^- B^{(-)} \end{array} \right\} \tag{218}$$

$$\begin{aligned}
&\text{with : } g^{\mu_1 \mu_2} B_{[\mu_1 \nu_1], [\mu_2 \nu_2]} = R_{\nu_1 \nu_2} \\
&- \varrho^{\mu \nu} = -R^{\mu \nu} + \frac{1}{4} g^{\mu \nu} R = \vartheta_{cl}^{\mu \nu} \\
&R = g^{\nu_1 \nu_2} R_{\nu_1 \nu_2} = 12 B^{(+)}.
\end{aligned}$$

Comparing the form of the adjoint string components in Eq. (218) with Eq. (209), we find

$$\begin{aligned}
B'_{[\mu_1 \nu_1], [\mu_2 \nu_2]} &= \frac{1}{2} \left(\begin{array}{l} g_{\mu_1 \mu_2} \varrho_{\nu_1 \nu_2} - g_{\nu_1 \mu_2} \varrho_{\mu_1 \nu_2} \\ -g_{\mu_1 \nu_2} \varrho_{\nu_1 \mu_2} + g_{\nu_1 \nu_2} \varrho_{\mu_1 \mu_2} \end{array} \right) \\
B' &\leftrightarrow \{II^+\} \longleftrightarrow \vartheta_{cl}^{\mu \nu}.
\end{aligned} \tag{219}$$

ii) The parallel to Abelian gauge fields.

The relations of the nonabelian adjoint string variables, contained in Eqs. (218) and (219), with the three spectral types, denoted I^+ , I^- and II^+ here, equally apply to the corresponding string variables pertaining to electromagnetic fields [6, 7]. This has not been explicitly done [5], since the structure of the two isolated decay photons yields a considerable simplification.

References

- [1] A. B. Kaidalov, V. A. Khoze, A. D. Martin and M. G. Ryskin, *Central exclusive diffractive production as a spin-parity analyser: from hadrons to Higgs*, Eur. Phys. J. C **31** (2003) 387; 2003hep-ph/0307064.
- [2] L. D. Landau and E. M. Lifschitz, *Production of electrons and positrons by a collision of two particles*, Phys. Z. Sowjetunion **6** (1934) 244; L. D. Landau and I. Pomeranchuk (in Russian), *Limits of applicability of the theory of Bremsstrahlung electrons and pair production at high energies*, Dokl. Akad. Nauk Ser. Fiz. **92** (1953) 535; L. D. Landau and I. Pomeranchuk (in Russian), *Electron cascade process at very high energies*, Dokl. Akad. Nauk Ser. Fiz. **92** (1953) 735; L. D. Landau (in Russian), *On the multiparticle production in high energy collisions*, Izv. Akad. Nauk Ser. Fiz. **17** (1953) 51.
- [3] H. Cheng and T. T. Wu, *High energy elastic scattering in quantum electrodynamics*, Phys. Rev. Lett. **22** (1969) 666; H. Cheng and T. T. Wu, *Impact picture and the eikonal approximation*, Phys. Lett. B **34** (1971) 647.
- [4] P. Minkowski and W. Ochs, *Identification of the glueballs and the scalar meson nonet of lowest mass*, Eur. Phys. J. C **9** (1999) 283, hep-ph/9811518; *Scalar mesons and glueball in B-decays and gluon jets*, hep-ph/0304144; *On the scalar nonet lowest in mass*, Nucl. Phys. Proc. Suppl. **121** (2003) 119; hep-ph/0209223; *The glueball among the light scalar mesons*, Nucl. Phys. Proc. Suppl. **121** (2003) 123; hep-ph/0209225;
- [5] H. Fritzsche and P. Minkowski, *Psi resonances, gluons and the Zweig rule*, Nuovo Cim. A **30** (1975) 393.
- [6] H. Landau, *On the angular momentum of a system of two photons*, Dokl. Akad. Nauk. SSSR **60** (1948) 207; see also in "Collected papers of L. D. Landau", D. ter Haar ed., Gordon and Breach, New York (1965).
- [7] C. N. Yang, *Selection rules for the dematerialization of a particle into two photons*, Phys. Rev. **77** (1950) 242.
- [8] I. Caprini, G. Colangelo and H. Leutwyler, work in progress; H. Leutwyler, *Electromagnetic form-factor of the pion*, Talk given at Continuous Advances in QCD 2002 / ARKADYFEST (honoring the 60th birthday of Prof. Arkady Vainshtein), Minneapolis, Minnesota, 17-23 May 2002, published in *Minneapolis 2002, Continuous advances in QCD* p.23, hep-ph/0212324.
- [9] The KLOE Collaboration, *Recent results from the KLOE experiment at DAΦNE*, AIP Conf.Proc. **698** (2004) 74; hep-ex/0308023.
- [10] H. Ichie, V. Bornyakov, T. Streuer and G. Schierholz, *The flux distribution of the three quark system in SU(3)*, Contributed to 20th International Symposium on Lattice Field Theory (LATTICE 2002), Boston, Massachusetts, 24-29 Jun 2002, hep-lat/0212024.
- [11] P. Minkowski, *On the Oscillatory Modes of Quarks in Baryons*, Nucl. Phys. B **174** (1980) 258.
- [12] The Particle Data Group, K. Hagiwara et al., Phys. Rev. D **66** (2002) 010001 and 2003 off-year partial update for the 2004 edition available on the PDG WWW pages (URL: <http://pdg.lbl.gov/>).
- [13] F. Niedermayer, P. Rüfenacht and U. Wenger, *Fixed point SU(3) gauge actions : scaling properties and glueballs*, Submitted to 18th Int. Symp. on Lattice Field Theory (Lattice 2000), Bangalore, India, 17-22 Aug 2000, Nucl. Phys. Proc. Suppl. **94** (2001) 636; hep-lat/0011041.
- [14] H. B. Meyer and M. J. Teper, *Glueballs and the Pomeron*, Nucl. Phys. Proc. Suppl. **129** (2004) 200; hep-lat/0308035.

- [15] C. Michael, *Hybrid Mesons from the Lattice*, hep-ph/0308293.
- [16] T. Kunihiro, S. Muroya, A. Nakamura, C. Nonaka, M. Sekiguchi and H. Wada, *Scalar Particles in Lattice QCD*, to be published in *Proc. Int. Symp. on Hadron Spectroscopy; Chiral Symmetry and Relativistic Description of Bound Systems*, in a series of KEK proceedings; hep-ph/0308291.
- [17] S. U. Chung, E. Klempt and J. G. Körner, *SU(3) Classification of p-wave $\eta\pi$ and $\eta'\pi$ Systems*, Eur. Phys. J. A **15** (2002) 539; hep-ph/0211100; D. R. Thompson et al., Phys. Rev. Lett **79** (1997) 1630; S. U. Chung et al., Phys. Rev. D **60** (1999) 092001; E. Ivanov et al., Phys. Rev. Lett. **86** (2001) 3977.
- [18] G. Colangelo, J. Gasser and H. Leutwyler, *Pi Pi scattering*, Nucl. Phys. B **603** (2001) 125; hep-ph/0103088.
- [19] R. Jost, *Über die falschen Nullstellen der Eigenwerte der S-Matrix*, Helv. Phys. Acta **20** (1947) 256.
- [20] R. Kaminski, L. Leśniak and B. Loiseau, *Elimination of ambiguities in pion-pion phase shifts using crossing symmetry*, Phys. Lett. B **551** (2003) 241; hep-ph/0210334; R. Kaminski, L. Leśniak and K. Rybicki, *A joint analysis of the S-wave in the $\pi^+\pi^-$ and $\pi^0\pi^0$ data*, Eur. Phys. J. direct C **4** (2002) 4; hep-ph/0109268, and references cited therein.
- [21] R. Kaminski, L. Leśniak and K. Rybicki, *Separation of S-wave pseudoscalar and pseudovector amplitudes in $\pi^-p \rightarrow \pi^+\pi^-n$ reaction on polarized target*, Z. Phys. C **74** (1997) 79; hep-ph/9606362.
- [22] *The crystal barrel collaboration*, CERN-PS-197 Experiment, C. Amsler et al., *High statistics study of $f_0(1500)$ decay into $\pi^0\pi^0$* , Phys. Lett. B **342** (1995) 433.
- [23] S. Spanier and N. A. Tornqvist, *Scalar mesons*, page 450 of the Review of Particle Properties in Ref. [12], and references cited therein.
- [24] C. Amsler, *Non $q\bar{q}$ candidates*, in Ref. [12], and references cited therein.
- [25] E. M. Aitala et al., E791 Collaboration, *Experimental evidence for a light and broad scalar resonance in $D^+ \rightarrow \pi^-\pi^+\pi^+$ decay*, Phys. Rev. Lett. **86** (2001) 770; hep-ex/0007028; E. M. Aitala et al., E791 Collaboration, *Study of the $D_s^+ \rightarrow \pi^-\pi^+\pi^+$ decay and measurement of f_0 masses and widths*, Phys. Rev. Lett. **86** (2001) 765; hep-ex/0007027.
- [26] P. L. Frabetti et al., E687 Collaboration, *Analysis of the $D^+, D_s^+ \rightarrow \pi^-\pi^+\pi^+$ Dalitz plots*, Phys. Lett. B **407** (1997) 79. and Phys. Lett. B **351** (1995) 591.
- [27] A. Garmash et al., Belle Collaboration, *Study of B meson decays to three body charmless hadronic final states*, Phys. Rev. D **69** (2001) 012001; hep-ex/0307082; A. Garmash et al., Belle Collaboration, *Three body charmless $B \rightarrow K h h$ decays at Belle*, hep-ex/0207003; K. Abe et al., Belle Collaboration, *Study of three body charmless B decays*, Phys. Rev. D **65** (2002) 092005, hep-ex/0201007; K. Abe et al., Belle Collaboration, *Study of charmless B decays to three kaon final states*, Contributed to *31st International Conference on High Energy Physics (ICHEP 2002)*, Amsterdam, The Netherlands, 24–31 July 2002, hep-ex/0208030.
- [28] B. Aubert et al., BABAR Collaboration, *Measurements of the branching fractions of charged B decays to $K^\pm\pi^\mp\pi^\pm$ final states*; Phys. Rev. D **70** (2004) 092001; hep-ex/0308065; B. Aubert et al., BABAR Collaboration, *Measurements of the branching fractions and charge asymmetries of charmless three body charged B decays*, Phys. Rev. Lett. **91** (2003) 051801; hep-ex/0304006; B. Aubert et al., BABAR Collaboration, *Measurements of the branching fractions of charged B decays to $K^+\pi^-\pi^+$ final states*;

- hep-ex/0303022; P. C. Bloom for the BABAR Collaboration, *Measurements of rare B decays at BABAR*, eConf C020805 (2002) TTH06, hep-ex/0302030; B. Aubert et al., BABAR Collaboration, *Measurements of the branching fractions of charmless three body charged B decays*, hep-ex/0206004.
- [29] C. Amsler, *Proton-antiproton annihilation and meson spectroscopy with the crystal barrel*, Rev. Mod. Phys. **70** (1998) 1293, hep-ex/9708025.
- [30] T. Akesson et al., AFS Collaboration, *A search for glueballs and a study of double pomeron exchange at the CERN intersecting storage rings*, Nucl. Phys. B **264** (1986) 154.
- [31] A. Singovsky for the WA102 collaboration, *New results from the WA102 experiment*, Nucl. Phys. A **675** (2000) 47c; A. Kirk, *Resonance production in central p p collisions at the CERN OMEGA spectrometer*, Phys. Lett. B **489** (2000) 29; hep-ph/0008053, and references cited therein.
- [32] F. Close, *Light hadron spectroscopy and experiment*, Int. J. Mod. Phys. A **17** (2002) 3239; hep-ph/0110081; F. Close and A. Kirk, *Scalar glueball $q\bar{q}$ mixing above 1 GeV and implications for lattice QCD*, Eur. Phys. J. C **21** (2001) 531; hep-ph/0103173; F. Close, *Glueballs: a central mystery*, Acta Phys. Polon. B **31** (2000) 2557; hep-ph/0006288; F. Close, A. Kirk and G. Schuler, *Dynamics of glueball and $q\bar{q}$ production in the central region of p p collisions*, Phys. Lett. B **477** (2000) 13; hep-ph/0001158; and references cited therein.
- [33] R. Jost, *The general theory of quantized fields*, American Mathematical Society, Providence R. I. (1965); R. Jost, *CTP-Invarianz der Streumatrix und interpolierende Felder*, Helv. Phys. Acta **36** (1963) 77; R. Jost, *Einiges über die Lorentzgruppe und das einäugige Sehen* (engl. transl.: *Some things on the Lorentz group and monocular vision*), Verein Schweizerischer Mathematik- und Physiklehrer, Bulletin Nr. 2, 1966.
- [34] For a review see M. Creutz, *The early days of lattice gauge theory*, AIP Conf. Proc. **690** (2003) 52; hep-lat/0306024; J. Greensite, *The confinement problem in lattice gauge theory*, Prog. Part. Nucl. Phys. **51** (2003) 1; hep-lat/0301023; M. Luescher, S. Sint, R. Sommer and P. Weisz, *Chiral symmetry and $O(a)$ improvement in lattice QCD*, Nucl. Phys. B **478** (1996) 365; hep-lat/9605038.
- [35] For a review see E. Alvarez, *Loops versus strings*, gr-qc/0307090; A. M. Polyakov and V. S. Rychkov, *Gauge fields-strings duality and the loop equation*, Nucl. Phys. B **581** (2000) 116; hep-th/0002106; Y. M. Makeenko and A. A. Migdal, *Exact equation for the loop average in multicolor QCD*, Phys. Lett. B **88** (1979) 135 and Erratum Phys. Lett. B **89** (1980) 437.
- [36] O. Nachtmann, *Perturbative and nonperturbative aspects of QCD*, H. Latal and W. Schweiger eds. Springer Verlag, Berlin, Heidelberg (1997); hep-ph/9609365.
- [37] Spider, *The Encyclopedia Americana, Int. edition*, Vol. **25**, p. 494, Americana Corporation 1976.
- [38] Photograph “Spinnennetz” (spider web), reproduction authorized by courtesy of Lui Bernard, www.onlinekunst.de/bernard/04.html.
- [39] M. Fierz, *Die unitären Darstellungen der homogenen Lorentzgruppe*, in *Preludes in theoretical physics*, in honor of V. F. Weisskopf, A. De-Shalit, H. Feshbach and L. van Hove eds., North Holland, Amsterdam (1966), p.1.

TVORBA HADRONA UKRŠTENIM HADRONSKIM SNOPOVIMA: FIZIČKI
POTENCIJAL OSNOVNOG EKSPERIMENTALNOG ISTRAŽIVANJA

Osnovni cilj ovog rada bio je dati kratak pregled gluonskih mezona, koji bi se tražili u središnjim sudarima hadrona relativno male mase, a u kojima bi se mogli odabrati pojasevi rapidnosti, i koji bi zahtijevali hadronske snopove dovoljne energije i intenziteta. Poglavlja 1–4 posvećena su tom cilju. Različite računalne vještine, koje su postigli mnogi tijekom posljednjih nekoliko desetljeća, uključujući i autora, opisuju se u pet dodataka posvećenih posebno gluonskim parovima u QCD-u i njihovoj polaznoj Yang-Millsovoj osnovnoj strukturi.